TECHNISCHE UNIVERSITÄT MÜNCHEN
Biologikum Weihenstephan
Lehrstuhl für Genetik

The role of the transcriptional coactivator MAL and its target genes in cell motility and EMT

Laura Leitner

Vollständiger Abdruck der von der Fakultät Wissenschaftszentrum Weihenstephan für Ernährung, Landnutzung und Umwelt der Technischen Universität München zur Erlangung des akademischen Grades eines

Doktors der Naturwissenschaften

genehmigten Dissertation.

Vorsitzender:	Univ.-Prof. Dr. E. Grill
Prüfer der Dissertation:	1. Univ.-Prof. Dr. K. Schneitz
	2. Priv.-Doz. Dr. G. Posern
	(Ludwig-Maximilians-Universität München)
	3. Univ.-Prof. Dr. M. Hrabé de Angelis

Die Dissertation wurde am 01.12.2010 bei der Technischen Universität München eingereicht und durch die Fakultät Wissenschaftszentrum Weihenstephan für Ernährung, Landnutzung und Umwelt am 20.06.2011 angenommen.

Index

I. Summary

Changes in actin dynamics are communicated to the nucleus by members of the MRTF (myocardin related transcription factors) family of transcriptional coactivators. Upon signal induction G-actin liberates MRTF cofactors, which subsequently bind to and activate the transcription factor Serum Response Factor (SRF). SRF target genes in turn include numerous structural and regulatory components of the actin cytoskeleton as well as cytoskeleton-associated proteins involved in adhesion and cell motility. Moreover MRTFs are implicated in epithelial-mesenchymal transition (EMT), a developmentally regulated process which is also involved in tumor progression. EMT is characterized by dissociation of cell-cell contacts and a morphological conversion towards unpolarized motile cells. Together, these findings suggest a role of actin-MAL-SRF signaling in cell motility.

I analyzed the migratory effects of actin-MAL mediated transcription in non-invasive cell lines and examined the regulation of MAL during EMT. An unbiased microarray screen identified Serpine1 (Pai-1) and the cytoskeleton-associated genes Four-and-a-half LIM domains 1 (Fhl1), Plakophilin 2 (Pkp2), Integrin α5 (Itga5) and Epithelial Protein Lost in Neoplasm α (Eplin-α) as novel G-actin regulated targets. I confirmed their transcriptional induction by quantitative RT-PCR. Moreover, retroviral infection with constitutively active, dominant negative and MAL knockdown constructs established these genes as MAL targets. The SRF responsive elements of Pkp2 and Eplin-α could be identified by chromatin IP and luciferase reporter assays.

Functionally, I showed that ectopic expression of active MAL impairs the migration of mesenchymal NIH 3T3 fibroblasts and epithelial EpRas cells in wound healing and Boyden chamber assays. Conversely, dominant negative constructs and partial knockdown of MAL enhanced motility in these non-invasive cells. I next asked how G-actin regulated cytoskeleton-associated targets are involved in the antimigratory function of MAL in non-invasive epithelial and mesenchymal cells. Knockdown of Integrin α5 and Plakophilin 2 (Pkp2) enhanced cell migration of fibroblasts, whereas Pkp2 and Fhl1 knockdown increased epithelial cell motility. In addition the reduced migration of epithelial cells stably expressing active MAL was partially restored by knockdown of either Pkp2 or Fhl1, or by double knockdown. Overall I concluded that MAL is implicated in antimigratory responses through upregulation of the cytoskeleton-associated proteins Integrin α5, PKP2 and FHL1 in non-invasive cells.

We have recently demonstrated that MAL is activated during EMT and calcium-dependent disassembly of epithelial junctions. I showed that MAL is upregulated on both mRNA and protein level upon EMT induction whereas MRTF-B expression was essentially unaffected. The microRNA miR-1 appeared to be involved in the regulation of MAL expression by binding to a highly conserved binding site in the MAL 3'UTR. Further analyses will have to determine how miR-1 contributes to the regulation of MAL during EMT induction.

My findings that MAL exhibits antimigratory functions in non-invasive cell lines is contrasted by the previously described requirement of MRTFs for motility and invasion of metastatic breast cancer cells.

To address the underlying discrepancies, I first reproduced the antimigratory effect of a partial Mrtf knockdown in the highly invasive MDA-MB-231 cells. In addition I could show that MAL enhances migration of invasive EpRasXT cells that have undergone EMT, which is in marked contrast to the antimigratory effect of MAL in the corresponding non-invasive epithelial EpRas cells. These findings demonstrated a fundamentally different migratory function of MRTFs in invasive and non-invasive cells.

Based on these results, I hypothesize that MAL activity directly correlates with adhesive strength through its numerous cytoskeleton-associated targets. As migration speed shows a biphasic dependence on the adhesiveness I speculate that increasing MAL signaling activity in non-invasive cell lines with an already large repertoire of cytoskeletal and adhesive components reduces motility. Conversely, weakly adherent cells respond with reduced motility to decreased MAL signaling.

II. Zusammenfassung

Veränderungen der Aktin-Zytoskelett-Dynamik werden durch Koaktivatoren der MRTF (myocardin related transcription factor) Familie dem Zellkern mitgeteilt. Die Induktion der Signalkaskade resultiert in verstärkter Aktinpolymerisation, wodurch MRTFs aus einem inhibierenden Komplex mit monomerem Aktin freigesetzt werden. Daraufhin können sie an den Transkriptionsfaktor Serum Response Factor (SRF) binden und diesen aktivieren. Viele der SRF Zielgene wiederum kodieren für Zytoskelett-assoziierte Proteine, die in Adhäsion und Migration involviert sind. Darüber hinaus sind MRTFs in epithelialer-mesenchymaler Transition (EMT) involviert, einem entwicklungsregulierten Prozess, der auch zur Tumorentstehung beiträgt. EMT ist durch die Dissoziation von Zell-Zellkontakten und dem morphologischen Übergang zu unpolarisierten, motilen Zellen charakterisiert. Insgesamt deuten diese Befunde auf eine Rolle des Aktin-MAL Signaltransduktionswegs in Zellmotilität hin.

In dieser Arbeit untersuchte ich, welchen Einfluss Aktin-MAL vermittelte Transkription auf die Migration nicht-invasiver Zellen hat. Des Weiteren analysierte ich die Regulation von MAL während der EMT. In einem Microarray Screen wurden Serpine1 (Pai-1) und die Zytoskelett-assoziierten Faktoren Four-and-a-half LIM domains 1(Fhl1), Plakophilin 2 (Pkp2), Integrin α5 (Itga5) und Epithelial Protein Lost in Neoplasm α (Eplin-α) als neue G-Aktin regulierte Gene identifiziert. Ich konnte die transkriptionelle Induktion dieser Gene mittels quantitativer RT-PCR verifizieren. Durch retrovirale Infektion mit konstitutiv aktiven, dominant negativen und MAL-Knockdownkonstrukten wurden diese Gene als MAL Zielgene charakterisiert. Die SRF-responsiven Elemente von Pkp2 und Eplin-α konnten durch Chromatin IP und Luciferase Assays identifiziert werden. Ich zeigte, dass die Überexpression von aktivem MAL die Migration mesenchymaler NIH 3T3 Zellen und epithelialer EpRas Zellen in Wundheilungs- und Boyden-Kammer-Assays beeinträchtigt. Dominant negative und MAL knockdown Konstrukte hingegen verstärkten die Motilität dieser nicht-invasiven Zellen.

Danach untersuchte ich, wie G-actin regulierte Gene mit Zytoskelett-assoziierten Funktionen zu dem antimigratorischen Effekt von MAL in nicht-invasiven epithelialen und mesenchymalen Zellen beitragen. Tatsächlich erhöhte der Knockdown von Integrin α5 und Plakophilin 2 die Migration von Fibroblasten, während Pkp2- und Fhl1-Knockdown epitheliale Zellmotilität verstärkte. Darüber hinaus wurde die verringerte Migration von epithelialen Zellen, die aktives MAL stabil exprimieren, durch den Knockdown von Pkp2 und/oder Fhl1 partiell aufgehoben. Insgesamt schließe ich, dass MAL durch die Hochregulierung der Zytoskelett-assoziierten Proteine Integrin α5, PKP2 und FHL1 eine antimigratorische Funktion in nicht invasiven Zellen ausübt.

Wir konnten kürzlich zeigen, dass MAL während der EMT und Kalzium-abhängiger Auflösung epithelialer Zellkontakte aktiviert wird. Ich zeigte in meiner Arbeit, dass MAL auf mRNA- und Protein-Ebene nach EMT Induktion hochreguliert wird, während die MRTF-B Expression im Wesentlichen unbeeinflusst bleibt. Die microRNA miR-1 scheint in die Regulation der MAL Expression involviert zu sein, in dem sie an eine hoch konservierte Bindestelle in der 3'UTR der MAL

mRNA bindet. Weitere Untersuchungen werden zeigen müssen, ob miR-1 zu der Regulation von MAL während der EMT Induktion beiträgt.

Mein Befund, dass MAL antimigratorische Funktionen in nicht-invasiven Zelllinien ausübt, steht der kürzlich beschriebenen Notwendigkeit von MRTFs für Motilität und Invasivität metastasierender Brustkrebszellen gegenüber. Um die zugrundeliegenden Ursachen zu untersuchen, reproduzierte ich zunächst den antimigratorische Effekt eines partiellen Mrtf Knockdowns in den hoch invasiven MDA-MB-231 Zellen. Darüber hinaus konnte ich zeigen, dass MAL die Migration invasiver EpRasXT Zellen, die eine epitheliale-mesenchymale Transition durchlaufen haben, verstärkt. Dies steht in klarem Gegensatz zu dem antimigratorischen Effekt von MAL in den entsprechenden nicht-invasiven epithelialen EpRas Zellen. Diese Ergebnisse zeigen eine prinzipiell unterschiedliche migratorische Funktion von MRTFs in invasiven und nicht-invasiven Zellen.

Basierend auf den Ergebnissen vermute ich, dass die MAL Aktivität durch die zahlreichen Zytoskelett-assoziierten Zielgene direkt mit der Adhäsionsstärke korreliert. Da die Migrationsgeschwindigkeit eine biphasische Abhängigkeit von der Adhäsivität zeigt, spekuliere ich, dass eine Erhöhung der MAL Signalaktivität in nicht-invasiven Zelllinien, die bereits mit einem großen Repertoire an zytoskelettalen und adhäsiven Komponenten ausgestattet sind, die Motilität verringert. Im Gegensatz dazu antworten weniger adhärente Zellen mit verringerter Motilität auf verminderte MAL Aktivität.

III. Introduction

1 The cytoskeleton

The cytoskeleton is a three dimensional, highly dynamic intracellular network of protein filaments extending throughout the cytoplasm. It plays pivotal roles in regulation of cell shape, cell division, organization of cellular components and coordinated movement. All these functions require a continuous reorganization of the cytoskeletal networks. The cytoskeleton is crucial for efficient signal transduction as it provides a scaffold to which many signaling molecules can bind upon activation of transmembrane receptors. Furthermore it represents a huge network on which motor proteins such as kinesins, dynein, and myosin can translocate to move organelles and vesicles. It consists of three major components: the intermediate filaments (IFs), microtubules (MTs), and actin filaments. These networks are built up by different protein subunits and display different mechanical properties.

1.1 Intermediate filaments

The intermediate filaments are the toughest and most durable of the cytoskeletal networks, providing cells with mechanical strength and crucial structural support.

IF proteins are encoded by a large family of about 70 conserved genes (Hesse et al., 2001) which are regulated in a cell type specific and differentiation-related manner. These genes can be classified according to sequence homology, polymerization properties of the encoded proteins, or their cellular distribution (Herrmann and Aebi, 2000).

Keratins are the most prominent IF proteins in epithelial cells whereas vimentin is the prototypic IF protein expressed in a plethora of non-epithelial cell types. Lamins form a meshwork of filaments termed the nuclear lamina, which underlies and strengthens the nuclear envelope.

The fibrous IF proteins contain an N-terminal globular head, a C-terminal globular tail and a central rod domain. The rod contains long-range heptad repeats of hydrophobic/apolar residues and highly conserved signature motifs at its N- and C-terminal extremities. It enables intermediate filament proteins to form stable dimers by wrapping around each other in a coiled-coil configuration, in which the two subunits exhibit a parallel alignment. Two coiled-coil dimers non-covalently form an apolar tetramer by associating along their lateral surfaces with an anti-parallel orientation; these tetramers bind to one another end-to-end and side by side, also by non-covalent bonding, forming long 10 – 12 nm wide ropes. The globular head and tail regions remain exposed in these filaments and can mediate the interaction with various proteins and other cytoskeletal networks.

Similar to F-actin and microtubules intermediate filaments show a highly regulated and dynamic organization that is controlled by accessory proteins (Coulombe et al., 2000) and post-translational modifications (Omary et al., 1998). Nevertheless IFs exhibit some features which are fundamentally different from F-actin and microtubules: IF proteins self-assemble in the absence of ATP or GTP into apolar heterogeneous filaments, which apparently don’t serve as tracks for molecular motors.

Intermediate filaments form a network throughout the cytoplasm that surrounds the nucleus and extends out to the cell periphery where it is anchored to cell-cell junctions such as desmosomes (Kottke et al., 2006). In epithelial cell layers keratin filaments of neighboring cells are connected via the desmosomes, which provides a continuous mechanical link throughout the tissue. IFs are also associated with other membrane-spanning adhesion complexes such as hemidesmosomes (Green and Jones, 1996; Litjens et al., 2006), "nonhemidesmosomal" integrin-mediated linkages to the substratum such as focal adhesions (Kreis et al., 2005; Tsuruta and Jones, 2003) and cell junctions mediated by classical cadherins (Kim et al., 2005; Kowalczyk et al., 1998). IFs take part in the regulation of integrin-based adhesion in migrating cells (Ivaska et al., 2005).

More than 40 genetically determined diseases have been related to mutations in IF encoding genes. The corresponding disorders range from ectodermal dysplasias, myopathies and cardiomyopathies and are caused by cell and tissue fragility.

1.2 Microtubules

Microtubules are long stiff hollow tubes, which can rapidly disassemble in one location and reassemble in another. Unlike intermediate filaments, microtubule extension requires an organizing center such as a centrosome, from which the microtubules grow out towards the cell periphery forming tracks along which vesicles, organelles and other cellular components are moved. The microtubule system is the main cytoskeletal network responsible for anchoring membrane enclosed organelles within the cell and for guiding intracellular transport. Kinesins and dyneins are motor proteins that can attach cargos to microtubule filaments. They use energy derived from repeated cycles of ATP hydrolysis to carry organelles and vesicles along the microtubules.

The microtubule cytoskeleton plays pivotal roles during mitosis, which requires disassembly of cytoplasmic microtubules and reassembly into mitotic spindles building up the machinery that segregates the chromosomes equally into two daughter cells. Whereas rapid remodeling of the microtubule network is essential at the onset of mitosis, microtubules are much more stable in differentiated cells, where they maintain the organization and the polarity of cells and help to position organelles in their required location.

They are built from tubulin subunits. These building blocks are dimers of two very similar globular proteins, α- and β-tubulin, which are tightly bound together by noncovalent bonding. The dimers form, again by noncovalent bonding, a linear chain, the protofilament, in which α- and β-tubulin alternate. Thirteen parallel protofilaments of the same polarity form a hollow cylindrical microtubule.

Centrosomes, the microtubule organizing centers, contain hundreds of ring-shaped structures formed from another type of tubulin, namely γ-tubulin. Each γ-tubulin ring serves as nucleation site for the outgrowth of one microtubule which occurs in a specific orientation at the plus end. In addition to the γ-tubulin rings a centrosome contains two centrioles made of a cylindrical array of short microtubules, which apparently have no role in the nucleation process.

Microtubules are in comparison to intermediate filaments relatively instable. Microtubule growth is a very dynamic process, a phenomenon that is referred to as dynamic instability. Free tubulin dimers contain tightly bound GTP which is hydrolyzed to GDP shortly after the subunit is added to a growing microtubule. This leads to a conformational change that weakens the binding strength between the tubulin subunits. If the addition of new subunits occurs faster than the hydrolysis of GTP, the newly added tubulin subunits form a GTP cap enabling the microtubule to grow further. If the bound GTP of a newly incorporated tubulin dimer is hydrolyzed before the addition of new subunits, rapid microtubule disassembly is favored. Released tubulin subunits then exchange their bound GDP to GTP and become available for polymerization to a growing microtubule.

Microtubule activity like those of other cytoskeletal filaments depends on a large variety of accessory proteins that mediate their stabilization and linkage to other filaments. Microtubules search the cytoplasmic space by continuously growing and shrinking at their plus ends, which project outward to the cell periphery (Kirschner and Mitchison, 1986). Microtubules are then captured and transiently stabilized at specific membrane target sites through plus end interacting proteins (+TIPs) such as EB-1 and CLIP-170 (Gundersen et al., 2004; Schuyler and Pellman, 2001). +TIPs are thought to act by protecting the growing ends of microtubules from catastrophe proteins that depolymerize microtubules (Komarova et al., 2002; Tirnauer et al., 2002). Coordinated interactions between microtubules and filamentous actin play pivotal roles in many polarized processes, including cell shape, mitotic spindle orientation, motility, growth cone guidance, and wound healing. During cell migration the actin-microtubule crosstalk occurs at focal adhesions, where the actin cytoskeleton is connected to the extracellular matrix. Microtubules grow towards focal adhesions, probably guided by actin stress fibers (Kaverina et al., 1998). Targeting of microtubules to focal adhesions leads to dissolution or turnover of the targeted focal adhesions (Kaverina et al., 1999). The microtubule dependent turnover may be important to limit adherence at the front of the cell and to dissolve focal adhesions at the rear.

Spectraplakins represent efficient eukaryotic scaffolding proteins strengthening interactions between microtubule- and actin-based structures. These proteins contain direct binding sites for +TIPs, F-actin and microtubules (Karakesisoglou et al., 2000; Leung et al., 1999; Subramanian et al., 2003; Yang et al., 1999) and at least some spektraplakins can also interact with IFs, dynein/dynactin, and cell junctions (Gregory and Brown, 1998; Karakesisoglou et al., 2000; Kodama et al., 2003; Leung et al., 1999; Roper and Brown, 2003).

An intact microtubule array was shown to be essential for directed migration (Goldman, 1971; Vasiliev et al., 1970). Microtubules are involved in restricting the activity of the actin cytoskeleton to the leading edge thereby contributing to lamellipodia formation (Liao et al., 1995; Mikhailov and Gundersen, 1998).

1.3 Actin filaments

The microfilament network is a complex structure essential for changes of cell shape, motor-based organelle transport, regulation of ion transport, receptor mediated signaling responses, and cell

movement. Two main steps of the migratory cycle depend on actin: the formation of protrusions by motor-independent actin polymerization and the generation of pulling forces through myosins.

The highly conserved actin genes are only found in eukaryotes and fall into three broad classes: α-, β-, and γ-isoforms (Vandekerckhove and Weber, 1978). Actin proteins are mainly located in the cytoplasm but also reside in the nucleus. In most eukaryotic cells actin is most abundant in the layer beneath the plasma membrane which is called the cell cortex. There the microfilaments are cross-linked in a dense meshwork, supporting the outer surface and giving mechanical strength.

Monomeric actin is 67 x 40 x 37 Å in size and has a molecular weight of 43,000 Da (Kabsch et al., 1990). It includes four quasi-subdomains (1-4), each having repeating motifs comprising a multi-stranded β-sheet. 40% of the structure is α-helical (Kabsch et al., 1990). The deep cleft in the center is usually occupied by a tightly bound ATP in monomeric actin or ADP-Pi (rather than ADP) in the majority of F-actin subunits (Kinosian et al., 1993). ATP binds as a complex with either Mg^{2+} or Ca^{2+} (De La Cruz and Pollard, 1995; Strzelecka-Golaszewska, 2001).

Although microfilaments are thinner, more flexible and usually shorter than microtubules, both filaments exhibit similar principles of assembly and disassembly. Actin filaments appear as a twisted chain of identical globular actin molecules all pointing in the same direction and are about 7 nm in diameter. The addition of actin monomers is possible at both ends of a microfilament, but occurs much faster at the (+) or “barbed” end. Three phases of actin polymerization can be distinguished: i) the slow initial association of G-actin subunits to a dimer that is more likely to dissociate again rapidly; ii) the formation of a stable trimer, which can be considered as the nucleus of polymerization; iii) the elongation phase, during which monomers are rapidly assembled (Oosawa et al., 1959).

Microfilaments are in a continuous state of assembly and disassembly (Kasai et al., 1962). Free actin monomers carry ATP which is hydrolyzed to ADP soon after incorporation. As for microtubule assembly a lag phase between the incorporation of ATP-G-actin and hydrolysis of ATP can be observed (Carlier, 1990; Carlier et al., 1984; De La Cruz et al., 2000; Pardee et al., 1982). The hydrolysis of ATP to ADP reduces the binding strength between the actin monomers and promotes depolymerization. Dissociated ADP-actin subunits rapidly exchange their bound ADP for ATP in solution (Neidl and Engel, 1979), a process that is accelerated by profilin. The polymerization of actin is not dependent on nucleotide hydrolysis (Cooke, 1975; Kasai et al., 1965; Pollard, 1984), but hydrolysis is required for the normal function of F-actin.

Filamentous actin can be found in multiple conformations depending on the type of the bound cation and nucleotide, the isoform of actin (Orlova et al., 1997; Orlova and Egelman, 1995) and the presence of other proteins bound to actin (McGough et al., 1997; Owen and DeRosier, 1993).

There is a large variety of actin binding proteins (ABPs) that regulate different aspects of the assembly and disassembly process. The association of microfilaments with microtubules and intermediate filaments also depends on linker proteins.

ABPs can be divided into the following groups (reviewed in (dos Remedios et al., 2003)

i) Monomer-binding proteins sequester G-actin and prevent its polymerization thus maintaining a pool of monomers in solution (e.g. thymosin β4, profilin, and DNase I).

ii) Filament-depolymerizing proteins induce the conversion of F- to G-actin (e.g. CapZ and cofilin).

iii) Filament end-binding proteins cap the ends of the actin filament preventing the exchange of monomers at the pointed end (e.g. tropomodulin) and at the barbed end (e.g. CapZ).

iv) Filament severing proteins shorten the average length of filaments by binding to the side of F-actin and cutting it into two pieces (e.g. gelsolin).

v) Cross-linking proteins contain at least two binding sites for F-actin, thus facilitating the formation of filament bundles, branching filaments and three-dimensional networks (e.g. actinin).

vi) Stabilizing proteins bind to the sides of actin filaments and prevent its depolymerization (e.g. tropomyosin).

vii) Motor proteins use F-actin as tracks upon which to move. All actin dependent motor proteins belong to the family of myosins. They bind to and hydrolyze ATP which provides the energy for the movement towards the plus end of the microfilaments. The myosin I and myosin II subfamilies are most abundant, myosin II is the major myosin involved in filament sliding whereas myosin I is critical for endocytosis. Myosins contain one head domain and a tail. The head interacts with actin filaments and has an ATP hydrolyzing motor activity that enables it to move along the filament in a cycle of binding, detachment and rebinding. The tail varies, determining which cell components will be dragged along the microfilaments.

viii) Actin nucleators promote the polymerization of the different types of actin arrays formed in a variety of cellular processes (e.g. Arp2/3, formins). Nucleation is the rate limiting step for actin filament polymerization

2 Cellular communities – epithelial sheets

Multicellular organisms are separated from the environment by a layer of epithelial cells which cover the external surface of the body and line all its internal cavities creating a protective barrier. Epithelia are multicellular sheets in which cells are densely packed side to side. Epithelia vary morphologically in thickness and form. Epithelial sheets have two faces: the apical surface that is exposed to the exterior or to internal cavities and the basal surface that is attached to some sort of connective tissue. The basal surface rests on the basal lamina, a thin sheet of extracellular matrix composed of Type IV collagen, laminin and other matrix proteins. The apical and basal surfaces of an epithelium are chemically different which is referred to as epithelial polarity. Epithelial integrity is maintained by intercellular junctional complexes composed of tight junctions, adherens junctions, and desmosomes, whereas gap junctions mediate intercellular communication. This organization further depends on junctions that epithelial cells form with the basal lamina, the hemidesmosomes and focal adhesions.

3 Cell junctions

Cell junctions are built up by protein complexes that provide contact between neighboring cells or a cell and the extracellular matrix. In multicellular organisms intercellular adhesion is critical for many processes such as tissue patterning, morphogenesis, and maintenance of normal tissues (Gumbiner, 1996). Intercellular junctions have most extensively been investigated in polarized epithelial cells where intercellular adhesion is mediated by a tripartite junctional complex comprised of tight junctions, adherens junctions and desmosomes.

Cell junctions can be classified according to their function as depicted below:

Table III-1: Cell-cell and cell-matrix junctions

Name	Function
Tight junctions (Occluding Junctions)	Seal neighboring epithelial cells to prevent leakage of molecules between them
Adherens junctions (Anchoring Junctions)	Join actin bundles of neighboring cells together
Desmosomes (Anchoring Junctions)	Join the intermediate filaments of neighboring cells together
Gap junctions (Communicating junctions)	Form channels that allow small water-soluble molecules, including ions, to pass from cell to cell
Hemidesmosomes	Anchor intermediate filaments in a cell to the basal lamina
Focal adhesions	Anchor actin filaments in a cell to the extracellular matrix

Adherens junctions, desmosomes and hemidesmosomes intracellularly associate with cytoskeletal filaments, thereby allowing the formation of a huge network that extends from cell to cell across the whole epithelial sheet. A second common function is the enrichment of signaling proteins at the junctional plaques.

Cell junctions are extremely dynamic structures that are tightly regulated. Their modulation mediated by extracellular signals allows for tissue remodeling during development, differentiation, wound healing, and invasion. Cell junctions do not only respond to extracellular stimuli, they also actively participate in signal cascades.

3.1 Tight junctions

Tight junctions (TJs), or zonula occludens, are the most apical component of the junctional complex. They form a continuous, circumferential, belt-like structure that holds the cells together and mediates a sealing function. Via tight junctions the membranes of two neighboring cells closely join together forming a virtually impermeable barrier to fluid. This defines two extremely different extracellular milieus, the apical and the basolateral compartment which is in continuity with the interstitial fluid. Furthermore TJs separate the apical and the basolateral domains of the plasma membrane, which differ in protein and lipid composition and carry out specialized functions. Tight junctions are composed of a

branching network of sealing strands of intramembrane particles. Rows of these transmembrane proteins are embedded in both plasma membranes, with extracellular domains joining one another directly. TJs contain two principal types of transmembrane components – tetraspan and single-span transmembrane proteins. The tetraspan proteins are occludin, tricellulin and the claudins.

There are 24 different human claudin genes that are expressed in a tissue-specific manner. The encoded proteins of 20-27 kDa are the main structural components of intramembrane strands (Furuse and Tsukita, 2006). The claudin composition determinates the ion selectivity of the paracellular pathway.

Like claudins occludin is associated with intramembrane strands, although it is not required for their assembly. It regulates the paracellular diffusion of small hydrophilic molecules.

Tricellulin is in contrast to occludin and claudins enriched at the junctions between three epithelial cells. It is thought to be required for junction formation (Ikenouchi et al., 2005) and shares a conserved domain with occludin that mediates binding to ZO-1.

Single-span transmembrane proteins such as JAMs, CRB3 and BVEs have also been found to be associated with tight junctions, mediating homotypic cell-cell adhesion (Bazzoni et al., 2000).

On the intracellular side of the plasma membrane these transmembrane proteins associate with a complex array of adaptors, scaffolding and cytoskeletal proteins components that build up the cytoplasmic plaque. Composition and complexity of the cytoplasmic plaque vary greatly among different epithelia. Many of the tight junction plaque proteins contain PDZ domains that serve as links to the actin cytoskeleton. Thus, tight junctions link the cytoskeleton of adjacent cells. Furthermore numerous accessory proteins interact with the cytoplasmic plaque mediating diverse processes such as tumor suppression, epithelial cell proliferation, polarization and differentiation. These signaling components include classical signaling proteins such as kinases and phosphatases, as well as dual-localization proteins that can reside at junctions as well as in the nucleus, affecting gene expression.

The major plaque components are ZO-1, ZO-2, cingulin, p130, and 7H6. Both ZO-1 and ZO-2 belong to the MAGUK protein family. Members of this family are often found at cell-cell contacts where they couple extracellular signaling pathways with the cytoskeleton. They share several conserved motifs including an SH3 domain, guanylate kinase domain, and PDZ domains. In tight junctions ZO-1 is located closest to the TJ membrane. It binds to the C-terminus of occludin via its GUK domain or to claudins via its PDZ domain and forms a heterodimer with ZO-2 or ZO-3 through its second PDZ domain. Furthermore it can directly bind to actin and α-actinin through its large C-terminal domain (Fanning, 2001). Via its SH3 domain ZO-1 is able to associate with a number of signaling molecules (Matter and Balda, 2007).

Although no cadherins are found in TJs, cadherin mediated cell-cell adhesion is believed to be critical in the establishment and maintenance of TJs. F-actin underlying the TJ membrane was also shown to play important roles in TJ maintenance and epithelial cell polarity.

Tight junctions are dynamic structures. During embryogenesis and epithelial-mesenchymal transition intercellular adhesion is decreased which requires the downregulation of tight junction and adherens junction proteins by the zinc finger transcription repressor Snail (Batlle E., 2000; Cano et al., 2000; Ikenouchi et al., 2005; Ikenouchi et al., 2003).

3.2 Adherens junctions

Adherens junctions zip cells together and thereby maintain cell and tissue polarity. Furthermore they anchor the cytoskeleton to the plasma membrane.

The transmembrane proteins forming adherens junctions (or zonula adherens) like those in desmosomes belong to the cadherin family. Cadherin molecules form homodimers in a calcium-dependent manner with other cadherin molecules on adjacent cells. At an adherens junction, the cadherin is tethered intracellularly via several linker proteins such as vinculin and catenins to actin filaments. The short intracellular domain of cadherin can bind to $p120^{ctn}$, β-catenin and γ-catenin (= plakoglobin). β-catenin binds to α-catenin, which recruits ZO-1, vinculin and α-actinin.

Often, the adherens junctions form a continuous adhesion belt around the whole epithelial cell that is located near the apical end of the cell, below the tight junctions. As the actin network spanning the whole epithelium is contractile the epithelial sheet has the capacity to develop tension and to change its shape dramatically. These epithelial movements are crucial during embryonic development, creating structures such as the neural tube. A similar cell junction in non-epithelial cells such as cardiomyocytes is the fascia adherens. It is structurally the same, but appears in ribbonlike patterns that do not completely encircle the cell.

In numerous cell types such as epithelial cells and fibroblasts an intercellular adhesions system containing nectin and afadin can be found at adherens junctions. Afadin associates with F-actin and the Ca^{2+}-independent cell-cell adhesion molecule nectin, linking it to the actin cytoskeleton. This adhesion system plays regulatory roles in the formation of adherens junctions and subsequently the formation of TJs in epithelial cells (Takai and Nakanishi, 2003). It also participates in the formation of several specialized cell-cell junctions, such as synapses in neurons (Takai and Nakanishi, 2003). Besides its adhesion properties nectin also induces activation of Cdc42 and Rac, which regulates reorganization of the actin cytoskeleton (Kawakatsu et al., 2002).

3.2.1 Eplin-α

Epithelial Protein Lost in Neoplasm α (Eplin-α) is a cytoskeleton-associated tumor suppressor whose expression inversely correlates with cell growth, motility, invasion and cancer mortality (Jiang et al., 2008; Maul and Chang, 1999). Eplin crosslinks, bundles and stabilizes F-actin filaments and stress fibers, which correlates with its ability to suppress anchorage-independent growth in transformed cells (Han et al., 2007; Maul et al., 2003; Song et al., 2002). In epithelial cells, Eplin is required for formation of the F-actin adhesion belt by binding to the E-cadherin-catenin complex through α-catenin (Abe and Takeichi, 2008).

3.3 Desmosomes

Desmosomes and hemidesmosomes are the major cell surface attachment sites for intermediate filaments at cell-cell and cell-substrate contacts, respectively (reviewed in (Green and Jones, 1996)). Desmosomes or maculae adherentes are localized spot-like adhesions subjacent to the adherens junctions and are more widely arranged along the lateral sides of plasma membranes.

They are composed of a tripartite electron-dense plaque that anchors intermediate filaments. Two cytosolic plaques of adjacent cells sandwich a membrane core region of 30 nm in width. This extracellular domain is called the extracellular core domain or the desmoglea. It is divided by an electron-dense midline where the desmosomal cadherins interact with each other.

The major components of the desmosomes belong to three different protein families: cadherins, armadillo proteins, and plakins.

The desmosomal cadherins desmoglein and desmocollin engage in calcium dependent homophilic binding (reviewed in (Garrod, 1993; Garrod et al., 2002; Koch and Franke, 1994)). They are single-pass, transmembrane-spanning glycoproteins with highly conserved repetitive regions of homology in the extracellular domain, which is thought to be involved in calcium binding and adhesion. A conserved region in the cytoplasmic domain is required for binding to cytoplasmic adaptor proteins of the armadillo and plakin family that mediate the link to IFs (Schmidt and Jager, 2005). There are three desmocollin (Dsc1-Dsc3) and four desmoglein (Dsg1-Dsg4) genes that are expressed in tissue- and stratification-specific patterns (King et al., 1995; Koch et al., 1992; Yue et al., 1995).

On the cytoplasmic side of the plasma membrane, there are two dense structures called the Outer Dense Plaque and the Inner Dense Plaque. These are spanned by the desmoplakin protein. The Outer Dense Plaque is where the cytoplasmic domains of the cadherins attach to desmoplakin (DP) via plakoglobin (Pg) and plakophilins (PKP 1-3). The Inner Dense Plaque is where desmoplakin attaches to the intermediate filaments of the cell. Figure III-1 shows the desmosome ultrastructure and the arrangement of desmosomal components.

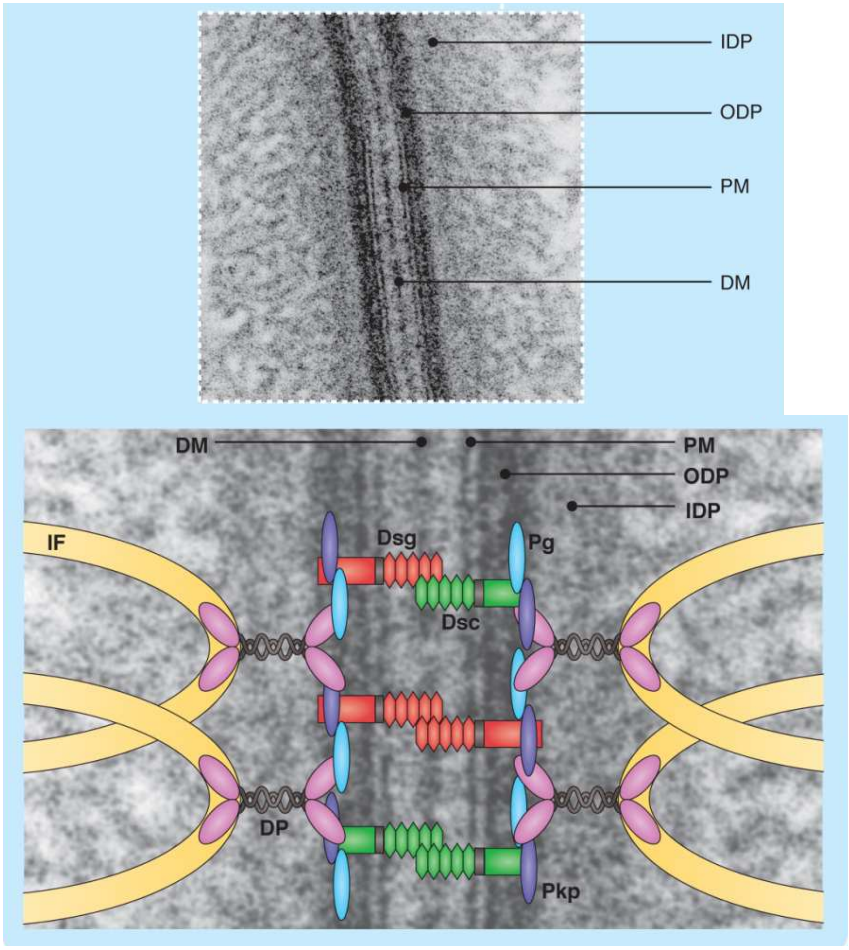

Figure III-1 Desmosome ultrastructure and arrangement of desmosomal components (from (Desai et al., 2009)). IDP, Inner Dense Plaque; ODP, Outer Dense Plaque; PM, plasma membrane; DM, dense midline; Pg, plakoglobin; Dsg, desmoglobin; Dsc, desmocollin; DP, desmoplakin; Pkp, Plakophilin.

Desmosomal armadillo family members include Pg and PKP1-3. Similar to their AJ counterparts β-catenin and p120, Pg and Pkps are also present in the nucleus. Members of this family contain a series of repeating armadillo motifs. In addition to their structural roles in intercellular junctions, armadillo family members act as signal transducers.

Plakoglobin binds to the cytoplasmic domain of desmocollins and desmogleins (Kowalczyk et al., 1994; Mathur et al., 1994; Roh and Stanley, 1995; Troyanovsky et al., 1994). It also associates with the N-terminus of the IF anchoring protein desmoplakin thereby representing a central desmosomal linker. It is not restricted to desmosomes but is a common component of adhesive junctions such as adherens junctions where it associates with the classic cadherins (Garrod, 1993; Schmidt et al., 1994), albeit more weakly than with desmosomal cadherins (Peifer et al., 1992).

Plakophilins are plakoglobin like molecules which bind directly to IFs (Hatzfeld et al., 1994) and numerous other proteins via their N-terminal head domains – they associate with DP (Chen et al., 2002), multiple desmosomal cadherins, Pg, β-catenin and cytokeratins. PKPs serve as scaffolds for positioning protein kinase C (PKC) and Rho GTPases during junction assembly (Bass-Zubek et al., 2008).

Plakins are a family of large modular proteins that link various cytoskeletal elements with each other and with adhesive junctions of the plasma membrane. Mutations in plakin family genes lead to defects in tissue integrity in skin, muscle and nervous system. Four desmoplakin family members can associate with desmosomes: DP, plectin, envoplakin and periplakin. Desmoplakin is indispensable for desmosome assembly and IF anchorage. It consists of a central α-helical coiled rod domain required for DP oligomerization that is flanked by two globular end domains. The N-terminal head domain binds to armadillo proteins and targets DP to the desmosomal plaque. The C-terminal domain directly associates with intermediate filaments (reviewed in (Godsel et al., 2004)).

Although a minimal set of these core proteins is required for desmosome formation, additional components can associate with desmosomes for specialized functions in a cell-type-specific manner. These include proteins required for junction assembly and integrity and proteins involved in cytoskeletal remodeling, differentiation, and signaling.

Connecting the keratin bundles of neighboring cells via desmosomes creates a transcellular network throughout a tissue that confers great tensile strength (reviewed in (Green et al., 1998)). Therefore desmosomes help to resist shearing forces that occur in tissues which experience mechanical stress such as the epidermis and heart. This network is additionally attached to the basal membrane via the hemidesmosomes. In epithelia desmosomes associate with keratin-containing IFs. They are not restricted to epithelia but can also be found in cardiac muscle, where they anchor desmin-containing IFs, as well as in dendritic cells where they associate with vimentin-containing IFs (Schmidt et al., 1994).

Desmosomes are dynamic structures. They have to be remodeled constantly. The de novo synthesis occurs from distinct cytoplasmic pools of cadherin core and plaque components (Godsel et al., 2005). Desmosomal cadherins are constitutively synthesized and transported to the membrane. Upon cell-cell contact, desmosomal cadherins become stabilized and cluster at the plasma membrane, associating with plaque components. DP enriched precursor particles translocate from the cytoplasm to nascent desmosomes to support the forming plaque. PKP2 associates with these DP precursors and plays pivotal roles in regulating the association of DP with IFs.

Desmosome formation depends on preexisting adherens junctions (Demlehner et al., 1995). On the other hand, maturation of AJs requires functional desmosomes. Armadillo proteins which have the capacity to associate with both classic and desmosomal cadherins might play important roles in this interplay.

Mis-sense, truncation and nonsense mutations leading to haplo-insufficiency have been identified in all major desmosomal components including DP, PKPs, Pg, and the desmosomal cadherins. These mutations can lead to inherited diseases of the skin such as blistering diseases and in heart defects (Gerull et al., 2004; McGrath et al., 1997; McKoy et al., 2000; Norgett et al., 2000).

3.3.1 Plakophilin 2

Plakophilins are armadillo family members that localize to the cytoplasmic plaque of intercellular desmosomal junctions, orchestrating junction formation (Bass-Zubek et al., 2009; Godsel et al., 2005). They were reported also to reside in the cytoplasm and the nucleus (Mertens et al., 1996; Schmidt et al., 1999; Schmidt et al., 1997). PKP1 is found only in desmosomes of complex epithelia, whereas PKP2 and PKP3 are more widely distributed. Alterations of plakophilin expression result in impaired cell adhesion and migration (Bass-Zubek et al., 2008; Grossmann et al., 2004; Kundu et al., 2008; South et al., 2003).

PKP2 is a major regulator of desmosome composition and positioning (Chen et al., 2002; Goossens et al., 2007). It coordinates actin-dependent maturation of desmosome precursors by interacting with the intermediate filament-desmoplakin complex, PKCα, and possibly F-actin (Bass-Zubek et al., 2008; Godsel et al., 2005). Nuclear PKP2 contributes to the RNA polymerase III holoenzyme complex.

Among the plakophilins, PKP2 shows the broadest tissue distribution (Bonne et al., 1999; Mertens et al., 1996; Schmidt et al., 1999) and is the only plakophilin expressed in the heart.

PKP2 is essential for cell-cell adhesion in cardiomyocytes (Grossmann et al., 2004; Pieperhoff et al., 2008). Ablation of plakophilin 2 in mouse results in lethality at mid-gestation due to defects in heart morphogenesis and stability (Grossmann et al., 2004).

3.4 Gap junction

Gap junctions are interspersed among desmosomes and mediate communication between cells by metabolically and electrically coupling them together. In a gap junction, the membranes of two adjacent cells are separated by a very narrow gap of 2-4 nm. This gap is spanned by the protruding ends of two transmembrane protein complexes of two adjacent cells facing each other. These protein complexes are called connexons and create a narrow passageway, which small inorganic ions and small water-soluble molecules can pass, moving directly from the cytosol of one cell to the cytosol of another. Several to hundreds of gap junctions can assemble into a macromolecular complex called a plaque. Connexons or hemichannels are homo- or hetero-hexamers of four-pass transmembrane proteins called connexins. The connexin gene family is diverse, with twenty-one identified members in the human genome, and twenty in the mouse. The various homomeric and heteromeric gap junctions can exhibit different functional properties regarding pore conductance, size selectivity, charge selectivity, voltage gating, and chemical gating.

The functions of gap junctions are diverse:

They allow for direct electrical communication between cells, as they mediate rapid transmission of action potentials in heart and in neuronal tissue via electrical synapses (Kirchhoff et al., 1998; Simon et al., 1998). In cardiac muscle the electrical coupling mediated by gap junctions allows for coordinated contraction of the cells. They also permit chemical communication between cells by providing passageways for small second messengers such as Ca^{2+}, inositol-triophosphate, and cyclic

nucleotides (Saez et al., 1989) . They mediate the free transport of metabolites and nutrients smaller than 1,000 Daltons such as nucleotides and glucose (Goldberg et al., 1999), whereas precluding the transport of large biomolecules. And they ensure that molecules and current passing through the gap junctions do not leak into the intercellular space.

Several human genetic disorders are associated with mutations in gap junction genes. Many of those affect the skin because this tissue is heavily dependent upon gap junction communication for the regulation of differentiation and proliferation.

Gap junction communication is regulated by signaling molecules associating with connexins such as phosphatases and kinases such as Src. Furthermore connexins are able to associate with proteins that are usually found at other cell-cell junctions such as ZO-1, which seems to play a role in gap junction turnover (Gaietta et al., 2002; Lauf et al., 2002). Cadherin mediated cell-cell adhesion is a prerequisite for gap junction formation.

3.5 Hemidesmosomes

Anchorage of epithelial cells to the underlying basal membrane is mediated by integrins that bind to the extracellular matrix protein laminin. Inside the cell they are linked to keratin filaments creating a structure that looks like half a desmosome, hence the name hemidesmosome.

Like desmosomes they also contain a tripartite electron-dense plaque located at the basal membrane that anchors intermediate filaments. Instead of using cadherins, hemidesmosomes contain integrin cell adhesion proteins. Integrins are composed of an α and a β subunit. They have a large extracellular domain responsible for ligand binding, a single transmembrane domain and a cytoplasmic domain (Hynes, 1992). There are several α- and β- subunit isoforms; the combination of these isoforms determines the binding specificity of the integrin to different ECM components. They do not only mediate the link between the extracellular matrix and the cytoskeleton of the cell, but they also transduce signals.

Laminin-5 is concentrated in the basement membrane zone immediately underlying each hemidesmosome in stratified squamous epithelial tissues (Jones et al., 1994). α3β1-integrin appears to initiate cell binding to laminin-5 (Carter et al., 1990) whereas α6β4-integrin is involved in the establishment of long term stable anchoring contacts of hemidesmosomes on laminin-5 rich matrices (Carter et al., 1990; Langhofer et al., 1993; Rousselle and Aumailley, 1994).

Hemidesmosomes of different epithelial tissues usually share their typical ultrastructure and composition. However, some simple epithelial cells such as those lining the gut express hemidesmosomal components that are not organized as ultrastructurally defined hemidesmosomes. These less organized multiprotein complexes are termed type II hemidesmosomes as opposed to the classical or type I hemidesmosomes of basal epidermal cells.

3.6 Focal adhesions

Cellular junctions with the ECM are required for cell migration, growth and differentiation. Focal adhesions, also known as focal contacts are large specialized multiprotein complexes where integrins cluster together to transduce transmembrane signals and link actin filaments to the ECM. They exist both between epithelia and the basal membrane and in mesenchymal cells linking them to ECM components such as collagens or fibronectin. These sites play an important role in the regulation of actin organization, thereby affecting cell spreading, morphogenesis and migration. The major transmembrane ECM receptors of focal adhesions belong to the integrin family. As mentioned above, integrins are heterodimers composed of α and β subunits. In mammals, 18 α and 8 β subunits combine in a restricted manner to form 24 specific dimers that have overlapping substrate specificity and cell-type specific expression patterns (Humphries et al., 2006; Hynes, 2002). Figure III-2 depicts the mammalian integrin heterodimers and their substrate specificities.

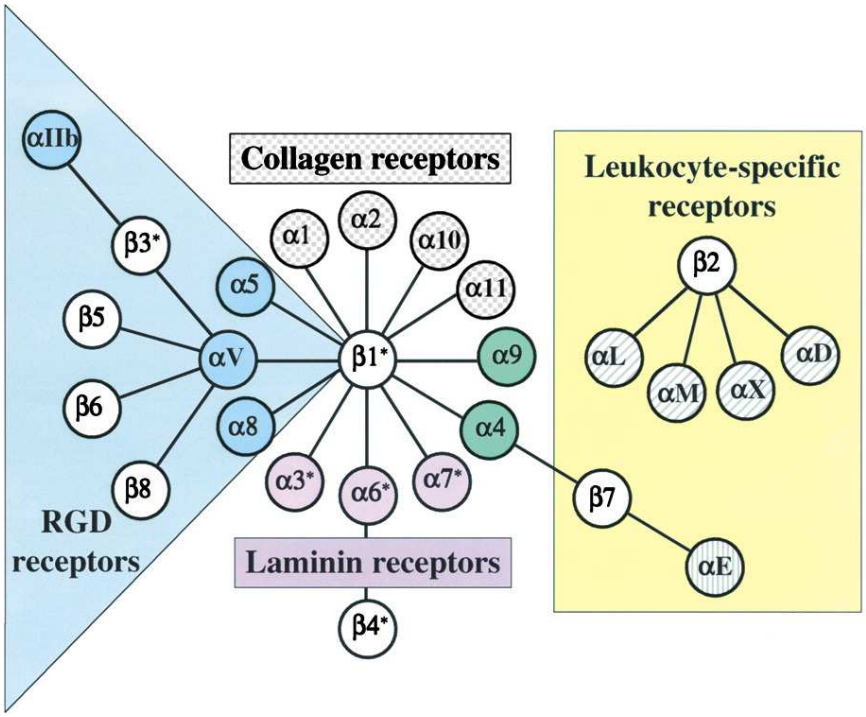

Figure III-2 Mammalian integrin heterodimers and their substrate specificities. (From (Hynes, 2002)). The blue subset of integrin heterodimers recognizes the tripeptide sequence RGD in molecules such as fibronectin and vitronectin.

Integrins transduce signals bidirectionally (reviewed in (Legate et al., 2009). Upon ligand binding they activate intracellular signaling pathways ("outside-in" signaling). On the other hand, intracellular stimuli can also cause extracellular changes via integrins. One example of inside-out signaling is the activation of integrins themselves, in which they shift from a low-affinity to a high-affinity conformation for ligand binding.

Besides integrin heterodimers additional transmembrane proteins such as heparan sulfate proteoglycans, layilin and urokinase receptor, also appear to be present at focal adhesions.

Large, multimolecular complexes assemble onto the cytoplasmic tails of activated integrins to transduce transmembrane signals and engage and organize actin filaments. More than 50 proteins were shown to be associated with focal contacts. The majority of these contain multiple domains that mediate binding to different components, forming dense and heterogeneous protein networks at the cytoplasmic faces of adhesions. Plaque composition is regulated by numerous mechanisms such as competitive binding of different partners, posttranslational modifications such as phosphorylation that modulate binding affinities and conformational changes of certain components.

Proteins associated with focal contacts can be divided into the following groups: cytoskeletal proteins (e.g. tensin, vinculin, paxillin, α-actinin, parvin, talin, and kindlin), tyrosin kinases (SRC, FAK, PYK2, CSK and ABL), serine/threonine kinases (ILK, PKC and PAK), modulators of small GTPases (ASAP1, Graf and PSGAP), tyrosine phosphatases (SHP-2, PAR PTP) and other enzymes (PI3 kinase, calpain II).

The adapter proteins talin and vinculin link the cytoplasmic domains of β integrins to actin filaments at the ends of stress fibers. Binding of talin to the cytoplasmic domain of integrin β subunits triggers the above mentioned conformational change in the αβ-integrin extracellular domain that increases its affinity for ECM components and promotes the assembly of focal adhesions (Calderwood, 2004). This activation is thought to be mediated by disruption of a salt bridge between the α- and β-integrin subunits, leading to separation of their cytoplasmic domains (Campbell and Ginsberg, 2004). Kindlin also directly interacts with β integrin tails. It thereby might cooperate with talin to regulate integrin affininty (Calderwood et al., 2002). Upon activation integrins cluster to form an adhesive unit tightly bound to the ECM. They first form unstable structures called nascent adhesion (Choi et al., 2008), a subset of which then progress to dot-like focal complexes that can mature to larger focal adhesions and finally into streak-like fibrillar adhesions (Geiger et al., 2001). These maturation processes are driven by actin-myosin contraction.

In non-motile cells focal contacts move centripetally whereas being rather stationary relative to the substrate in motile cells. In migrating cells, three different zones of distinct focal contact behavior can be defined: a focal contact formation zone between the leading edge and the nucleus, a persistence zone between the nucleus and the tail, and a culling zone where focal contacts disassemble (Smilenov et al., 1999).

Upon activation and clustering integrins are able to transduce signals “outside-in”. Paxillin links integrins to signaling proteins, forming a scaffold for SRC family tyrosine kinases. Integrin signaling modifies cellular adhesion, locomotion, and gene expression, which in turn influences survival, growth and differentiation of cells.

3.6.1 FHL1

The LIM-only proteins FHL 1-3 are characterized by four complete LIM domains, preceded by an N-terminal half LIM domain (Johannessen et al., 2006). Lim domains are cysteine-rich zinc finger motifs mediating protein-protein interactions with transcription factors, cell-signaling molecules, and

cytoskeleton-associated proteins. FHL family members are thought to act as scaffolds and to interact with F-actin and focal adhesions (Robinson et al., 2003; Shen et al., 2006; Wixler et al., 2007). They exert important roles in focal adhesion and transcriptional regulation by binding and modulating the activity of multiple transcription factors.

The tumor suppressor FHL1 plays important roles in muscle growth (Chu et al., 2000; McGrath et al., 2003) and carcinogenesis (Shen et al., 2006). It can move between intercellular junctions, focal adhesions (Brown et al., 1999), and the nucleus (Taniguchi et al., 1998) to affect gene expression. FHL1 expression is down-regulated in various types of malignancies including breast cancer, gastric cancer, lung cancer, prostate cancer, ovary cancer, colon cancer, thyroid cancer, brain tumor, renal cancer, liver cancer, and melanoma (Shen et al., 2006)

FHL1was reported to inhibit hepatoma cell growth (Ding et al., 2009b) and anchorage-dependent and –independent breast cancer cell growth (Ding et al., 2009a). SRC suppresses FHL1 in order to promote non-anchored tumor cell growth and migration (Shen et al., 2006). Recently FHL1 was shown to interact with estrogen receptors, which are involved in breast cancer development and progression, and to repress estrogen-responsive gene transcription (Ding et al., 2009a).

4 Cell migration

Cell migration is a complex and highly regulated process that is fundamental for tissue formation, maintenance and regeneration. Cell motility plays crucial roles in embryonic development, where it occurs during morphogenic processes such as gastrulation, and remains pivotal in the adult organism; skin and intestine epithelia are constantly renewed which requires migration of fresh epithelial cells up from the basal layer. During the inflammatory response leukocytes immigrate into areas of insult, and migration of fibroblasts and epithelial cells is essential for wound healing. Misregulated cell migration can lead to pathological conditions such as vascular disease, osteoporosis, chronic inflammatory diseases, mental retardation and cancer. In principle all nucleated cell types have the ability to migrate during certain stages of their development. For most cells, including epithelial, stromal, and neuronal cells, migration takes place during morphogenesis, stops with terminal differentiation and can be reactivated for tissue regeneration and neoplasia. Other cell types such as leukocytes are able to migrate throughout their entire life span, as motility is essential for their functional role. Also the requirements concerning substrate and environment differ greatly between cells.

4.1 General mechanism of cell migration

Migration is strictly regulated both spatially and temporally. It requires a tightly coordinated interplay between cell-cell adhesion, cell-matrix adhesion and localized cytoskeletal reorganization. Therefore changes in the expression of adhesion receptors or cytoskeletal-linking proteins can affect migratory behavior (Huttenlocher et al., 1995).

The basic common process of migration requires polarized actomyosin-driven shape change of the cell body (Lauffenburger and Horwitz, 1996). The cell interacts with the surrounding tissue structures. The

ECM provides the substrate for migration and represents a barrier that has to be overcome by the advancing cell. The basic mesenchymal type of cell migration can be described as a continuous cycle of 5 interdependent steps. The cell first becomes polarized and elongates, forming protrusions at the leading edge. These protrusions differ in morphology and can be divided in lamellipodia, filopodia, pseudopods and invadopods. (Adams, 2001). The formation of these protrusions is driven by actin polymerization. It seems to be independent of actomyosin contractility. In a next step adhesions between the protrusion and the ECM are formed. Transmembrane integrins bind to different ECM components dependent on the combination of integrin α and β subunit. Via a number of adaptor proteins integrins are coupled to the actin cytoskeleton. Integrins then cluster in the plasma membrane and form initial small focal complexes. These nascent adhesive complexes can grow and mature to larger more organized focal adhesions that serve as points of traction over which the cell body moves. If the cell migrates through a three dimensional environment, the extracellular matrix that represents a barrier for the migrating cell must be proteolytically remodeled. Surface proteases are recruited to the attachment sites. Soluble proteases, for instance, can directly bind to integrins and become concentrated at ECM contacts. These proteases then degrade ECM components such as collagen, fibronectin, and laminins.

Actin filaments elongate and bundle together, forming stress fibers. These stress fibers then contract, which generates inward tension towards the substrate binding sites and mediates contraction of the whole cell body. The traction force derives from the interaction of microfilaments connected to cell-substrate adhesions with myosin II. Myosin II is activated by phosphorylation of myosin light-chain (MLC) via myosin light-chain kinase (MLCK) or Rho kinase (ROCK). Myosin light-chain phosphorylation is inhibited by MLC phosphatase, which is itself inhibited by ROCK.

As a last step, cell-matrix attachments resolve preferentially in the back of the cell. Focal contact disassembly can occur by different mechanisms. Microtubule dependent targeting of dynamin promotes endocytosis of some adhesion components (Ezratty et al., 2005). Actin filament strand breakage is mediated by actin severing proteins (Wear et al., 2000). The affinity of attachments at the rear can be weakened by phosphorylation, and components like talin can be cleaved by proteases (Franco et al., 2004). After focal contact disassembly integrins get either internalized via endocytosis or remain on the substratum as the cell detaches and moves forward (Regen and Horwitz, 1992).

The migration speed is limited by the rate of focal contact formation and disassembly. A biphasic dependence of migration speed on adhesiveness has long been proposed (DiMilla et al., 1991): a certain degree of cell-matrix attachment is essential for cell migration as it enables the cell to exert traction on the substratum. Nevertheless, further stabilization of attachment to the point at which detachment is abolished impairs migration. Cell attachment is determined by the density of adhesive ligands on the substrate, the density of adhesion receptors on the cell, and the affinity of the receptors for the ECM ligands. Experimental evidence for a biphasic dependence of migration speed on the amount of integrin α5 and its ligand fibronectin (Palecek et al., 1997) confirms this prediction.

4.2 Rho GTPases in cell migration

The Rho family of small GTPases comprises essential regulators of actin polymerization, adhesion and formation of lamellipodia and filopodia. When bound to GTP, they are in their active state and interact with their downstream effectors.

The cyclical activation and inactivation of these small G proteins are regulated by three types of regulators: Rho GDP/GTP exchange factors (GEFs), Rho GTPase-activating proteins (GAPs), and Rho GDP dissociation inhibitors (GDIs) (Takai et al., 2001). The Rho proteins remain in the active state until acted upon by GAPs. GAPs boost the slow intrinsic rate of GTP hydrolysis by the Rho GTPases. GEFs modulate the exchange of GDP for GTP on GTPases to promote their activation. GDIs inhibit Rho GTPases in resting cells by blocking the dissociation of GDP; upon cell stimulation, GDIs dissociate from Rho GTPases to allow activation and targeting of the GTPase.

Rac, Cdc42, and RhoG are involved in formation of lamellipodia and filopodia. Rac mainly activates WAVE proteins (Cory and Ridley, 2002), the most prominent targets of Cdc42 mediating actin polymerization in protrusion are WASP proteins. The WASP/WAVE family then activates the Arp2/3 complex thereby inducing dendritic actin polymerization (Welch and Mullins, 2002).

The establishment and maintenance of cell polarity, which is crucial for migration, is mediated by several interdependent positive feedback loops that involve Rho family GTPases. Especially Cdc42 plays a decisive role in cell polarization. In migrating cells Cdc42 is active at the front; both inhibition and global activation interferes with directionality of migration. Cdc42 establishes cell polarity by two main mechanisms. It restricts protrusion formation to the leading edge and localizes the golgi apparatus and the microtubule-organizing center (MTOC) in front of the nucleus (Gotlieb et al., 1981; Malech et al., 1977), which results in microtubule growth and vesicle delivery into this region (Nabi, 1999). Cdc42 activity at the leading edge is maintained by a positive feedback loop. The Cdc42 target PAK1 itself mediates Cdc42 activation downstream of G protein-coupled receptor induction by chemoattractants. Cdc42 activity defines the localization of Rac activity via PAK, thereby mediating actin polymerization and protrusion at the leading edge (Cau and Hall, 2005). Rac activity is similar to Cdc42 activity maintained by several positive feedback mechanisms, including PI3Ks, microtubules, and integrins, respectively.

The localized activity of Cdc42 and Rac at the leading edge alone is not sufficient for effective mesenchymal cell migration. Rho activity defining the tail of the cell and mediating cell contractility is also required. At the trailing edge active Rho stabilizes microtubules, thereby promoting focal adhesion turnover. Active Rac inhibits Rho activity and vice versa, thereby allowing a distinctive mutually exclusive distribution of these two Rho GTPase family members in the polarized cell.

Adhesion to the substrate is yet another pivotal aspect of cell migration dependent on Rho GTPases. The formation of focal complexes at the leading edge is mediated by Rac and Cdc42. The assembly of larger integrin clusters, the so called focal adhesions, involves Rho and myosin induced contractility.

The effect of Rho inhibition on cell migration depends on the cell type, probably reflecting different basal levels of stress fibers and focal adhesions. Cultured fibroblasts have high amounts of stress fibers and focal adhesions; the strong cell-matrix attachment impairs migration (Cox and Huttenlocher, 1998). Inhibition of Rho in such highly adherent cells can have opposing effects as it leads to decreased cell-substrate adhesion but also negatively effects cell body contraction. In less adherent cells that lack focal adhesions such as macrophages, Rho inhibition does not alter adhesion but impairs cell body contractility, thereby decreasing cell migration (Allen et al., 1998).

4.3 Different modes of cell migration

Dependent on the cell type and the tissue environment cells can migrate individually (through amoeboid or mesenchymal modes) or collectively. Collective cell migration plays important roles in tissue formation, maintenance and remodeling. It also occurs during cancer progression (Alexander et al., 2008; Friedl et al., 1998). Single-cell migration is essential for immune cell trafficking (Lammermann and Sixt, 2009) and cancer metastasis to distant sites (Thiery, 2002). Many different parameters of the extracellular matrix such as dimension, density, stiffness, and orientation as well as structural and molecular characteristics of the cell such as cell-cell adhesion, cell-matrix adhesion, cytoskeletal polarity and stiffness, and pericellular proteolysis determine migration mode and efficiency (Friedl and Wolf, 2010).

Motile rounded or ellipsoid cells that lack focal adhesions and stress fibers show amoeboid migration (Friedl et al., 2001; Lammermann and Sixt, 2009). In mesenchymal migration highly adherent single cells form strong focalized cell-matrix interactions (Kaye et al., 1971).

Some cells migrate as chains in a tail-to head fashion. The cells of such a chain follow a common track and transiently form and resolve cell-cell contacts. This migration mode is called chain migration or cell streaming (Davis and Trinkaus, 1981).

In collective migration, a group of cells maintains its cell-cell adhesions during motility. The cortical actin of neighboring cells can assemble across cell-cell junctions, allowing for the formation of a large, multicellular contractile body with non-migratory cells inside the group. In collective migration cells with different characteristics can join together thereby increasing efficiency of for instance tumor invasion and survival. Cells can move collectively as multicellular tubes, strands, irregular shaped masses, or sheets (Farooqui and Fenteany, 2005; Friedl et al., 1995).

These different modes of migration yield in varying migration speeds; leukocytes show fast amoeboid movement, as compared to the much slower migration of fibroblasts into a wound or the even slower collective movement during organ formation (Friedl et al., 1998).

Each cell type preferentially uses a particular migration mode. But cells have the capacity to react to modulation of either the environment or the cell properties by adaptation reactions that change the migration mode. Upon down-regulation of cell-cell junctions in a multicellular system such as an epithelial sheet, single cells can detach and disseminate individually. Epithelial-to-mesenchymal transition has been implicated in carcinoma progression and several developmental processes: single

spindle-shaped cells detach from a multicellular unit to invade the surrounding tissue in a fribroblastoid manner (Thiery, 2002).

The conversion between mesenchymal and amoeboid migration, the so called mesenchymal-to-amoeboid transition (MAT), is not only characterized by a change in cell morphology from spindle-shaped fribroblastoid cells towards roundish cells but is also accompanied by an altered integrin distribution and microfilament organization. MAT is regulated by the balance between Rac and Rho signaling (Sahai and Marshall, 2003). In most cells, Rac-mediated protrusion of the leading edge is counteracted by Rho/ROCK signaling, which controls actomyosin mediated retraction of the trailing edge. High Rac activity therefore results in mesenchymal migration of elongated cells, whereas active Rho in the presence of little or no Rac activity leads to amoeboid migration of rounded cells (Sahai and Marshall, 2003). Active Rac inhibits Rho/ROCK signaling and vice versa (Sahai and Marshall, 2003; Sanz-Moreno et al., 2008). Inhibition of Rho signaling and matrix proteases as well as weakening of cell-matrix adhesion can cause a mesenchymal-amoeboid transition.

Collective-to-amoeboid transitions (Hegerfeldt et al., 2002) as well as individual-to-collective transitions (Thiery, 2002) have also been observed.

5 The actin-MAL-SRF signaling pathway

5.1 Signal transduction

In multicellular organisms, signal transduction processes are required for coordinating the behavior of individual cells to support the function of the organism as a whole. These molecular circuits detect, amplify, and integrate diverse external signals to generate responses such as gene expression, helping the cell to adapt to the altered conditions. Signal transduction pathways follow a broadly similar course involving membrane receptors that transfer information from the environment to the cell's interior. The information is then relayed by changes in either the concentration of small molecules (the so called second messengers) or the posttranslational modification of proteins (e.g. phosphorylation). Furthermore signal transduction molecules often translocate to other compartments of the cell or elicit novel protein-protein interactions. If the cell responds to the external cue by altered gene expression, transcription factors are usually involved downstream of the signaling cascade. These proteins bind to specific DNA sequences in promoter regions adjacent to genes thereby controlling gene transcription.

5.2 Serum response factor

The ubiquitously expressed transcription factor serum response factor (SRF) regulates expression of numerous muscle specific (reviewed in (Pipes et al., 2006)) and “immediate early” genes, whose expression is activated by mitogenic stimuli independently of new protein synthesis (Philippar et al., 2004; Sun et al., 2006a). These growth factor-regulated genes encode signaling molecules, transcription factors, and many cytoskeletal components (Miano, 2003; Pipes et al., 2006; Posern and Treisman, 2006). SRF is a 67 kDa protein conserved in all higher eukaryotes and the founding

member of the MADS (MCM1, Agamous, Deficiens, SRF) family of transcription factors. Members of this protein family are characterized by a conserved 56 amino acid MADS-box mediating DNA binding, homodimerization and protein-protein interactions. The DNA binding site for SRF is a 10 base pair motif with the consensus sequence $CC(A/T)_6GG$, termed the CArG box. Its dyadic symmetry reflects binding of SRF as a homodimer (Shore and Sharrocks, 1995). On its own, SRF is a weak transcription factor. It generally interacts with co-activators to mediate gene transcription. Expression of two subgroups of SRF target genes is differentially controlled by co-factors that are regulated by separate signaling pathways (Posern and Treisman, 2006) and bind to SRF in a mutually exclusive manner (Miralles et al., 2003; Murai and Treisman, 2002). Members of the ternary complex factor (TCF) family of Ets domain proteins (Elk-1, Sap-1 and Net) are activated by mitogen activated protein (MAP) kinase phosphorylation (Buchwalter et al., 2004; Treisman, 1994). Regulation of myocardin-related transcription factors (MRTFs comprising MRTF-A or MAL and MRTF-B) on the other hand is controlled trough actin dynamics (Miralles et al., 2003) and is tightly linked to cytoskeletal-based events such as cell shape, polarity and motility (Posern and Treisman, 2006). In contrast, SRF activation by the MRTF family member myocardin is constitutive (Wang et al., 2001).

5.3 The Rho-actin signaling pathway

Activation of Rho family GTPases RhoA, Rac1, and Cdc42 leads to changes in actin dynamics that are sensed by MRTFs (Busche et al., 2008; Du et al., 2004; Kuwahara et al., 2005; Posern et al., 2002; Sotiropoulos et al., 1999); (reviewed in (Olson and Nordheim, 2010). The Rho GTPase effectors LIM kinase and Diaphanous cooperate to stabilize F-actin, which leads to a depletion of the G-actin pool in the cell (Geneste et al., 2002). Upon RhoA activation, mDia mediates de novo F-actin assembly via VASP activation, whereas Rho kinase (ROCK) promotes F-actin stabilization by phosphorylating LIM kinase, which in turn phosphorylates and thereby inactivates the actin depolymerizing factor cofilin (Copeland and Treisman, 2002; Geneste et al., 2002; Sotiropoulos et al., 1999). MAL-dependent SRF activity responds to the G-actin level in the cell rather than the ratio of G-actin to F-actin as shown by actin binding drugs and ectopic expression of wild type actin and non-polymerizable mutant actins (Posern et al., 2002; Sotiropoulos et al., 1999). Upon G-actin depletion MAL, which harbors G-actin-binding RPEL motifs at the N terminus, is released from an inhibitory complex with monomeric actin and strongly activates SRF-controlled transcription (Lockman et al., 2004; Miralles et al., 2003; Posern et al., 2004; Vartiainen et al., 2007). Figure III-3 depicts the Rho-actin-MAL-SRF signaling pathway.

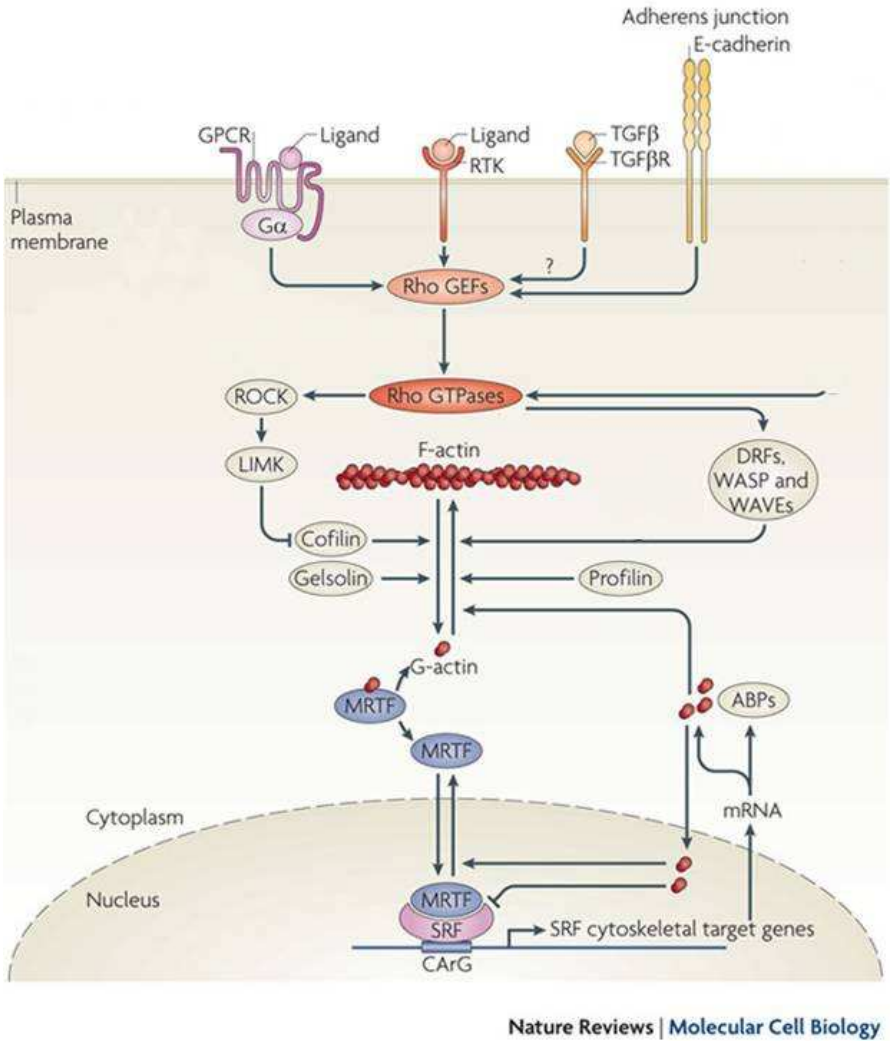

Figure III-3 The Rho-actin-MAL signaling pathway (modified from (Olson and Nordheim, 2010)). Cytoskeletal actin microfilament dynamics are affected by the activation of receptor Tyr kinases (RTKs), G protein-coupled receptors (GPCRs; with α-subunits of Gα12/13, Gαq/11 or Gαi/0), transforming growth factor-β receptors (TGFβRs), and E-cadherins at adherens junctions. This triggers expression of a subset of SRF target genes, namely cytoskeletal genes, actin itself and many genes that modulate actin dynamics, such as gelsolin and vinculin. LIMK, LIM domain kinase. GEFs, Rho guanine nucleotide exchange factors. ROCKs, Rho-associated kinases. DRFs, Diaphanous-related formins. WASP, Wiskott–Aldrich syndrome protein. WAVEs, WASP-family verprolin homologues. ARP2/3, actin-related protein 2/3. ABPs, actin-binding proteins.

FRAP (Fluorescence Recovery After Photobleaching) analysis showed that the actin-MAL complex is constantly shuttling between the nucleus and the cytoplasm. High export rates ensure that MAL is mainly cytoplasmic. However upon serum stimulation, export decreases, allowing for MAL nuclear accumulation. The G-actin depletion leads to the release of MAL from the inhibitory actin-MAL complex mediating SRF activation (Vartiainen et al., 2007).

5.4 Actin binding drugs

MAL-dependent SRF activity is responsive to actin binding drugs that change actin dynamics. The cyclic peptide jasplakinolide isolated from the marine sponge *Jaspis johnstoni* binds to and stabilizes F-actin, thereby inducing SRF activity. The G-actin binding drug cytochalasin D isolated from *Zygusporium mansonii* depolymerizes actin by capping F-actin barbed ends and stimulating hydrolysis

of the actin bound ATP (Sampath and Pollard, 1991). It apparently also binds to monomeric actin (Posern et al., 2002). The G-actin binding drug latrunculin B isolated from *Latrunculia magnificans* blocks actin polymerization. Although both drugs depolymerize F-actin thereby increasing the endogenous G-actin pool in the cell, they have opposing effects on MAL-SRF signaling. Treatment with cytochalasin D activates transcription by releasing MAL from G-actin, whilst latrunculin B rather stabilises the G-actin-MAL complex and inhibits gene expression (Gineitis and Treisman, 2001; Miralles et al., 2003; Mouilleron et al., 2008; Posern et al., 2004; Posern et al., 2002; Vartiainen et al., 2007).

5.5 Identifying SRF target genes on a genome wide scale

In recent years various genome-wide approaches to identify SRF targets were performed. The earlier approaches mainly identified SRF target genes irrespectively of the upstream signalling pathway. These approaches included microarray expression analysis upon transient overexpression of constitutively active SRF-VP16 in Srf-deficient ES cells (Philippar et al., 2004) and platelet-derived growth factor stimulation of glioblastoma cells (Tullai et al., 2004), SRF chromatin IP in pluripotent P19 cells undergoing Cardiac Cell Differentiation after Me_2SO treatment (Zhang et al., 2005), and a computational approach to screen for functional SRF-binding sites on a genome-wide scale (Sun et al., 2006a).

In order to identify serum-inducible MAL target genes Selvaraj and Prywes performed microarray analyses of NIH 3T3 fibroblasts expressing dominant negative MAL upon serum stimulation (Selvaraj and Prywes, 2004). As serum treatment triggers not only Rho-actin but also MAPK signalling, the effects of dominant negative MAL could be masked by MAPK targets. Furthermore binding of dominant negative MAL to SRF could titrate TCF factors, making it difficult to distinguish between targets of these two pathways. Indeed some of the SRF targets that were claimed to be dependent on MAPK signalling are actually Rho-actin pathway targets and vice versa. The same group very recently analyzed NIH 3T3 cell expressing shRNA targeting both MRTF-A and MRTF-B for serum induction by a microarray approach (Lee et al., 2010), circumventing the risk of TCF factor titration by dominant negative MAL. Nevertheless the use of serum as SRF inducer requires to artificially set a cut-off value for the reduction of target activation by the MRTF knockdown that defines a target gene as being MRTF dependent. Serum mediated Pai-1 activation was for instance reduced less than 25% percent by MRTF depletion defining Pai-1 as MRTF independent, conversely to our own findings.

We recently searched for genes directly regulated by G-actin in NIH 3T3 fibroblasts (Descot et al., 2009) benefitting from the differential effect of the G-actin binding drugs cytochalasin D and latrunculin B on SRF activity. As both drugs depolymerise F-actin, genes affected by cytoskeleton rearrangements rather than by the G-actin switch should not score as differentially expressed. Indeed, several known MAL/SRF targets were identified as G-actin regulated genes in this microarray screen, validating the approach (Descot et al., 2009).

Recent transcriptome analysis of Mrtf depleted B16 and MDA-MB-231 cells (Medjkane et al., 2009) identified only a relatively small number of MRTF target genes, but included several known targets such as Ctgf, Cyr61, Fos, Myh9, and Myl9. The small number of identified target genes and the weak fold changes of expression might be explained by principle differences of MAL-SRF signalling in epithelial and fibroblast cells. Microarray analysis on cortical samples of Mrtf-A/B double knockout mice identified few known MAL-SRF targets (Mokalled et al., 2010), but again, target expression in this cell system might be entirely differently effected by MAL-SRF signalling. Furthermore, it is important to note, that whole transcriptome analyses of transgenic mouse tissue or stable cell lines has some shortcomings in comparison to a short-term drug treatment in the presence of a translation inhibitor as performed by our group, as they usually identify not only direct targets but also numerous indirectly regulated genes. On the other hand, stable ectopic gene expression or depletion can prompt cells to establish compensation mechanisms, which counteract and thereby mask the differential regulation of direct target genes.

5.6 Cellular functions of MAL-SRF mediated transcription

5.6.1 Srf and MAL knockout phenotypes

Functions of the transcription factor SRF were first studied in Drosophila. Mutations in the Drosophila Srf homolog DSRF impaired formation and maintenance of the trachea due to cytoskeletal defects (Affolter et al., 1994; Guillemin et al., 1996).

SRF plays pivotal roles in murine embryogenesis. Srf knockout mice die at the onset of gastrulation lacking any detectable mesoderm (Arsenian et al., 1998). This developmental defect is caused by a non-cell-autonomous defect in differentiation towards mesoderm (Weinhold et al., 2000). Srf(-/-) embryonic stem cells show impaired cell spreading, adhesion, and migration due to defective formation of actin stress fibers and focal adhesion plaques. The defective cytoskeleton organization was reflected by a downregulation and/or mislocalization of FA kinase, β1-integrin, talin, zyxin, vinculin, and actin (Schratt et al., 2002). Similarly, Srf(-/-) hematopoetic stem cells displayed decreased expression of the integrin network and impaired adherence. The mice with SRF-depleted hematopoietic cells show increased numbers of circulating stem and progenitor cells, most likely due to their reduced retention in the bone marrow caused by the adhesion defect (Ragu et al., 2010).

Cytoskeletal abnormalities and adhesion defects are also the primary cause for the edema and skin blistering phenotype of keratinocyte-specific Srf depletion (Koegel et al., 2009).

Other tissue specific Srf knockouts have demonstrated diverse functions of Srf for skeletal muscle growth, maturation, and regeneration (Charvet et al., 2006; Li et al., 2005b), liver regeneration (Latasa et al., 2007), cardiogenesis (Miano et al., 2004; Niu et al., 2005), cardiac function and integrity (Parlakian et al., 2005), as well as neurite outgrowth, axon guidance, neuron migration (Alberti et al., 2005; Knoll et al., 2006), oligodendrocyte differentiation (Stritt et al., 2009), and memory formation (Etkin et al., 2006; Ramanan et al., 2005; Smith-Hicks et al., 2010).

Mice lacking only one member of the MRTF family of transcriptional coactivators fail to phenocopy Srf loss-of-function mutations suggesting either functional redundancy between MRTF members or the involvement of other coactivators in the observed in vivo SRF functions. Mrtf-A knockout mice have defects in mammary myoepithelial cell differentiation preventing female mice from nursing their offspring (Li et al., 2006; Sun et al., 2006b). Depletion of Mrtf-B results in defects in smooth muscle cell differentiation and cardiovascular development causing death of knockout mice during mid-gestation (Li et al., 2005a; Oh et al., 2005). Remarkably, MRTF-B restoration only in cardiac neural crest was sufficient to rescue this pathology.

However, brain-specific deletion of Mrtf-A in Mrtf-B(-/-) mice causes lethality between P16 and P21 and results in several morphological abnormalities that phenocopy the brain-specific Srf knockout (Mokalled et al., 2010).

5.6.2 Cell differentiation, proliferation and apoptosis

MRTFs were shown to regulate the switch from proliferation to differentiation of smooth muscle cells by competing with TCFs (Wang et al., 2004). Furthermore, MAL is a regulator of megakaryocyte differentiation (Cheng et al., 2009).

Whole transcriptome analysis identified a number of antiproliferative G-actin regulated genes (Descot et al., 2009). MAL exhibited strong antoproliferative effects via transcriptional regulation of Mig6/Errfi-1, a negative regulator of the EGFR family, demonstrating antagonistic functions of MAL on EGF signalling (Descot et al., 2009). Preliminary results of our group show that overexpression of MAL in NIH 3T3 fibroblasts not only strongly represses proliferation but also induces apoptosis. Furthermore MAL was demonstrated to control the expression of at least two known pro-apoptotic genes Bok and Noxa ((Descot, 2010), doctoral dissertation).

5.6.3 Cytoskeletal organization, adhesion and migration

MAL and SRF play crucial roles in cytoskeletal organization, actin turnover and adhesion (Miano et al., 2007; Schratt et al., 2002). Previous studies identified numerous cytoskeleton-associated SRF targets with potential roles in cell migration such as β-actin, vinculin, zyxin, or gelsolin (Miralles et al., 2003; Philippar et al., 2004; Schratt et al., 2002). These findings were confirmed by our screen for G-actin regulated genes, which identified numerous actin microfilament effectors such as the known SRF targets Acta1, Acta2, Actg2, Myl9, Vcl, and Tagln (Descot et al., 2009). This demonstrates the existence of an actin-MRTF-SRF circuit: rearrangements of the cytoskeletal actin microfilament are communicated to the nucleus by MRTFs, which in turn leads to the expression of structural components of the microfilament and regulators of actin dynamics (reviewed in (Olson and Nordheim, 2010). This circuit can be assumed to play pivotal roles in motile cell functions. Furthermore, in addition to the known cytoskeleton-associated SRF targets a number of novel G-actin regulated targets with potential roles in cell motility were shown to be upregulated by cytochalasin D treatment and downregulated by simultaneous treatment with latrunculin B.

MAL/MRTF-A and MRTF-B have recently been implicated in tumor cell invasion and metastasis (Medjkane et al., 2009). Knockdown of both MAL and Mrtf-B strongly reduced adhesion, spreading, invasion and motility of highly invasive breast cancer and melanoma cells (Medjkane et al., 2009).
In line with this, suppression of the MAL inhibitor SCAI in breast cancer cells promoted matrigel invasion via β1-integrin upregulation (Brandt et al., 2009).
Finally, MAL depletion in megakaryocyte progenitors was reported to reduce filopodia, lamellipodia and stress fiber formation and to impair megakaryocyte migration through matrigel (Gilles et al., 2009).
Epithelial-mesenchymal transition (EMT) is a cellular process that can be observed during experimental pancreas adenocarcinoma progression: cell-cell contacts dissociate and epithelial cells transform into unpolarized motile ones (Perl et al., 1998). We have recently demonstrated that MAL is activated during EMT and calcium-dependent disassembly of E-cadherins through activation of Rac and dissociation of MAL from G-actin (Busche et al., 2008; Busche et al., 2010). Furthermore, MRTFs were reported to be required for TGF-β induced EMT, acting by transcriptional upregulation of slug and actin remodeling (Morita et al., 2007).

5.6.4 Regulation of tumor suppressor genes

Myocardin was proposed to act as a tumor suppressor (Milyavsky et al., 2007). Overexpression of myocardin in human sarcoma cells induced the expression of differentiation markers and blocked malignant growth (Milyavsky et al., 2007). In line with this, myocardin was recently shown to activate expression of the cyclin-dependent kinase inhibitor p21 (Kimura et al., 2010). Interestingly, several novel G-actin regulated target genes such as Mig6, Cyr61, Epithelial protein lost in neoplasm α (Eplin-α), and Fhl1 were reported to have tumor suppressor functions.

IV. Aims of this thesis

Cell motility is a fundamental process for tissue formation, maintenance and regeneration. Misregulated cell migration can lead to pathological conditions such as cancer. Numerous SRF target genes, whose expression is induced upon recruitment of the MRTF transcriptional coactivators, play important roles in cytoskeletal activities. They encode structural components of the microfilament cytoskeleton and focal adhesions, regulators of actin dynamics and proteins involved in actomyosin contractility. Moreover, MRTF coactivators were recently implied in epithelial-mesenchymal transition (EMT), a cellular process which has been implicated in carcinoma progression and is characterized by the dissociation of cell-cell contacts and the transformation of epithelial cells into unpolarized motile cells. Our lab recently demonstrated that MAL transcriptional activity is induced during EMT and calcium-dependent disassembly of epithelial junctions. Together, these findings pointed towards a role of MAL-SRF signaling in cell motility.

The aim of this study was to investigate the regulation of MAL during EMT and to analyze the effect of MAL and a set of newly identified target genes on cell migration. Firstly, I wanted to study whether in addition to the induction of MAL transcriptional activity, MAL expression is also altered upon EMT induction and whether regulation by miRNAs is involved. Secondly, I investigated the migratory behavior upon ectopic expression of active, dominant negative and knockdown constructs of MAL. For this I initially chose non-invasive NIH 3T3 fibroblasts as the characterization of the MAL-SRF signaling pathway and the identification of novel G-actin regulated genes was performed in this cell system. Ectopic MAL expression in epithelial cells was performed to determine whether the migratory effect of MAL in different non-invasive cells was similar or whether MAL plays distinct roles in mesenchymal and epithelial cell migration. Potential new target genes mediating the migratory functions of MAL were to be characterized with regard to their precise transcriptional regulation by the actin-MAL signaling pathway. Functionally, the effect of target depletion in mesenchymal and epithelial cells was tested. Finally, in order to demonstrate that the migratory effects of MAL are directly mediated by its cytoskeletal targets I analyzed whether target depletion counteracts the MAL knockdown, rescuing the migratory phenotype.

V. Materials and Methods

1 Materials

1.1 Laboratory hardware

Table V-1: List of laboratory hardware used in this study.

ABI 3730 sequencer	Applied Biosystems (Darmstadt)
Agarose gel electrophoresis system	Workshop MPI of Biochemistry (Martinsried)
Balances	Kern 572, Kern & Sohn GmbH (Balingen) Mettler AE200, Mettler Toledo (Giessen)
Celloshaker	Renner GmbH (Dannstadt)
Centrifuges	Eppendorf 5417R (Wesseling-Berzdorf) Eppendorf 5417C (Wesseling-Berzdorf) Beckman Coulter Allegra 6KR (Krefeld) Sorvall Evolution RC, Thermo Fisher Scientific (Schwerte) Hettich Universal 16 (Kirchlengern)
Dark Reader®	Clare Chemical Research (Dolores, USA)
Duomax 1030	Heidolph (Kelheim)
Polyacrylamide gel electrophoresis casting stand, casting frames, glass plates, combs & sample loading guide	Bio-Rad (Munich)
Polyacrylamide gel electrophoresis system Vertical Elpho "B"	Workshop MPI of Biochemistry (Martinsried)
Elisareader	BioTek (Winooski, USA)
Fireboy plus	Integra Biosciences (Fernwald)
GelAir dryer	Bio-Rad (Munich)
Gel chambers	Workshop MPI for Biochemistry (Martinsried)
Genepulser XCell™	BioRad (Munich)
Icemachine	Ziegra (Isernhagen)
IDA gel documentation system	Raytest (Straubenhardt)
Immersol™ 518F	Zeiss (Jena)
Incubator HERAcell® 150i	Thermo Fisher Scientific (Schwerte)
LightCycler instrument	Roche (Penzberg) Applied Biosystems (Darmstadt)
Microplate Luminometer LB 96V	EG and G Berthold (Schwerzenbach, CH)
Microscopes	Zeiss Axio Observer.A1 (Jena) Zeiss Axiovert 200M (Jena)
Microwave	Siemens (Munich)
Power supply	Consort EV 261 (Turnhout, B)
Spectrophotometer	BioPhotometer, Eppendorf (Wesseling-Berzdorf) Nanodrop ND 1000, Thermo Fisher Scientific (Schwerte)
Sterile Lamin Air Hood	Lamin Air Model 1.2, Heraeus (Hanau) Lamin Air HA 2472 GS, Holten (Allerod, DK)
Thermocycler	Biometra T3000 (Göttingen)
Thermomixer Comfort	Eppendorf (Wesseling-Berzdorf)
Vortex Genie 2™	Bender and Hobein (Zurich, CH)
Western Blotting Chamber Mini Trans-Blot Cell	Bio-Rad (Munich)

1.2 Chemicals and reagents

Table V-2: List of chemicals and reagents used in this study

Acetic acid	Merck (Darmstadt)
Acrylamide	Serva (Heidelberg)
Agar (Difco™)	BD Biosciences (Heidelberg)
Agarose	Eurogentec (Cologne)
Ampicillin	Roche (Mannheim)
Ammonium peroxodisulfate (APS)	Bio-Rad (Munich)
BES	Merck (Darmstadt)
Bisacrylamide	Serva (Heidelberg)
Bovine serum albumin (BSA)	Sigma-Aldrich (Steinheim)
Bradford reagent	Sigma-Aldrich (Steinheim)
Bromphenol blue	Sigma-Aldrich (Steinheim)
Calcium chloride	Merck (Darmstadt)
Chloramphenicol	Merck (Darmstadt)
Chlorophenolred-β-D-galactopyranosid	Merck (Darmstadt)
Chloroquine	Sigma-Aldrich (Steinheim)
CompleteTM Protease Inhibitor Cocktail Tablets	Roche (Mannheim)
Coomassie Brilliant Blue G-250	Serva (Heidelberg)
Crystal violet	Sigma (Taufkirchen)
Cycloheximide	Sigma (Taufkirchen)
Cytochalasin D	Calbiochem (Beeston, UK)
Deoxyribonucleotides (dG/A/T/CTP)	Roche (Mannheim)
4',6-diamidino-2-phenylindole hydrochloride (DAPI)	Roche (Mannheim)
Dimethyl sulfoxide (DMSO)	Riedel-de Haën (Seelze)
Dithiothreitol (DTT)	Sigma-Aldrich (Steinheim)
EDTA (Ethylenediaminetetraacetic acid)	Merck (Darmstadt)
EGF, human recombinant	Peprotech (Hamburg)
Ethanol p.a.	Riedel-de Haën (Seelze)
Ethidium bromide	Roth (Karlsruhe)
EGF	Sigma (Taufkirchen)
Gelatine from cold water fish skin	Sigma-Aldrich (Steinheim)
G418	Invitrogen (Karsruhe)
4-(2-Hydroxyethyl)piperazine-1-ethanesulfonic acid (HEPES)	Biomol (Hamburg)
Hoechst 33258	Sigma-Aldrich (Steinheim)
Glycerol 100%	Merck (Darmstadt)
HCl (Hydrochloric acid),37%	Merck (Darmstadt)
Isopropanol	Fluka (Buchs, Switzerland)
Isopropyl thiogalactopyranoside (IPTG)	Fermentas (St. Leon-Rot)
Jasplakinolide	Calbiochem (Beeston, UK)
Kanamycin	Invitrogen (Karlsruhe)
KCl	Merck (Darmstadt)
KH2PO4	Merck (Darmstadt)
K2HPO4, 3H2O	Merck (Darmstadt)
Latrunculin B	Calbiochem (Beeston, UK)
Lipofectamine® (GibCo)	Invitrogen (Karsruhe)
Lipofectamine 2000® (GibCo)	Invitrogen (Karsruhe)
Lipofectamine® RNAiMAX	Invitrogen (Karlsruhe)
beta-Mercaptoethanol	Merck (Darmstadt)
Methanol	Fisher Scientific (Schwerte)
$MgCl_2$	Merck (Darmstadt)
Mitomycin C	Sigma (Taufkirchen)
NaCl	Merck (Darmstadt)
Na2HPO4	Merck (Darmstadt)

NaOH	Merck (Darmstadt)
N,N,N',N'-Tetramethylethylenediamine (TEMED)	Serva (Heidelberg)
Non fat milk powder	Töpfer Naturaflor (Kempten)
PBS	Merck (Darmstadt)
Phenol	Roth (Karlsruhe)
PMSF (Phenylmethylsulfonylfluoride)	Sigma (Taufkirchen)
Polybren (Hexadimethrinbromide)	Sigma (Taufkirchen)
Ponceau S	Sigma (Taufkirchen)
Puromycin Dichloride	Calbiochem (Beeston, UK)
Sodium azide	Serva (Heidelberg)
Sodium dodecyl sulfate (SDS)	Serva (Heidelberg)
Sodium fluoride	Sigma-Aldrich (Steinheim)
Sodium orthovanadate	Sigma-Aldrich (Steinheim)
TGF-β1, human recombinant	Peprotech (Hamburg)
Tris	Sigma-Aldrich (Steinheim)
Triton X-100	Roth (Karlsruhe)
Tryptone (Bacto™)	BD Biosciences (Heidelberg)
Tween 20	Sigma-Aldrich (Steinheim)
UO126	Calbiochem (Beeston, UK)
Yeast extract (Bacto™)	BD Biosciences (Heidelberg)

1.3 Kits and miscellaneous materials

Table V-3: List of kits and miscellaneous materials used in this study.

Cell culture inserts, 8 µm pore size	BD Falcon (Heidelberg)
Cellophane	Pütz Folien (Taunusstein)
Chromatography paper 3MM	Whatman (Dassel)
CryoTube™ vials	Nunc (Roskilde, DK)
Dual-Glo™ Luciferase Assay Kit	Promega (Madison, USA)
ECL Plus™	GE Healthcare (Munich)
Electroporation cuvettes (0.2 cm)	Bio-Rad (Munich)
Electroporation cuvettes (0.4 cm)	Bio-Rad (Munich)
LightCycler® FastStart DNA Master SYBR Green I mix	Roche (Penzberg)
Micro BCA Protein Assay Kit	Pierce (Sankt Augustin)
Migration Culture Inserts	ibidi GmbH (Martinsried)
Parafilm	Pechiney Plastic Packaging (Chicago, USA)
Plastic ware	BD Falcon (Heidelberg) Eppendorf (Wesseling-Berzdorf) Greiner bio-one (Frickenhausen) Nunc (Roskilde, DK)
Precision Plus ProteinTM Dual Color Standard	Bio-Rad (Munich)
PVDF membrane Immobilion-P Transfer 0.45 µm	Millipore (Billerica, USA)
QIAquick Gel Extraction Kit	Qiagen (Hilden)
QIAquick PCR Purification Kit	Qiagen (Hilden)
QIAGEN Plasmid Mini Kit	Qiagen (Hilden)
QIAGEN Plasmid Maxi Kit	Qiagen (Hilden)
QIAGEN RNeasy Mini Kit	Qiagen (Hilden)
Reverse-iT-1st-Strand-Synthesis-Kit	ABgene (Hamburg)
SmartLadder DNA marker	Eurogentec (Cologne)
Sterile filter 0.22 µm, cellulose acetate	Thermo Fisher Scientific (Schwerte)
Sterile filter 0.45 µm, cellulose acetate	Thermo Fisher Scientific (Schwerte)
Vivaspin 20 column	Satorius Stedim Biotech (Aubagne Cedex, F)
Western Lightning™ Chemoluminescence Reagent Plus	PerkinElmer (Boston, USA)

1.4 Media, buffers and solutions

1.4.1 Bacterial media

Luria-Bertani (LB) broth (1% Tryptone, 0.5% yeast extract, 1% NaCl. pH 7.2) was used for cultivation of *Escherichia* (*E.*) *coli* bacteria. If required, 100 µg/ml Ampecillin, 70 µg/ml Kanamycin or 34 µg/ml Chloramphenicol were added to the medium after autoclavation. For plate preparation, 1.5% Agar was added.
SOC broth (2% Tryptone, 0.5% yeast extract, 10 mM NaCl, 2.5 mM KCl, 10 mM $MgCl_2$, 10 mM $MgSO_4$, 20 mM glucose) was added to electrocompetent bacteria directly after electrotransformation.

1.4.2 Cell culture media

All cell lines used in this study were cultured in Dulbecco's Modified Eagle Medium (DMEM) supplemented with 4.5 mg/ml glucose (high glucose) and L-glutamine (all obtained from Invitrogen (Gibco™)), and were further supplemented with 4 – 10% fetal calf serum (FCS), 2 mM L-glutamine, 1 mM sodium-pyruvate, 50 U/ml penicillin and 50 µg/ml streptomycin (all obtained from Invitrogen (Gibco™)). Freeze medium consisted of growth medium with 20% FCS and 10% DMSO.
For calcium switch experiments (2.3.3) the culture medium was exchanged to medium with reduced calcium. Calcium reduced medium was prepared as normal medium, but with calcium free DMEM and FCS and supplemented with the desired amount of calcium (usually 0.02 mM). Calcium free DMEM was obtained from Invitrogen (Gibco™), calcium free FCS was generated using Chelex® 100 chelating ion exchange resin according to Brennan and colleagues (Brennan et al., 1975).

1.4.3 Buffers and solutions

All buffers and solutions were prepared in Millipore water if not indicated otherwise.

Table V-4: List of buffers and solutions used in this study.

Acrylamide solution (30/0.8)	30% (w/v) acrylamide 0.8% (w/v) bisacrylamide
Annealing buffer	20 mM Tris-HCl pH 7.5 100 mM NaCl 2 mM EDTA
5x Bradford solution	20% (v/v) Bradford solution (prepared according to manufacturer's instructions) 10% (v/v) H2O 20% (v/v) ethanol 50% (v/v) H3PO4 after mixing filter through paper filter
Coomassie R-250 solution	0.25% (w/v) Serva Blue R 45% (v/v) methanol 10% (v/v) acetic acid
Coomassie destaining solution	10% (v/v) methanol 10% (v/v) acetic acid
DNA loading buffer (6x)	30 % (v/v) glycerol 0.3% (w/v) bromophenole blue 0.3% (w/v) xylene cyanol 100 mM EDTA
Crystal violet staining solution	0.5% (w/v) crystal violet 25% (v/v) methanol
Laemmli buffer (3x)	10 mM EDTA 3% (w/v) SDS 20% (v/v) glycerol 0.05% (w/v) bromophenole blue 3% (v/v) β-Mercaptoethanol

Milk	5% (w/v) milk powder in TBST buffer
PBS	137.0 mM NaCl 27.0 mM KCl 80.9 mM Na2HPO4 1.5 mM KH2PO4 pH 7.4
Radioimmunoprecipitation Assay (RIPA) buffer	20 mM Tris HCl pH 8.0 150 mM NaCl 5% (v/v) glycerol 10 mM MgCl2 1% (v/v) Triton X-100 0.5% (w/v) desoxycholat 0.1% (v/v) SDS
Strip buffer	65 mM Tris/HCl, pH 6.8 2% (w/v) SDS 100 mM β-Mercaptoethanol
TAE buffer	40 mM Tris/Acetate pH 8.0 1 mM EDTA
TBE buffer	90 mM Tris/HCl, pH 8.0 90 mM boric acid 3 mM EDTA
TBS buffer	20 mM Tris/HCl, pH 7.5 150 mM NaCl
TBST buffer	20 mM Tris/HCl, pH 7.5 150 mM NaCl 0.1% (v/v) Triton X-100
TE (10/0.1)	10 mM Tris/HCl, pH 8.0 0.1 mM EDTA
Tris-Glycin-SDS buffer	25 mM Tris/HCl, pH 8.8 192 mM glycine 1% (w/v) SDS
Western blotting buffer	25 mM Tris 190 mM glycine 20% (v/v) methanol 0.1% (v/v) SDS (for proteins > 80 kDa)

1.5 Oligonucleotides

All DNA oligonucleotides were purchased from Eurofins MWG Operon (Ebersberg) as HPSF purified oligos. siRNAs were purchased from Applied Biosystems / Ambion (Darmstadt) in standard purity. 2'O-Me antisense-RNAs directed against endogenous miRNAs were synthesized at the Core Facility MPI of Biochemistry (Martinsried).

1.5.1 Sequencing primers

The oligonucleotides listed in Table V-5 served as primers used in the sequencing reaction (2.2.7) together with the indicated plasmids (Table V-12).

Table V-5: Oligonucleotides used for sequencing reactions.

Plasmid	Primer name	Sequence (5’ → 3’)
pGL3	GLprimer2	CTTTATGTTTTTGGCGTCTTCCA
pGL3	RVprimer4	GACGATAGTCATGCCCCGCG
pSUPER.retro.puro	pRSpuroF1241	GGAAGCCTTGGCTTTTG
pSUPER.retro.puro	pRSpuroR1532	TCGCTATGTGTTCTGGGAAA
pMirRNL	pMRSeqF	ACACAGATCCAATGAAAATAAAAG
pMirRNL	pMRSeqR	TACCGGAAAACTCGACGCAAGAAA

1.5.2 Cloning primers

The primers listed in Table V-6 were used to amplify genomic regions like promoter sequences or 3'UTR regions in a PCR reaction (2.2.11) to subsequently clone it into a vector of interest, thereby engineering the constructs listed in Table V-12. Besides the sequence complementary to the desired genomic region, they harbor an endonuclease restriction site flanked by four randomly chosen bases to allow endonuclease binding.

Table V-6: Cloning primers used in this study

Primer name	Sequence (5' → 3'; restriction sequence underlined)	cloned region
Eα-1802_F	CTGAGAGCTCTGAGTTCCAGGGGAGAGAGAGA	Eplin-α-prom-1802
Eα-1802_R	CATGCTCGAGGGGGCAGACTTTCAGGGTTCTA	Eplin-α-prom-1802
Eα-1115_F	CTGAGAGCTCATGTCTCCCTGCTGTGTGGT	Eplin-α-prom-1115
Eα-1115_R	CATGCTCGAGAGGCTTGTCCGTCACTTCA	Eplin-α-prom-1115
Eα-915_F	CTGAGAGCTCGGCGTTTGGTTTGATTAGGA	Eplin-α-prom-915
Eα-915_R	CATGCTCGAGAGGCTTGTCCGTCACTTCA	Eplin-α-prom-915
Eβ-1249_F	CTGAGAGCTCATGTCCTGTGCCCTTTGC	Eplin-β-prom-1249
Eβ-1249_R	CATGCTCGAGGCCTCCTGCTCCTGCTAC	Eplin-β-prom-1249
Pai-1-2011_F	CTGAGGTACCGGCTGGTTGCCTTGGTATCTGT	PAI-prom-1
Pai-1-2011_R	CATGAGATCTGCTGTGGTTGGCTGTGTGCT	PAI-prom-1
Pai-1-1548_F	CTGAGGTACCGAGGGAGGTGGGTCAGAAT	PAI-prom-2
Pai-1-1548_R	CATGAGATCTGATTGGCTCTTGTTGGCTGT	PAI-prom-2
Pai-1-567_F	CTGAGGTACCGGAGGGAGGAGGAAAGGACT	PAI-prom-3
Pai-1-567_R	CATGAGATCTGATTGGCTCTTGTTGGCTGT	PAI-prom-3
UTRh_F	CTGAACTAGTCTGGCTCAAGACGGGGTGGGGAAGG	hum Mal3'UTR
UTRh_R	CATGGTTTAAACTTTTTCCTGTGTTTTTGTGTTTATTT	hum Mal3'UTR
UTRr_F	CTGAACTAGTCTGACTCAGACATGGGCTAGGGAAGG	rat Mal3'UTR
UTRr_R	CATGGTTTAAACCTGGCAAGTCAGTGTTTTTGTTTTAT	rat Mal3'UTR
UTRm_F	CTGAACTAGTCAGACATGCGCTAGGGAAGGGTCAGA	mouse Mal3'UTR
UTRm_R	CATGGTTTAAACTGGCAAGTCAGTGTTTTTGTTTTATT	mouse Mal3'UTR

1.5.3 Small hairpin RNA encoding oligonucleotides

Sense strand (ss) and antisense strand (as) oligonucleotides were annealed and cloned in the small hairpin RNA (shRNA) expression vector pSUPER.retro.puro (Table V-11). Upon retroviral infection of mammalian cells the encoded shRNA is expressed.

MRTF shRNAss:
gatccccgCATGGAGCTGGTGGAGAAGAAttcaagagatTCTTCTCCACCAGCTCCATGtttttggaaa

MRTF shRNAas:
agcttttccaaaaaCATGGAGCTGGTGGAGAAGAAtctcttgaaTTCTTCTCCACCAGCTCCATGcggg

1.5.4 Quantitative real-time RT-PCR primer

The oligonucleotides listed in Table V-7 were used as primers in quantitative RT-PCR (1.5.4) for expression analysis

Table V-7: Oligonucleotides used as primers in quantitative RT-PCR analysis.

Gene	species	direction	Sequence (5' → 3')
alas1	human	forward	CTGCAAAGATCTGACCCCTC
alas1	human	reverse	CCTCATCCACGAAGGTGATT
Eplin-α	mouse	forward	GCTGTTTCCGATGCTCCTAC
Eplin-α	mouse	reverse	CTCATTGTCGCTCTTGCTTG
Eplin-β	mouse	forward	CAAGAACAAGTCATCCGCAAT
Eplin-β	mouse	reverse	AGGAGGGTAGTCCGCTGTGT

Ereg	mouse	forward	CAGTTATCAGCACAACCGTGA
Ereg	mouse	reverse	ACATCGCAGACCAGTGTAGC
Fam126b	mouse	forward	TTCTCAGCCACTCTTGGTG
Fam126b	mouse	reverse	ATTCTCGGCACTGTTGGAG
Fhl1	mouse	forward	GCCAGTGAGACCTTTGTGTC
Fhl1	mouse	reverse	CCAGACGGTGCCCTTGTA
hprt	mouse	forward	TCAGTCAACGGGGGACATAAA
hprt	mouse	reverse	GGGGCTGTACTGCTTAACCAG
ITGA5	mouse	forward	CCTGGACCAAGACGGCTACAATGA
ITGA5	mouse	reverse	GGCTGCAACTGCGCTCCTCTG
MAL	mouse	forward	CCAGGACCGAGGACTATTTG
MAL	mouse	reverse	CGAAGGAGGAACTGTCTGCTA
MAL	rat	forward	CCAGGACCGAGGACTATTTG
MAL	rat	reverse	CAAAGGAGGAACTGTCTGCTA
MAL	human	forward	TGTGTCTCAACTTCCGATGG
MAL	human	reverse	CCCTGTCCTGCTTCTGGTC
Mrtf-B	mouse	forward	CCCACCCCAGCAGTTTGTTGTT
Mrtf-B	mouse	reverse	TGCTGGCTGTCACTGGTTTCATC
Mrtf-B	rat	forward	AAGCAAAGCCATCCCAAGAATCCA
Mrtf-B	rat	reverse	CCTCCTCGCCGGCACACCTG
Mrtf-B	human	forward	AATTATAGGCGTTGGGAAGGAG
Mrtf-B	human	reverse	CTGCGCTGGAGTGTTTGTAGTCA
Nexn	mouse	forward	ACCGAGTCCGCATCAGAG
Nexn	mouse	reverse	GGTTGGTTCTCCCATTTCCT
Pkp2	mouse	forward	TGATGAGAAGGTGTGATGGTC
Pkp2	mouse	reverse	GCTGGTAGGAGAGGTTATGAAG
Plaur	mouse	forward	GGCTTAGATGTGCTGGGAAA
Plaur	mouse	reverse	AGAGAGGCAATGAGGCTGAG
Serpine1(Pai-1)	mouse	forward	CAACAAGAGCCAATCACAAGG
Serpine1(Pai-1)	mouse	reverse	ATAGCCAGCACCGAGGACA

1.5.5 Primers for quantification of chromatin immunoprecipitations

Table V-8: Oligonucleotides used as primers for quantitative RT-PCR following ChIP

Promoter	direction	Sequence (5’ → 3’)
Eplin-α	forward	AAAAAGTCTCTCCCTTCCAATGT
Eplin-α	reverse	GTTACTGCCCTGCCACAAG
Pkp2	forward	TTGTTGACATACCAGAAAGGATGAGG
Pkp2	reverse	TTCCAGGGAAACCATACACCGTAAGA
Srf	forward	GGCTCCACTGTTCCTTTAAGGAGTTGGC
Srf	reverse	CCCCCATATAAAGAGATACAATGTTTCCTTT
Gapdh	forward	CCCTGCTTATCCAGTCCTAGCTCAAGG
Gapdh	reverse	CTCGGGAAGCAGCATTCAGGTCTCTGG

1.5.6 2'-O-methyl antisense-RNAs targeting endogenous miRNAs

Table V-9: 2’-O-methyl antisense-RNAs used for knockdown of endogenous miRNAs *1 nt mismatch. After deprotection 5’ carries an OH-group; all 2’ OH groups are modified to 2’-OMe groups

Oligo name	targeted miRNA	Sequence (5’ → 3’)
as_mir_1	hsa/mmu/rno*-mir-1	r(AUACAUACUUCUUUACAUUCCA)dT
as_mir_206	hsa/mmu/rno-mir206	r(CCACACACUUCCUUACAUUCCA)dT
as_mir_219	hsa/mmu/rno-mir219-1-5p	r(AGAAUUGCGUUUGGACAAUCA)dT
as_mir_124	hsa/ mmu/rno-mir124	r(GGCAUUCACCGCGUGCCUUA)dT

1.5.7 siRNAs

Table V-10: siRNAs used in this study.

siRNA name	sense (5' → 3')	antisense (5' → 3')
GL2 ctrl siRNA	CGUACGCGGAAUACUUCGAtt	UCGAAGUAUUCCGCGUACGtt
Itga5 siRNA #1	GUGUGAGGCUGUAUAUGAAtt	UUCAUAUACAGCCUCACACtg
Itga5 siRNA#2	CAGGAGGACUGAGCACUAAtt	UUAGUGCUCAGUCCUCCUGgg
Pkp2 siRNA#1	GCUAUACGUUGAACAAUUUtt	AAAUUGUUCAACGUAUAGCtt
Pkp2 siRNA#2	GGAUGUAUUUGUCCUUAAUtt	AUUAAGGACAAAUACAUCCtt
Fhl1 siRNA#1	ACGAGCCAAUAUCAAAGUAtt	UACUUUGAUAUUGGCUCGUtt
Fhl1 siRNA#2	GGAGGUGCAUUAUAAGAAUtt	AUUCUUAUAAUGCACCUCCtt

1.6 Plasmids

1.6.1 Basic vectors

Table V-11: List of basic vectors used in this study

Plasmid	Description	Source
pEF plink	mammalian expression vector, pUC12 backbone, EF1α enhancer/promoter, Ampr	G. Posern (Sotiropoulos et al., 1999)
pEF-Flag plink	like pEF plink, with 5' Flag-tag	G. Posern (Sotiropoulos et al., 1999)
pGL3-Basic	reporter vector encoding for firefly (*Photinus pyralis*) luciferase, Ampr	Promega (Madison, USA)
pRL-TK	internal control reporter for pGL3, herpes simplex virus thymidine kinase promoter driving *Renilla reniformis* luciferase expression, Ampr	Promega (Madison, USA)
pSUPER.retro	shRNA expression vector for retroviral infection, Ampr, Puror, H1 promoter	OligoEngine (Seattle, USA)
pMIR-RNL-CMV	reporter plasmid containing a CMV promoter driven firefly luciferase gene and a MCS for miRNA binding site insertion behind it. Harbors a SV40 promoter driven renilla luciferase gene for normalization	G. Meister
pMIR-RNL-TK	reporter plasmid containing a TK promoter driven firefly luciferase gene and a MCS for miRNA binding site insertion behind it. Harbors a SV40 promoter driven renilla luciferase gene for normalization	G. Meister
pLPCX	expression vector for retroviral infection, Ampr, Puror, CMV promoter	Clontech (Mountain View, USA)

1.6.2 Modified vectors

The vectors were generated by cloning or shRNA encoding oligonucleotide insertion into the basic vectors Table V-11. Vectors are mammalian expression vectors, if not indicated otherwise.

Table V-12: List of modified vectors used in this study.

Plasmid	Description	Source/Reference
p3D.A-Luc	three c-fos derived SRF binding sites in front of a *Xenopus laevis* type 5 actin TATA-Box in pGL3-basic driving the expression of the firefly luciferase gene	G. Posern (Geneste et al., 2002)
pEF-Flag-G15S	cDNA of β-actin, hyperpolymerizable by replacement of G15 with S, Flag-tagged	G. Posern (Posern et al., 2004)

pEF-Flag-R62D	cDNA of β-actin, nonpolymerizable by replacement of R62 with D, Flag-tagged	G. Posern (Posern et al., 2002)
pEF-Flag-wt-actin	cDNA of wild type β-actin, Flag-tagged	G. Posern (Posern et al., 2002)
pGL3_E-α-1802	Eplin-α promoter starting at -1802 inserted in pGL3 luciferase reporter	this study
pGL3_E-α-1115	Eplin-α promoter starting at -1115 inserted in pGL3 luciferase reporter	this study
pGL3_E-α-915	Eplin-α promoter starting at -915 inserted in pGL3 luciferase reporter	this study
pGL3_E-β-1249	Eplin-β promoter starting at -1249 inserted in pGL3 luciferase reporter	this study
pGL3_Pai-2011	Pai-1 promoter starting at –2011 inserted in pGL3 luciferase reporter	this study
pGL3_Pai-1548	Pai-1 promoter starting at –1548 inserted in pGL3 luciferase reporter	this study
pGL3_Pai-567	Pai-1 promoter starting at –567 inserted in pGL3 luciferase reporter	this study
pLPCX_eGFP	pLPCX containing eGFP cDNA	G. Posern
pLPCX_MAL (fl.)	pLPCX containing cDNA of murine full length MAL, HA-tagged	(Descot et al., 2009)
pLPCX_MAL (met)	pLPCX containing cDNA of murine MAL with N-terminal truncation (amino acids 1-91)	G. Posern (Descot et al., 2009)
pLPCX_MAL ΔN	pLPCX containing cDNA of murine MAL with constitutive active N-terminal truncation (amino acids 1 – 171), HA-tagged	G. Posern (Descot et al., 2009)
pLPCX_MAL ΔNΔB	pLPCX containing cDNA of murine MAL with dominant negative truncation (amino acids 1 – 171 and 316 – 341), HA-tagged	G. Posern (Descot et al., 2009)
pLPCX_MAL ΔNΔC	pLPCX containing cDNA of murine MAL with dominant negative truncation (amino acids 1 – 171 and 563 – 1021), HA-tagged	G. Posern (Descot et al., 2009)
pMIR-C-MAL_hum	pMIR-RNL-CMV reporter plasmid harboring the human MAL 3'UTR behind the firefly luciferase gene	this study
pMIR-C-MAL_rno	pMIR-RNL-CMV reporter plasmid harboring the rat MAL 3'UTR behind the firefly luciferase gene	this study
pMIR-C-MAL_mmu	pMIR-RNL-CMV reporter plasmid harboring the mouse MAL 3'UTR behind the firefly luciferase gene	this study
pMIR-T-MAL_hum	pMIR-RNL-TK reporter plasmid harboring the human MAL 3'UTR behind the firefly luciferase gene	this study
pMIR-T-MAL_rno	pMIR-RNL-TK reporter plasmid harboring the rat MAL 3'UTR behind the firefly luciferase gene	this study
pMIR-T-MAL_mmu	pMIR-RNL-TK reporter plasmid harboring the mouse MAL 3'UTR behind the firefly luciferase gene	this study
pSR_MAL_sh	pSUPER.retro.puro encoding shRNA against MAL and MRTF-B	this study

1.7 Antibodies

1.7.1 Primary antibodies

The antibodies listed in Table V-13 were used as primary antibodies in immunoblot or chromatin immunoprecipitations (ChIP) analysis.

Table V-13: Primary antibodies used in immunoblot or ChIP analysis.

Antibody	Description	Source
FHL1	rabbit, polyclonal	ProteinTech Group Inc.; (Chicago, USA)
HA p.c. (3F10)	monoclonal, recognizes the BAbCO influenza hemagglutinin epitope, peroxidase conjugated	BAbCO (Richmond, USA)
MRTF	rabbit, polyclonal, recognizes MRTF-A and MRTF-B	homemade (Posern Lab)
PAI-1	sheep, polyclonal	American Diagnostica Inc.; (Greenwitch, USA)
PKP2	mouse, polyclonal	Acris Antibodies GmbH; (Hiddenhausen, Germany)
SRF	rabbit, polyclonal, recognizes epitope within the C-terminus of human SRF	Santa Cruz (G-20); (Heidelberg, Germany)
αTubulin	mouse, monoclonal	ProteinTech Group Inc., (Chicago, USA)

1.7.2 Secondary antibodies

For immunoblot analysis the horseradish peroxidase (HRP) conjugated anti-IgG antibodies listed in Table V-14 were used in this study.

Table V-14: Secondary horseradish peroxidase (HRP) conjugated anti-IgG antibodies used in immunoblot analysis

Antibody	Source
Polyclonal goat anti-sheep-HRP	Jackson ImmunoResearch (Newmarket, GB)
Polyclonal goat anti-mouse-HRP	DakoCytomation (Glostrup, DK)
Polyclonal swine anti-rabbit-HRP	DakoCytomation (Glostrup, DK)

1.8 Enzymes

Table V-15: Enzymes used in this study

Enzyme	Source
Calf Intestinal Alkaline Phosphatase	NEB (Frankfurt/Main)
DNAse I, RNAse free	Roche (Mannheim)
Phusion™ High-Fidelity DNA-Polymerase	Finnzymes (Espoo, FI)
Restriction Endonucleases	NEB (Frankfurt/Main) MBI (Fermentas, St. Leon-Rot)
T4-DNA Ligase	NEB (Frankfurt/Main)
Trypsine (Gibco)	Invitrogen (Karsruhe)

1.9 Cells

1.9.1 Bacterial strains

The *Escherichia coli* (*E.coli*) DH5α strain was used for transformations to amplify plasmids.

Table V-16: Bacterial strain used in this study.

Genotype/Properties	Origin
DH5α F- φ80dlacZM15 (lacZYA-argF)U169 deoR recA1 endA1 hsdR17 (r k- m k+) phoA supE44 thi-1 gyrA96 relA1 λ-	Invitrogen (Karlsruhe)

1.9.2 Mammalian cell lines

Table V-17: Mammalian cell lines used in this study. ATCC, American Type Culture Collection.

Cell line	Description	Origin/Reference
EpH4	mouse mammary epithelia cells	H.Beug, IMP (Vienna, A)
EpRas	EpH4 cells stably expressing v-Ha-Ras. Cells undergo EMT upon TGF-β treatment (Oft et al., 1996).	H.Beug, IMP (Vienna, A)
HaCaT	human keratinocytes, undergo EMT upon TGF-β treatment	A.Ullrich, MPI Biochemistry (Martinsried)
MDCK	canine kidney normal epithelial cells	ATCC (Manassas, USA)
MDA-MB-231	human breast carcinoma cell line	A.Ullrich, MPI Biochemistry (Martinsried)
NBT-II	rat bladder carcinoma cell line, cells undergo EMT upon EGF treatment	S. Julien /L. Larue (Paris, France)
NIH 3T3	mouse embryonic fibroblasts	R.Treisman, CRUK (London, GB)
PANC-1	human pancreatic carcinoma cell line, cells undergo EMT upon TGF-β treatment	A.Ullrich, MPI Biochemistry (Martinsried)
PhoenixA	amphotropic retrovirus producing cell line derived from the Human Embryonic Kidney (HEK) 293T cell line	A.Ullrich, MPI Biochemistry (Martinsried) / G.P. Nolan (Stanford, USA)
PhoenixE	ecotropic retrovirus producing cell line derived from the Human Embryonic Kidney (HEK 293T) cell line	A. Ullrich, MPI Biochemistry (Martinsried)./ G.P. Nolan (Stanford, USA)

2 Methods

2.1 Microbiological techniques

2.1.1 Cultivation and maintenance of bacterial strains

E. coli strains were grown at 37°C for 12 – 16 h either in LB medium or on LB agar plates supplemented with antibiotics for selection if required. For short-term storage, E. coli cultures were kept on LB agar plates at 4°C. For long-term storage 1 ml glycerol stocks containing 50% (v/v) glycerol in LB medium were stored in screw-top vials at -80°C.

2.1.2 Generation of competent bacteria

To generate electrocompetent bacteria a single bacterial colony grown on LB agar was inoculated in 5 ml LB medium and incubated shaking (180 rpm) at 37°C over night. The next day the overnight culture was diluted 1:100 in fresh LB medium and incubated as before until the cell density reached the optical density of 0.5 at 600 nm. At this point the bacteria were harvested by centrifugation at 1200 x g and 4°C for 10 minutes. The supernatant was then decanted and the bacteria were resuspended in sterile ice-cold 10% glycerol (same volume than supernatant decanted) and incubated for 20 minutes on ice. Afterwards the bacteria were pelleted as before and resuspended in 10% glycerol ($1/10^{th}$ of the amount of decanted supernatant) followed by another incubation on ice for 20 minutes. Thereafter the bacteria were pelleted again as before and resuspended in 10% glycerol ($1/5^{th}$ of the amount of decanted supernatant). The now electrocompetent bacteria were shock frozen as 40 µl aliquots in liquid nitrogen and stored at -80°C. Newly generated competent bacteria were tested for efficiency by transformation of 0.1 ng of a known plasmid, which should result in $10^8 – 10^9$ colonies per µg DNA.

2.1.3 Transformation of competent bacteria

Competent bacteria were transformed by electroporation. For each electroporation 50 µl of electrocompetent bacteria were thawed on ice and supplemented with 2 µl ligation reaction. The

mixture was then transferred into an ice-cold 0.2 cm electroporation cuvette and electoporated with the Genepulser XCell™ at 2.5 kV, 25 µF and 200 Ohm. Immediately afterwards 1 ml of SOC medium were added, followed by incubation on a rotating wheel at 37°C for 1 h. Thereafter 20 µl and 200 µl of the mixture were plated on LB agar containing antibiotics for selection.

2.2 DNA modification

2.2.1 Genomic DNA isolation

For cloning of target promoters into the luciferase reporter plasmid pGL3 promoter fragments were amplified by PCR from genomic DNA prepared from mouse liver. Livers of C57BL/6 mice were cut into 25 mg pieces, snap frozen in liquid nitrogen and stored at -80°C until DNA preparation. Isolation of genomic DNA was done using the QIAGEN DNeasy Kit according to manufacturer's instructions. Genomic DNA was stored at +4°C.

2.2.2 Plasmid preparation

Plasmids were prepared using the QIAGEN Plasmid Mini Kit for small amount of DNA and the QIAGEN Plasmid Maxi Kit for larger amounts of DNA according to manufacturer's instructions.

2.2.3 Restriction digestion of DNA

For restriction digestion approximately 0.5 – 2 µg of DNA were digested in 20 µl reaction volume with the required endonuclease according to manufacturer's instructions.

2.2.4 Dephosphorylation of DNA 5'-termini

To prevent self-ligation of vector termini generated by restriction digestion, the 5'- termini of digested vectors were dephosphorylated with Calf Intestinal Alkaline Phosphatase for 30 min at 37°C according to manufacturer's protocols. The reaction was stopped by either heat inactivation at 65°C for 5 minutes or direct purification of the DNA via the QIAquick PCR Purification Kit.

2.2.5 Ligation of DNA fragments

Before ligation, the fragments were purified by agarose gel electrophoresis followed by gel extraction with the QIAquick Gel Extraction Kit. Dephosphorylated and QIAquick PCR Purification Kit purified vector fragments were directly used for ligation. 100 ng of vector and the 3 fold molar amount of insert (10 fold for ligation of shRNA coding inserts) were incubated in 1x T4 Ligase buffer with 400 U of T4 DNA Ligase in 20 µl reaction volume at 16°C over night. As control, the ligation was performed as described above without insert DNA. After ligation 2 µl of the reaction were transformed into competent *E. coli DH5α*.

2.2.6 Generation of shRNA expressing plasmids

For annealing 3 µg of the sense and the corresponding antisense shRNA oligonucleotide strand were mixed in a total of 50 µl Annealing buffer. The mixture was heated to 95°C for 10 minutes and then cooled down with 0.01°C per second to 4°C in a Biometra T3000 Thermocycler. The annealed shRNAs harboring a BglII and HindIII overhang were purified via agarose gel electrophoresis and extracted. The insertion into the desired shRNA expression vector was done as described above.

2.2.7 Sequencing

DNA samples were sequenced on an ABI 3730 sequencer by the core facility of the Max Planck Institute of Biochemistry (Martinsried).

2.2.8 Agarose gel electrophoresis

DNA fragments were separated by agarose gel electrophoresis (Sambrook, 1989). Gels were prepared as follows: 0.7 – 2 % (w/v) agarose in TAE or TBE buffer was boiled and afterwards supplemented with 0.01% (v/v) ethidium bromide. After gel polymerization, DNA samples were mixed with the

corresponding amount of DNA loading buffer and loaded on the agarose gel together with the SmartLadder DNA marker for size determination. Electrophoresis was performed in TAE or TBE buffer, according to gel preparation, at 70 – 120 V for 20 – 60 minutes in a agarose gel electrophoresis system Horizontal-Elpho. After electrophoresis, the DNA was visualized at 302 nm and photographs were taken with the IDA gel documentation system. If the separated DNA fragments or plasmids were used for further experiments, they were visualized with a Dark Reader® at 460 nm to avoid the insertion of mutations.

2.2.9 Isolation of DNA fragments and plasmids from agarose gels

The DNA fragments or plasmids of interest were cut out of the gel with a sterile blade and purified using the QIAquick Gel Extraction Kit according to manufacturer's instructions.

2.2.10 Determination of DNA concentration

The concentration of plasmid preparations and purified DNA fragments was measured with a spectrophotometer Nanodrop (Thermo Scientific).

2.2.11 DNA amplification by Polymerase Chain Reaction

DNA fragments of interest were exponentially amplified via Polymerase Chain Reaction (PCR) by a repeating cycle of denaturation, primer annealing and polymerase-driven primer elongation (Mullis and Faloona, 1987). The Phusion™ High-Fidelity DNA Polymerase was used according to manufacturer's instructions with the cloning primers depicted in Table V-6. PCR was carried out in a Biometra T3000 Thermocycler. PCR products were analyzed via agarose gel electrophoreses and positive products were extracted from the gel as described above.

2.2.12 Quantitative real-time PCR

Total RNA was prepared with the QIAGEN RNeasy Mini Kit and the concentration was measured with a spectrophotometer Nanodrop (Thermo Scientific). First-strand cDNA synthesis was done with the Reverse-iT-1st-Strand-Synthesis-Kit (Thermo Scientific) according to manufacturer's instruction using 1 µg of total RNA and 500 ng of anchored oligo-dT primer. For cDNA quantitation, one-fortieth of the RT reaction was mixed with gene-specific primers (0.5 µM) and Fast SYBR Green Master mix (Applied Biosystems; Darmstadt, Germany) to a total volume of 15 µl. The PCR was carried out on a StepOnePlus instrument (Applied Biosystems; Darmstadt, Germany), according to the manufacturer's instructions. Calculations were done using the ΔΔCt method (Winer et al., 1999). Gene-specific primers are listed in Table V-7.

2.2.13 Chromatin Immunoprecipitations

10^7 NIH 3T3 cells for each IP were fixed with 1% formaldehyde for 10 min at RT. Cross-linked cells were sonicated in RIPA buffer (0.1% SDS) using Bandelin HD2200 sonicator with MS72 tip. Sonicated chromatin was incubated with 5 µg of anti-SRF (G-20, Santa Cruz) or home-made anti-MRTF rabbit serum, precoupled to 40 µl of Dynabeads (Invitrogen). Immune complexes were captured overnight at 4°C. DNA-protein complexes were eluted with 0.1 M NaHCO3/0.1% SDS, crosslinks were reversed overnight at 65°C, and DNA was purified using PCR Purification Kit (QIAGEN). Immunoprecipitated DNA was analyzed using the primers listed in Table V-8. Quantitation was done by real-time PCR and is shown as the percentage of input chromatin.

2.3 Methods in mammalian cell culture

2.3.1 General cell culture methods

All cell lines were cultivated in a HERAcell® 150i CO_2 incubator in a 90% air and 10% CO_2 atmosphere at 37°C. All working steps were carried out in sterile Lamin Air hoods. EpRas, EpH4, PANC-1, HaCaT, NBT-II, NIH 3T3, MDCK, PhoenixA and PhoenixE cells were routinely cultured in fresh DMEM containing 4.5 g/L D-glucose and L-glutamine additionally supplemented with 10% FCS (4% FCS for EpRas), 2 mM L-glutamine, 1 mM sodium pyruvate, 50 U/ml penicillin and 50 µg/ml

streptomycin and passaged constantly. MDA-MB-231 cells were cultured in RPMI supplemented with 10% FCS, 2 mM L-glutamine, 50 U/ml penicillin, and 50 µg/ml streptomycin. Prior to seeding cells were counted manually in a Neubauer counter chamber. For long time storage cells were transferred in freeze medium (growth medium with 20% FCS and 10% DMSO) to CryoTube™ vials and after slow freezing stored in liquid nitrogen.

2.3.2 Generation of stable cell lines

To generate stable EpRas cell pools harboring an expression vector of interest, cells were retrovirally infected, split after two days and supplemented with 3 µg/ml puromycin. Surviving cells were then maintained in medium containing 1 mg/ml puromycin.

2.3.3 Calcium withdrawal

In order to induce the dissociation of epithelial junctions, MDCK cells were seeded at high density to form a confluent monolayer. 24 h after seeding the medium was exchanged to normal medium as control or reduced calcium medium containing 0.02 mM calcium.

2.3.4 EMT induction

To induce epithelial-mesenchymal transition, EpRas, PANC-1, and HaCaT cells were treated with recombinant human TGF-β1 (5 ng/ml, 10 ng/ml, and 2.5 ng/ml, respectively). NBT-II cells were treated with recombinant human EGF (10 ng/ml). The medium was changed every second day.

2.3.5 MAL-SRF activation by treatment with serum and actin binding drugs

Serum stimulation of NIH 3T3 was done as previously described (Posern et al., 2002). Briefly cells were seeded at subconfluent density, serum starved for 24 h and stimulated with 15% FCS. Actin binding drugs were added after 24 h serum starvation at the following concentrations:

Latrunculin B: 5 µM
Cytochalasin D: 2 µM
Jaspakinolide: 0.5 µM

2.3.6 Methods to introduce DNA in mammalian cells

2.3.6.1 Calcium phosphate mediated transfection

The PhoenixE and PhoenixA retrovirus producing cell lines were transfected with the calcium phosphate method as described before (Sambrook, 2001). 18-24 hours prior to transfection 6 x 10^6 cells per 10 cm plate were seeded in 10 ml medium without Penicillin/Streptomycin. 1 hour prior to transfection the cell medium was replaced with 9 ml fresh media for each 10 cm plate supplemented with 25 µM chloroquine. For each transfection, 500 µl $CaCl_2$ (250 mM) were mixed with 20 µg of retroviral vector DNA. This mixture was added dropwise while swirling on vortex to 500 µl 2 x BBS solution to initiate precipitation. After 20 minutes of incubation at RT, the mixture was added dropwise into the growth medium while swirling the cells. The transfected cells were incubated at 3% CO_2 and 37°C to enhance precipitate formation. 24 h post transfection the cells were washed once with medium and cultured in fresh medium without penicillin/streptomycin.

2.3.6.2 Lipofection

NIH 3T3 cells were transfected with DNA using Lipofectamine® and with siRNA using RNAiMAX®. EpH4, EpRas, NBT-II, HaCaT, PANC-1, and MDA-MB-231 cells were transfected with Lipofectamine 2000® according to manufacturer's instructions. The individual cell numbers seeded per well of a 12-well plate 18 – 24 h prior to infection, total amount of nucleic acid transfected and amount of transfection reagent (TR) used are summarized in Table V-18.

Table V-18: Cell numbers, the amount of DNA and transfection reagent used for lipofection of mammalian cell lines.

	Cell number	Nucleic acid	TR
NIH 3T3 + DNA	3.5×10^4	0.5 µg	2 µl
NIH 3T3 + siRNA	1.5×10^4	10 pmol	1.5 µl
EpH4	8.5×10^4	1.6 µg	4 µl
EpRas	8.5×10^4	1.6 µg	4 µl
NBT-II	3×10^5	1.6 µg	4 µl
HaCaT	1.28×10^5	1.6 µg	4 µl
PANC-1	5.6×10^4	1.6 µg	4 µl
MDA-MB-231	1.1×10^5	1.6 µg	4 µl

2.3.6.3 Electroporation

For Electroporation 5×10^6 EpRas cells in 200 µl Opti-MEM (Gibco) were mixed with 600 pmol siRNA in a 4 mm cuvette (Bio-Rad). Electroporation was performed with a GenePulser Xcell with CE and PC modules using the time constant protocol (voltage, 250 V; pulse length, 70 ms).

2.3.6.4 Retroviral infection

For retroviral infection of NIH 3T3 cells, 10^7 cells of the retroviral packaging line Phoenix E were transfected on a 15 cm dish with 50 µg of plasmid using calcium phosphate. 24 h post transfection the cells were washed once with medium and then cultured in 16 ml DMEM without Penicillin/Streptomycin at 7% CO_2 and 32°C to enhance virus stability. Following virus production for 24 hours, the virus-containing medium was filtered through a 0.45 µm PVDF membrane (Millipore; Eschborn, Germany), concentrated on a Vivaspin 20 column (MW cutoff, 30,000 Da; PES; Sartorius; Goettingen, Germany), and used to infect 1.53×10^5 NIH 3T3 cells seeded in 6 cm dishes the day before. Infection occurred in the presence of polybrene (8 µg/ml). The procedure was repeated 8 hours later. 24 h post infection the medium of the target cells was replaced by normal growth medium. 48 h post infection the infection efficiency was monitored by EGFP expression of a control infection. For retroviral infection of EpRas and MDA-MB-231 cells, virus containing supernatant of 3×10^7 and 10^7 Phoenix A cells was used to infect 3.36×10^5 and 4.5×10^5 cells per 6 cm dish, respectively.

2.3.7 Luciferase reporter assay

All cell lines were transfected by lipofection as described in 2.3.6.2. For luciferase assays in NIH 3T3 fibroblasts 3.5×10^4 cells per well of a 12-well plate were transfected with 6 - 25 ng of the firefly luciferase reporter plasmid, 50 ng pRL-TK and optionally 200 ng of actin expressing plasmid in a total of 500 ng DNA.
Epithelial cells in one 1 cm dish (12-well plate) were transfected with 800 ng luciferase reporter plasmid and 300 ng pRL-TK in a total of 1600 ng DNA, using Lipofectamine 2000®.
To test the effect of miR inhibition on MAL 3'UTR driven reporter activity, cells in one 1 cm dish (12-well plate) were transfected with 40 ng of the reporter plasmid pMIR-RNL-TK, 160 pmol of synthetic 2'-O-methyl antisense RNA and 1.08 µg of empty plasmid using Lipofectamine 2000®.

Upon transfection, serum starvation, MAL-SRF activation or EMT induction was done as indicated in the figure legends.
The luciferase reporter assay was carried out with reagents from the Dual-Glo™ Luciferase Assay Kit. After the indicated cells were washed twice with ice-cold PBS and lysed by incubation in 100 µl Passive Lysis Buffer (PLB) per 12 well on ice for 10 minutes. Thereafter, cells were scraped of the plate, the lysate collected in an Eppendorf tube and centrifuged at 20000 x g and 4°C for 10 minutes. 20 µl of the supernatant were transferred into a well in a white 96 well microtiter plate and mixed with 45 µl LARII solution. The emitted Firefly luminescence was detected in a Microplate Luminometer LB 96V. After detection 45 µl of Stop & Glow reagent supplemented with Stop & Glow substrate were added to the well to stop the Firefly reaction and start Renilla luminescence emission, which was detected as above. The protein content of each lysate was determined by Bradford assay (V.2.4.2.1).

Firefly luciferase activity was normalized to either protein content or Renilla luciferase activity, as indicated in the figure legend.

2.3.8 Wound closure assay

2 x 10^4 NIH 3T3 cells and 5 x 10^4 MDA-MB-231 in 70 µl medium were seeded into each of two reservoirs of migration inserts (Ibidi). After attachment overnight, medium containing 10 µg/ml mitomycin C was added, the inserts were removed and cells started to migrate into the separating zone of 500 µm between the two cell patches. Micrographs were taken at time point zero and after 12 or 24 hours. After precisely marking the migration front, the free area devoid of migrated cells was measured using the MetaVue software. The area difference of experiment starting and end point was normalized to the control.

2.3.9 Transwell migration assay

Cell were seeded into polycarbonate transwells of 8 µm pore size at a density of 9 x10^4 (EpRas/EpRasXT), 3.75 x 10^4 (NIH 3T3), and 3 x 10^4 (MDA-MB-231) cells in 300 µl medium, respectively. Migration conditions were as follows: EpRas, directed movement: 16 h from serum-free medium containing 0.2% BSA towards 10% FCS; EpRas, undirected movement: 23 h in serum-free medium; EpRas XT, directed movement: 24 h from serum-free medium towards 10% FCS; NIH 3T3, directed movement: 2 h from serum free medium towards 1% FCS; NIH 3T3, undirected movement: 8 h in 10% FCS, MDA-MB-231, directed movement: 15 h from serum-free medium towards 10% FCS. After removing the non-migrating cells and staining the transmigrated cell with crystal violet, micrographs were taken at 5x magnification. Cell migration was deduced by measuring the membrane area covered with migrated cells using the Photoshop CS3 Extended Measurement feature.

2.3.10 Conventional microscopy

Phase contrast and fluorescence micrographs were taken using a Zeiss AxioObserver A1 microscope with MetaVue™ imaging software.

2.4 Protein analytical methods

2.4.1 Lysis of cells with Triton X-100

Prior to lysis the cells were washed with twice cold PBS and then lysed for 3 minutes on ice in RIPA buffer containing protease (Complete™ Protease Inhibitor Cocktail Tablets) and phosphatase (2 mM sodium orthovanadate, 10 mM sodium fluoride) inhibitors. After scraping the lysates were precleared by centrifugation at 20000 x g and 4°C for 10 min.

2.4.2 Determination of protein concentration

2.4.2.1 Bradford protein assay

For protein concentration measurement using the Bradford method the protein lysate of interest was mixed with 100 µl of Bradford solution and incubated for 5 minutes at room temperature. Then the absorption was measured at 595 nm in a BioTek Elisareader. The protein concentration was determined by comparison with a standard curve of BSA (1 - 10 µg).

2.4.2.2 BCA protein assay

Protein concentration measurement using the BCA assay was carried out with the Micro BCA Protein Assay Kit according to manufacturer's instructions. The absorption was measured at 570 nm in a BioTek Elisareader. The protein concentration was determined by comparison with a standard curve of BSA.

2.4.3 SDS-Polyacrylamide Gel Electrophoresis

SDS-Polyacrylamide Gel Electrophoresis (SDS-PAGE) was carried out as described before (Laemmli, 1970). Samples were run on two-layered gels consisting of stacking and separating gel in a polyacrylamide gel electrophoresis system Vertical Elpho "B". The stacking gel contained 5% acrylamide solution in 127 mM Tris-HCl pH 6.8, 0.1% (w/v) SDS, 4.5% (v/v) glycerol and 0.1% (w/v) APS. The separating gel contained 7 – 15% acrylamide solution (according to protein size) in 377 mM Tris-HCl pH 8.8, 0.1% (w/v) SDS and 0.1% (w/v) APS. To start the polymerization reaction 0.1% (v/v) TEMED was added. Before SDS-PAGE all samples were mixed with the appropriate amount of Laemmli buffer and boiled at 95 °C for 2 minutes to remove all secondary, tertiary and quaternary structures. The Precision Plus Protein™ Dual Color Standard was used as molecular weight standard. SDS-PAGE was performed at 80 – 140 V. After proteins separated by electrophoresis were transferred to a PVDF membrane for western blotting (2.4.4).

2.4.4 Western blotting

For Western blotting electrophoretically separated proteins were transferred to a PVDF membrane in a Mini Trans-Blot Cell. Blotting was performed in Tris-Glycin-SDS buffer at 100 V for 1 h.

2.4.5 Immunoblot detection

PVDF membranes were incubated in 5% milk powder in TBST for at least 1 h at room temperature or 4°C over night in order to block unspecific binding sites. Afterwards the milk was removed and the membrane was incubated with the first antibody (see Table V-13) in milk for at least 1 h at room temperature or 4°C over night, afterwards washed five times in TBST buffer for 3 minutes and incubated with the secondary horseradish peroxidase conjugated anti-IgG antibody (see Table V-14) diluted in milk for 1 – 2 h. Thereafter the membrane was washed again five times in TBST buffer for 3 minutes incubated in Western Lightning™ Chemoluminescence Reagent Plus for 1 minute. Luminescent bands were detected on Hyperfilm.

2.4.6 Stripping

To reincubate with a different set of antibodies the membrane was stripped to remove all bound antibodies. Therefore, the membrane was washed two times for 10 minutes in TBST buffer and then incubated at 50°C in a closed container in stripping buffer. Afterwards the membrane was washed three more times in TBST buffer for 5 minutes before it was ready to be incubated with another antibody

VI. Results

1 Identification of novel G-actin regulated genes with putative roles in cell motility

In order to screen for G-actin regulated genes our group previously performed whole genome microarrays. The expression profile of untreated NIH 3T3 cells was compared to that of cells treated with the G-actin binding drug cytochalasin D that induces actin-MAL-SRF signaling by dissociating the inhibitory G-actin-MAL complex. Furthermore, the expression profile of NIH 3T3 cells simultaneously treated with cytochalasin D and the G-actin binding drug latrunculin B was analyzed. As described above, latrunculin B stabilizes the inhibitory G-actin-MAL complex and can prevent cytochalasin D mediated pathway induction. As both drugs depolymerise F-actin, genes affected by cytoskeleton rearrangements rather than by the G-actin switch should not score as differentially expressed. In order to minimize indirect gene activation the translation inhibitor cycloheximide was added to all samples. We obtained a list of about 200 genes differentially expressed under these conditions (GEO dataset GSE17105) (Descot et al., 2009). The statistical significance of all the selected genes scoring as G-actin regulated targets was high, indicated by the q-value which represents the lowest false discovery rate at which the specific probe sets are detected as differentially expressed. More than 30% of the genes that scored as G-actin regulated in our analysis are known SRF targets, validating the approach. For example, several actin genes, the early marker of smooth muscle cell development Sm22, the connective tissue growth factor (Ctgf), myosin light chain 9 (Myl9), the extracellular matrix-associated signaling molecule Cyr61, the fibronectin receptor integrin α 5 (Itga5), the four-and-a-half-LIM-only proteins Fhl1 and Fhl2, the cytoskeleton associated adaptor vinculin or Srf itself were found.

Previous studies identified numerous cytoskeleton-associated SRF targets with potential roles in cell migration such as β-actin, vinculin, zyxin, or gelsolin (Miralles et al., 2003; Philippar et al., 2004; Schratt et al., 2002). These findings were confirmed by our screen for G-actin regulated genes. The above mentioned known SRF targets Acta1, Acta2, Actg2, Myl9, Vcl, and Tagln that were also identified in our screen are all actin microfilament effectors consistent with the important role of MAL and SRF in cytoskeletal organisation and actin turnover (Miano et al., 2007; Schratt et al., 2002); (reviewed in (Olson and Nordheim, 2010)) and pointing to an involvement of MAL in cell adhesion and motility.

Besides these known cytoskeleton-associated SRF targets a number of novel G-actin regulated targets with potential roles in cell motility were shown to be upregulated by cytochalasin D treatment and downregulated by simultaneous treatment with latrunculin B. I particularly focused on those novel targets in my further investigation.

Table VI-1 lists the differentially regulated probe sets and their corresponding q-values of the selected novel G-actin regulated targets with potential migratory roles. They included all four independent

probe sets of the Eplin gene, two independent probe sets for Plakophilin 2 and Integrin α5, and one probe set for the Four-and-a-half LIM domain protein Fhl1.

Table VI-1: Differential regulation of novel target genes implicated in cell motility by G-actin signaling. Genes potentially relevant for migration are differentially regulated by actin binding drugs. G-actin regulated genes were induced by treatment with cytochalasin D (*CD*, 2 μM, 90 min). This induction was repressed by latrunculin B (*LB*, 5 μM). All samples were pretreated with cycloheximide (3 μg/ml) to enrich for primary targets. Results shown are from Affymetrix microarray analysis of NIH 3T3 fibroblasts as previously described (Descot et al., 2009). The q-value is the lowest false discovery rate at which the differentially expressed probe set is called significant.

			Induction		
Probe Set ID	Gene ID	Name	CD	CD+LB	q-value
1429183_at	Pkp2	Plakophilin-2	12.85	2.08	0
1449799_s_at	Pkp2	Plakophilin-2	7.07	1.64	1.14
1423267_s_at	Itga5	Integrin α5	4.09	1.55	0
1423268_at	Itga5	Integrin α5	5.39	1.84	3.75
1417872_at	Fhl1	Fhl1	4.14	1.06	0
1419149_at	Serpine1	Pai-1	3.98	2.13	3.01
1425654_a_at	Lima1	Eplin	5.21	2.43	1.14
1435727_s_at	Lima1	Eplin	3.98	2.38	1.99
1450629_at	Lima1	Eplin	3.71	2.08	0
1422499_at	Lima1	Eplin	3.51	2.17	0
1435649_at	Nexn	Nelin	3.82	1.48	3.01
1419431_at	Ereg	Epiregulin	3.33	1.55	1.99
1456320_at	Fam126b	Fam126b	7.79	3.09	0
1452521_a_at	Plaur	uPAR	5.39	1.66	3.01

Firstly, I validated the microarray results for these genes using quantitative RT-PCR. The novel tumor suppressor Epithelial Protein Lost in Neoplasm referred to as Eplin is expressed in two isoforms. The longer Eplin-β contains all eleven exons, whereas the shorter Eplin-α is transcribed from a different promoter and comprises exons four to eleven. To determine the regulated Eplin isoform, I performed quantititative RT-PCR with primers that detect both Eplin-α and Eplin-β and additionally with Eplin-β specific primers.

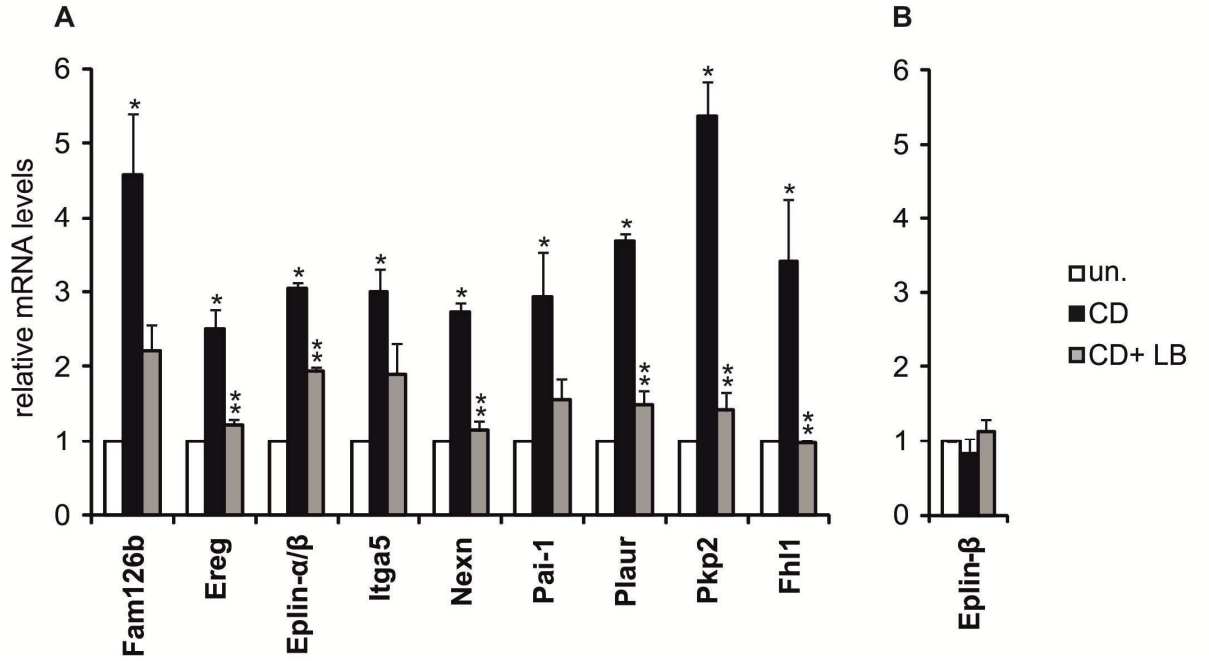

Figure VI-1: Validation of novel target genes implicated in cell motility for differential regulation by G-actin signaling. Newly identified target genes implicated in cell motility are responsive to actin binding drugs. NIH 3T3 cells were treated with cytochalasin D (2 µM) for 90 min, or with cytochalasin following 15 min pretreatment with latrunculin B (5 µM). All samples were pretreated with cycloheximide (3 µg/ml) as before. Shown is the average induction of mRNA after normalization to Hprt. Error bars indicate SEM (n=3) (A), and half range for Eplin-β (B), respectively. Asterisk, significant activation compared to untreated; double asterisk, significant repression compared to CD-induced ($p<0.05$, unpaired student's t-test).

All mRNAs were upregulated by cytochalasin D treatment which was prevented by the simultaneous treatment with latrunculin B (Figure VI-1). In most cases the results of the quantitative RT-PCR and the microarray analysis were well comparable. In the case of Ereg and Fhl1 the mRNA induction assessed by quantitative RT-PCR correlated especially well with the microarray data, Fam126b, Lima1 and Pkp2 showed slightly higher induction in the microarray analysis compared to the quantitative RT-PCR.

Quantititative RT-PCR with Eplin-β specific primers revealed, that this longer isoform is in contrast to the shorter Eplin-α not affected by treatment with the G-actin binding drugs cytochalasin D and latrunculin B. This suggests that transcription from the Eplin-α promoter, but not from the Eplin-β promoter, is regulated by G-actin. Note that the Eplin-α/β RT-PCR primers detect both the α- and the β-isoform. Similarly the probe sets of the Lima1 gene are bound by both isoforms. The actual induction of the Eplin-α transcription by cytochalasin D is therefore higher as assessed by both microarray analysis and quantitative RT-PCR. The difference between actual and assessed fold induction depends on the relative levels of Eplin-α and Eplin-β mRNA in the cell.

The microarray data and the verification by quantitative RT-PCR showed that all the selected genes with potential roles in cell motility respond to changes in the G-actin level, which is known to control MAL/MRTF activity. As the translation inhibitor cycloheximide was added in the microarray analysis and the quantititative RT-PCR experiments it can be concluded that the selected genes are novel targets directly regulated by G-actin.

2 Characterization of novel G-actin regulated genes as direct MAL targets

2.1 Assessment of a potential involvement of MAPK signaling in target regulation

To exclude the involvement of MAPK signaling in the observed expression induction I repeated quantitative RT-PCR upon cytochalasin D treatment for most of the selected targets in the presence of the MEK inhibitor UO126. As expected cytochalasin D mediated target induction was essentially unaffected by inhibition of MAPK signaling (Figure VI-2).

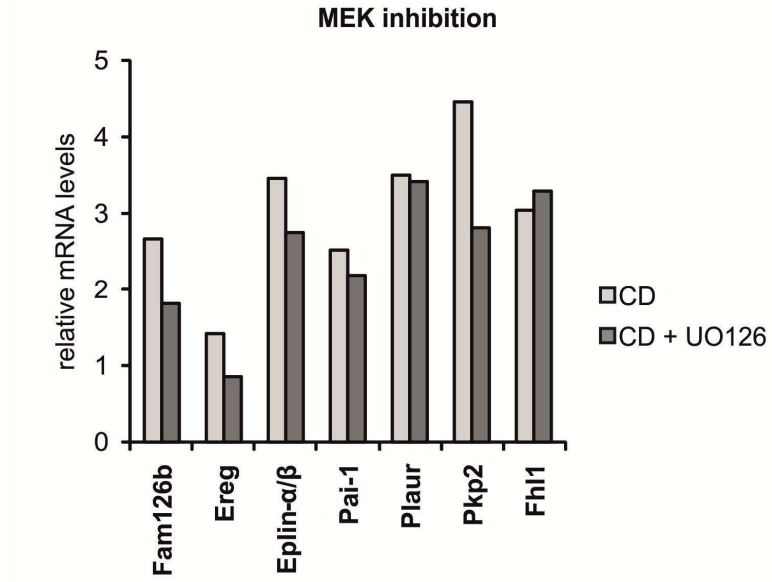

Figure VI-2: MAPK signaling does not contribute to the induction of novel G-actin target genes by cytochalasin D. Effect of pretreatment with UO126 (10 µM, 30 min) on the average induction target mRNA by CD (2µM, 90 min) as assessed by qRT-PCR. Shown are the relative target mRNA levels after normalization to Hprt.

The possible regulation of the novel G-actin targets Fhl1, Pkp2, Pai-1 and Eplin-α by MAL/SRF signaling was then examined in more detail.

Eplin-α was described earlier as an immediate-early serum responsive gene (Chen et al., 2000). Indeed quantititative RT-PCR in the presence of cycloheximide showed that Eplin-α was induced by serum independent from protein translation (Figure VI-3). As serum stimulation also activates the MAPK pathway in parallel to Rho-actin signaling it is important to note, that the serum mediated induction of Eplin-α was significantly inhibited by latrunculin B pretreatment, which has no effect on MAPK signaling towards SRF-dependent transcription (Figure VI-3).

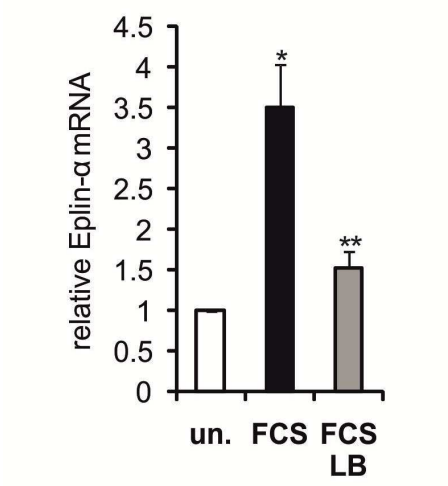

Figure VI-3: Serum mediated induction of Eplin-α is dependent on actin-MAL signaling. Effect of 15 min pretreatment with latrunculin B (5 µM) on the average induction of Eplin-a mRNA by serum (FCS, 15%, 90 min) as assessed by quantitative RT-PCR. Shown is the average induction of mRNA after normalization to Hprt. Error bars indicate SEM of at least three independent experiments. Asterisk, significant activation; double asterisk, significant repression ($p < 0.01$, unpaired student's t-test).

To examine a potential involvement of MAPK signaling in Eplin-α regulation more precisely, cells were pretreated with the MEK inhibitor UO126 before addition of serum and cytochalasin D, respectively. A slight but significant reduction of serum-mediated Eplin-α upregulation was observed, whereas cytochalasin D induction was essentially unaffected (Figure VI-4). This suggests that MAPK-TCF signals might contribute to Eplin-α regulation, whilst actin-MAL signaling is strictly required.

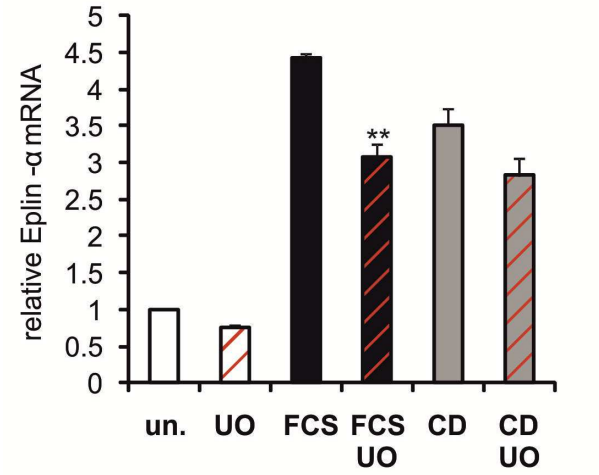

Figure VI-4: MAPK signaling might contribute to the serum mediated induction of Eplin-α. Effect of pretreatment with UO126 (10 µM, 30 min) on the average induction of Eplin-α mRNA by serum (FCS, 15%, 90 min) and CD (2µM, 90 min) as assessed by quantitative RT-PCR. Shown is the average induction of mRNA after normalization to Hprt. Error bars indicate SEM of at least three independent experiments. Double asterisk, significant repression ($p < 0.01$, unpaired student's t-test).

2.2 Target promoter characterization

Next I searched for the MAL-SRF responsive element in the Eplin-α promoter. I tested whether a 2 kb long fragment of the murine Eplin-α promoter containing the transcription start site mediated

differential expression of a heterologous luciferase reporter. Indeed this 2 kb promoter fragment was induced by serum and cytochalasin D in NIH 3T3 cells, and its induction was reduced significantly by latrunculin B pretreatment as assessed by luciferase assays (Figure VI-5).

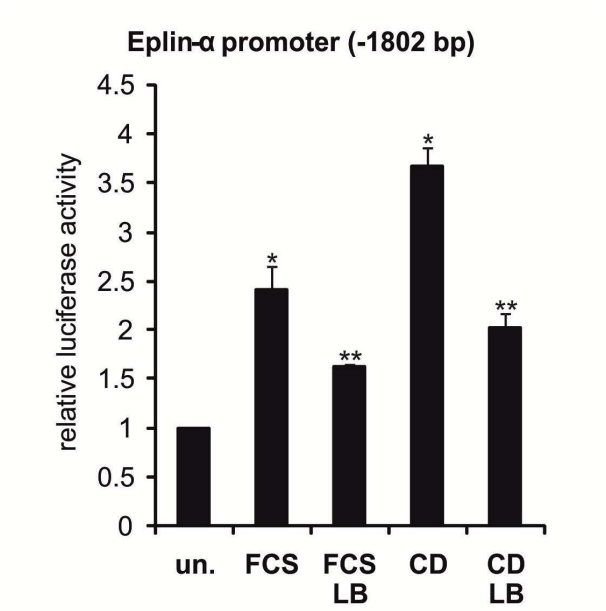

Figure VI-5: The proximal promoter of Eplin-α is regulated through actin. A fragment of the Eplin-α promoter ranging from nucleotides -1802 to +132 relative to the putative transcription start site confers differential regulation to a luciferase reporter gene. NIH 3T3 cells transiently transfected with the luciferase reporter construct were treated with latrunculin B (5 µM; 30 min pretreatment), serum (15%, 7 hours) or cytochalasin D (2 µM, 7 hours) as indicated. Thereupon luciferase activity was measured and normalized to renilla luciferase activity. Shown is the mean relative luciferase activity. Error bars, SEM (n = 3). Asterisk, significant activation; double asterisk, significant repression ($p < 0.05$, unpaired student's t-test).

The genomic region encoding the two Eplin isoforms is schematically represented in Figure VI-6.

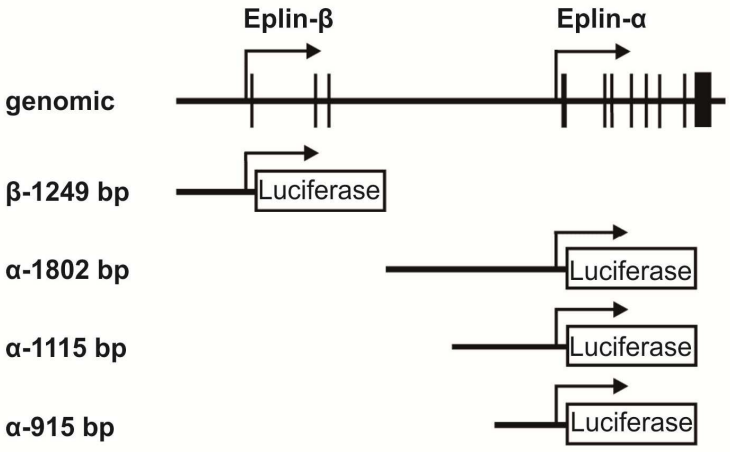

Figure VI-6: Genomic organization of the Eplin-α and Eplin-β promoter regions. Schematic diagram of the genomic structure of the Eplin gene, and the promoter reporter constructs used. The Eplin-β reporter ranges from -1249 to +71, and the truncated Eplin-α fragments range from the indicated nucleotide to +284, relative to the transcription start site. Bars in the genomic structure indicate exons.

The 2 kb long promoter fragment contains two potential SRF binding sites: a CArG-like element at position -1050 relative to the transcription start site and a consensus CArG Box at -124. I therefore

additionally cloned two promoter deletions into the luciferase reporter construct and tested their ability to mediate regulation of the luciferase reporter expression (see Figure VI-7).

The longer deletion construct comprised both potential SRF binding sites whereas the shorter one lacked the CArG-like element at -1050 but still contained the proximal CArG consensus box at -124. Both deletion constructs show very similar regulation by serum and cytochalasin D than the original 2 kb long promoter fragment suggesting that the consensus CArG Box at -124 near the transcription start site mediates Eplin-α responsiveness to MAL-SRF signaling. This consensus SRF binding site is conserved in the human promoter. Consistent with a possible involvement of MAPK signaling in Eplin-α regulation, a TCF-binding site is located adjacent to this CArG Box (Chen et al., 2000).

As a control I analyzed a 1.3 kb long Eplin-β promoter fragment. The putative Eplin-β promoter contains no potential SRF binding site. As expected the analyzed fragment containing the transcription start site mediated basal transcription of the luciferase reporter but was neither induced by serum nor cytochalasin D (Figure VI-7).

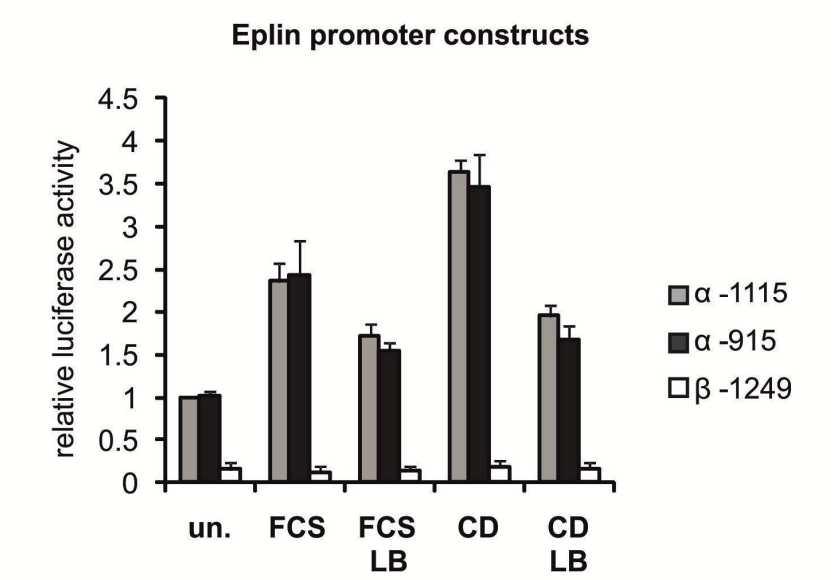

Figure VI-7: A proximal CArG consensus element at position -124 mediates Eplin-α responsiveness to MAL-SRF signaling. Analysis of the indicated Eplin promoter reporter constructs by transient luciferase assays in NIH 3T3 fibroblasts. Luciferase activity was measured after treatment with latrunculin B (5 µM; 30 min pretreatment), serum (15%, 7 hours) or cytochalasin D (2 µM, 7 hours) as indicated. Shown is the mean relative luciferase activity normalized to renilla luciferase activity. Error bars, SEM (n = 3).

Since Eplin-α was described as an epithelial protein with a critical role in junction formation, I next tested the regulation of the shortest promoter fragment in mouse mammary epithelial EpRas cells. As observed before for other known SRF targets (Busche et al., 2008), the Eplin-α induction mediated by actin binding drugs was generally lower than in NIH 3T3 fibroblasts. Nevertheless, the principle regulation of the Eplin-α promoter by changes in actin dynamics was comparable in epithelial cells: the reporter was upregulated by both cytochalasin D and the F-actin stabilizing drug jaspakinolide, which also induces actin-MAL signaling (Figure VI-8). In both cases the induction was repressed by

latrunculin B pretreatment. This suggests that the mode of Eplin-α regulation is not fundamentally different in epithelial cells.

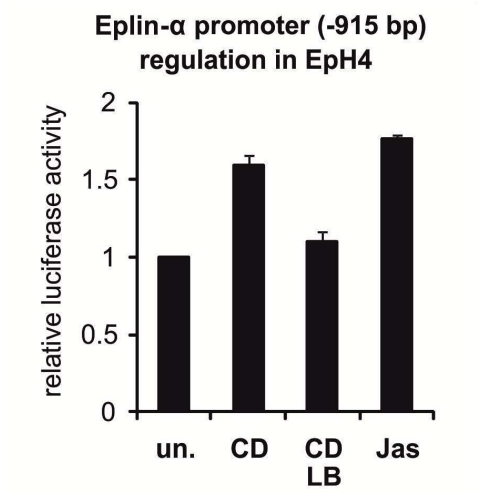

Figure VI-8: The proximal Eplin-α promoter is differentially regulated by actin binding drugs in mouse mammary epithelial EpH4 cells. Cells were transiently transfected with the Eplin-α (-915) promoter reporter construct, treated with cytochalasin D (2µM, 7 hours), latrunculin B (5 µM, 30 min pretreatment), or jasplakinolide (0.5 µM, 7 h), and by luciferase assays. Shown is the mean relative luciferase activity normalized to renilla luciferase activity, with error bars indicating half range.

To test the regulation of the Eplin-α promoter by actin in a more direct way I analyzed the effect of different actin mutants on the luciferase reporter activity.

R62D is a nonpolymerizable point mutant actin that is not incorporated into actin filaments, but increases the total cellular G-actin level, binds to MAL and consequently inhibits SRF activation (Miralles et al., 2003; Posern et al., 2002). In contrast, the actin mutant G15S enhances F-actin formation and constitutively activates MAL-SRF signaling (Posern et al., 2004). Thus I ectopically expressed these two actin mutants and wild type actin, respectively, together with the shortest Eplin-α promoter construct in NIH 3T3 cells. Actin R62D as well as actin wildtype significantly inhibited the cytochalasin D mediated induction of luciferase reporter activity (Figure VI-9). Inhibition of serum-mediated reporter activation was also observable. Conversely, G15S activated the Eplin-α promoter independently of external stimuli and the reporter activation was even slightly further increased by cytochalasin D and serum, respectively (Figure VI-9).

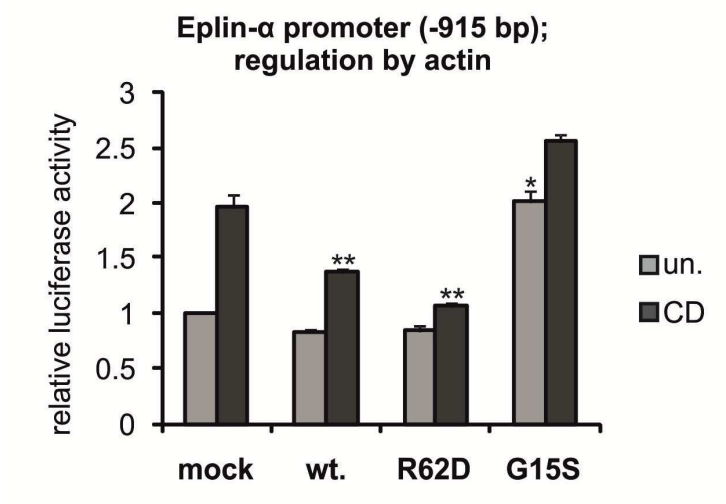

Figure VI-9 Eplin-α expression is controlled by mutant actins. Cotransfection of NIH 3T3 cells with the shortest proximal Eplin-α reporter and actin wildtype (wt), non-polymerizable mutant actin R62D, and F-actin stabilizing mutant actin G15S. Following cytochalasin treatment, the luciferase activity was determined in luciferase assays. Shown is the mean relative luciferase activity normalized to renilla luciferase activity. Error bars, SEM (n = 3). Asterisk, significant activation; double asterisk, significant repression ($p < 0.01$, unpaired student's t-test).

Next I investigated whether G-actin responsive elements exist also in the promoter of Pai-1, Pkp2 and Fhl1.

I cloned a 2.2 kb long fragment of the murine Pai-1 promoter containing the transcription start site into the luciferase reporter plasmid pGL3. The genomic organization of the Pai-1 gene and its proximal promoter region is depicted in Figure VI-10.

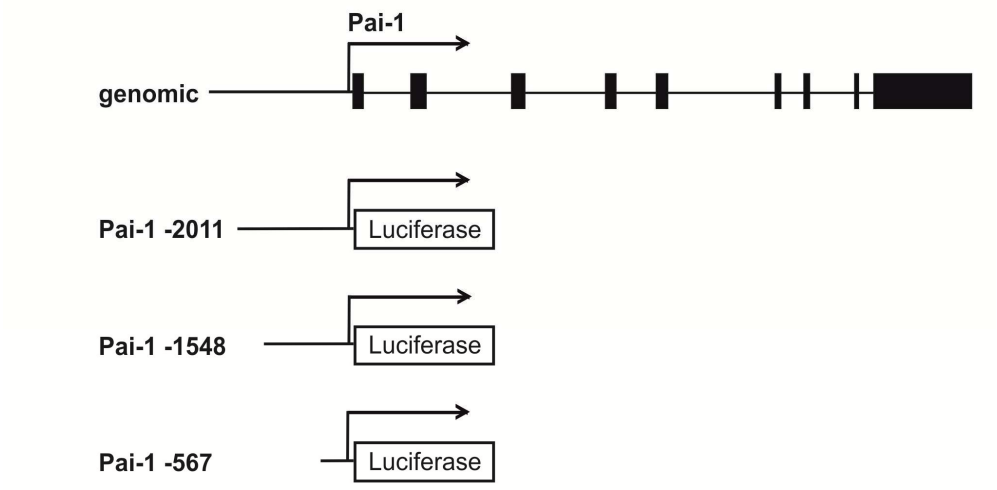

Figure VI-10: Genomic organization of the Pai-1 promoter region. Schematic diagram of the genomic structure of the Pai-1 gene, and the promoter reporter constructs used. The original Pai-1 reporter ranges from -2093 to +92, and the truncated Pai-1 fragments range from the indicated nucleotide to +118, relative to the transcription start site.

By luciferase assays I tested whether the 2.2 kb long fragment of the Pai-1 promoter mediated differential expression of the heterologous luciferase reporter. Indeed this 2.2 kb promoter fragment

was induced by serum and to a lesser degree by cytochalasin D in NIH 3T3 cells, but surprisingly its induction was unaffected by latrunculin B pretreatment (Figure VI-11A).

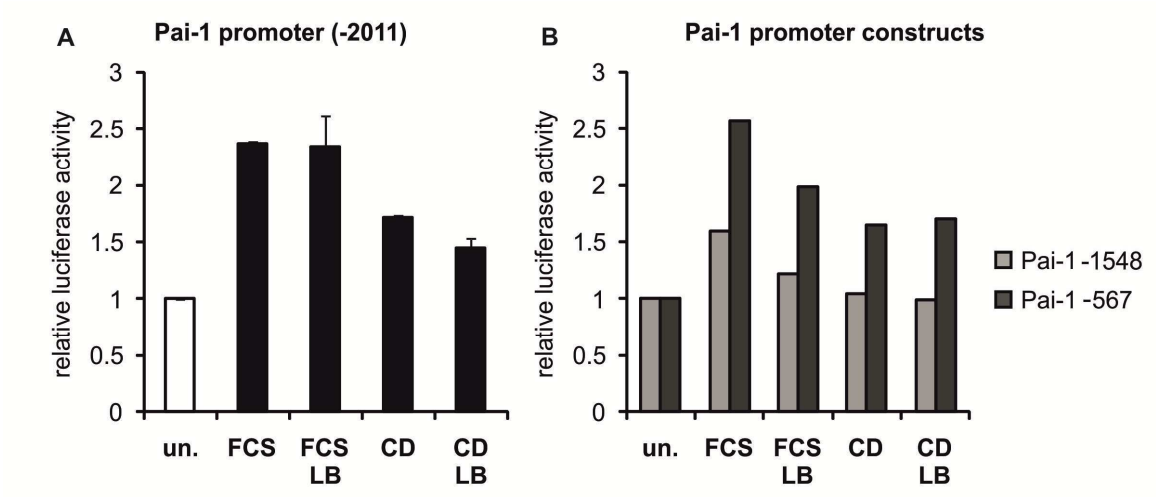

Figure VI-11 The proximal promoter of Pai-1 is serum responsive. A fragment of the Pai-1 promoter ranging from nucleotides -2011 to +92 relative to the putative transcription start site confers differential regulation by serum to a luciferase reporter gene. (A) Analysis of the indicated Pai-1 promoter reporter constructs by transient luciferase assays in NIH 3T3 fibroblasts (B). NIH 3T3 cells transiently transfected with the luciferase reporter constructs were treated with latrunculin B (5 µM; 30 min pretreatment), serum (15%, 7 hours) or cytochalasin D (2 µM, 7 hours) as indicated. Thereupon luciferase activity was measured and normalized to renilla luciferase activity. Shown is the mean relative luciferase activity. Error bars indicate half range (A).

The 2.2 kb long promoter fragment contains three CArG-like elements at positions -1736, -1193, and -354 relative to the transcription start site. I therefore additionally tested the regulation of two promoter deletions by serum and G-actin binding drugs.

The longer deletion construct comprises the two potential SRF binding sites at -1193 and -354 whereas the shortest one only contains the most proximal element at -354. The shortest promoter construct showed a very similar regulation than the original longest Pai-1 promoter fragment. It was induced by serum and to a lesser degree by cytochalsin D. The -1548 construct was more weakly induced by serum and unaffected by cytochalsin D. Again latrunculin B did not affect the inducibility of both truncated fragments (see Figure VI-11B). As all three promoter fragments were induced by serum but unaffected or only marginally activated by cytochalasin D and the serum mediated upregulation was unaffected by latrunculin B treatment I seems likely that the most proximal CArG-like element at position -354 mediates regulation of Pai-1 by MAPK signaling or other pathways but is not responsive to actin-MAL signaling. The MAL-SRF responsive element has therefore yet to be identified. Unfortunately I was not able to clone the MAL-SRF responsive promoter fragments of Pkp2 and Fhl1; the created reporter constructs failed to show considerable responsiveness to either stimuli (data not shown).

2.3 Regulation of target expression by MAL

To determine whether these G-actin regulated genes are direct targets of MRTF signaling I transiently retrovirally infected NIH 3T3 cells with various MAL constructs and examined the effect on target expression by quantitative RT-PCR.

The different MAL constructs used are schematically represented in Figure VI-12.

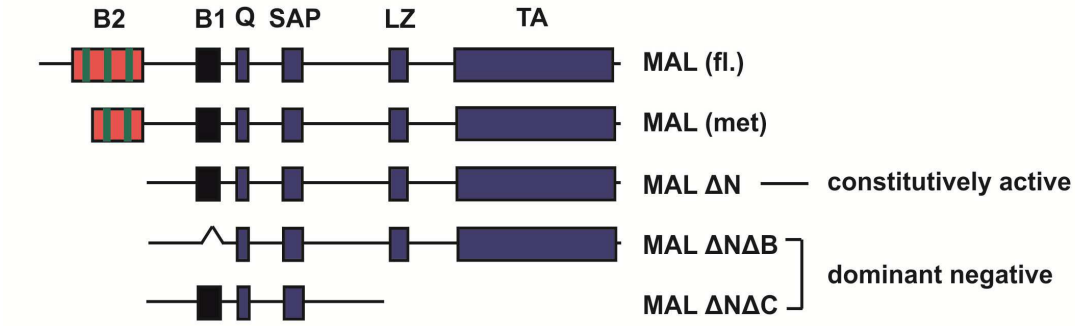

Figure VI-12: Schematic diagram of the MAL mutants used in this study. Conserved sequence motifs in the mouse MAL protein family are highlighted as boxes. RPEL motifs are indicated by green bars, basic boxes are in black, and other conserved elements in blue. The transcriptional activation domain is contained in the C-terminal region. Structures of five different MAL mutants are shown.

The upper panel shows wild type MAL with the three RPEL-motifs at the N terminus by which MAL binds to G-actin. The B-1 domain is essential for nuclear import and SRF binding, the leucine zipper mediates dimerization and the C-terminal part contains the transactivation domain. MAL (met) starts from the first methionine and therefore lacks one of the three RPEL-motifs, thus the negative regulation of MAL by G-actin is weakened. MAL ΔN lacks all three RPEL-motifs, the negative regulation by G-actin is completely abolished and this construct is therefore constitutively active (Miralles et al., 2003; Mouilleron et al., 2008). MAL ΔN additionally lacking the B1 domain is thought to associate with MAL via the leucine-zipper retaining it in an inactive, cytoplasmic state (Knoll et al., 2006; Zaromytidou et al., 2006). This construct is therefore dominant negative such as MAL ΔNΔC which has no transactivation domain (Wang et al., 2004; Zaromytidou et al., 2006).

Transient retroviral infection of NIH 3T3cells was highly efficient; the GFP control shows an infection rate of more than 90% (Figure VI-13).

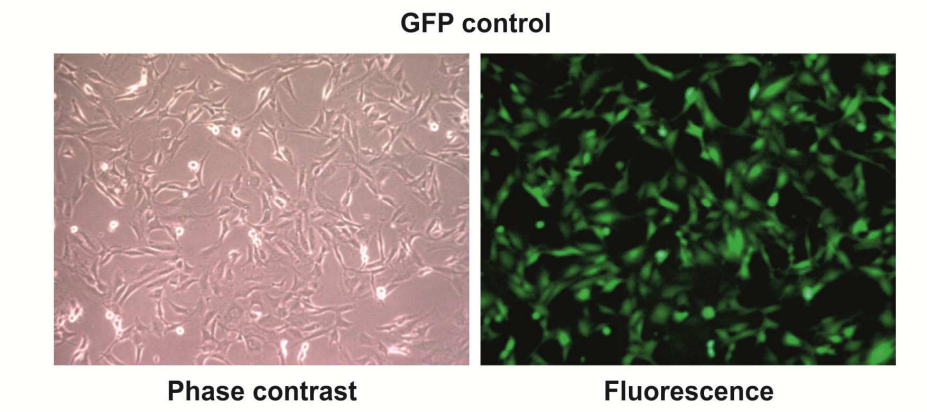

Figure VI-13: Expression analysis of GFP in control infected NIH 3T3 cells by fluorescence microscopy. Roughly more than 90% of NIH 3T3 cells express high amounts of GFP as judged by comparing fluorescence microscopy and phase contrast pictures.

All MAL constructs were highly expressed in these cells, as shown by western blotting (Figure VI-14).

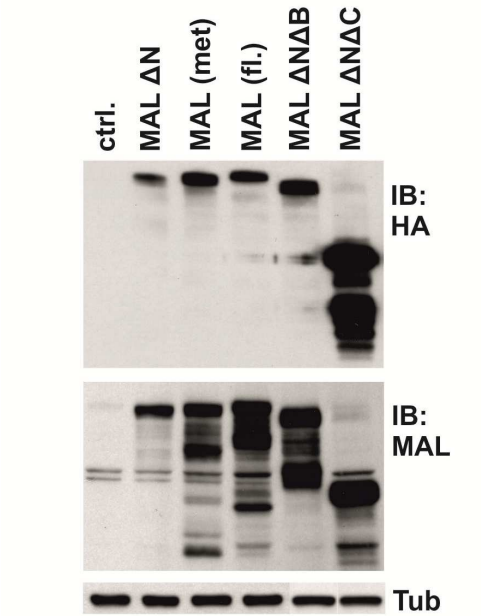

Figure VI-14: Transient retroviral infection of NIH 3T3 cells yields high expression levels of the MAL mutants. Expression analysis of MAL constructs in infected cells using anti-HA antibodies (top), anti-MAL antibodies (middle), and anti-tubulin as a control (bottom).

Transient retroviral infection with an Mrtf-shRNA construct targeting both murine MAL and Mrtf-B resulted only in partial knockdown; the knockdown efficiency was analyzed by quantitative RT-PCR and was about 60% for both Mrtf-A and B (Figure VI-15).

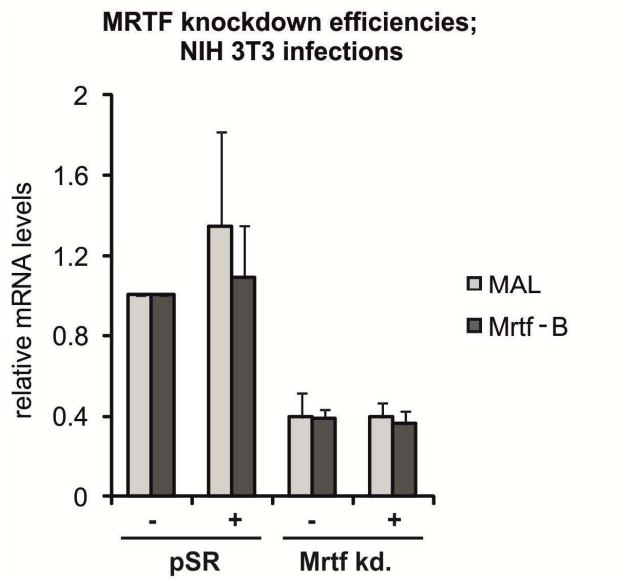

Figure VI-15 Determination of knockdown efficiencies yielded by transient retroviral infection with Mrtf knockdown construct. MAL and Mrtf-B expression was analyzed by qRT-PCR upon knockdown. mRNA was isolated from transiently infected cells, reversely transcribed and quantitated by real-time PCR. The relative mRNA levels after normalization to Hprt are depicted. Error bars, SEM (n=3)

Two days after retroviral infection total RNA was prepared and endogenous levels of target mRNA was determined by quantitative RT-PCR. Although the fold variations in relation to the control varied greatly among the different analyzed target genes, the principal pattern of regulation by the various MAL constructs was strikingly similar in all cases (Figure VI-16). Target expression was significantly induced by the constitutive active MAL constructs. MAL full length exhibited the weakest activity, consistent with its tightest regulation through actin. MAL ΔN, which lacks all RPEL motifs and cannot be bound by G-actin mediated the strongest target induction. Endogenous Fhl1 mRNA was upregulated most strongly, retroviral infection with MAL ΔN lead to an almost 100fold induction. Fhl1 is the only target which was also significantly upregulated by wild type MAL that only mediated a slight induction of the other genes examined (Figure VI-16).

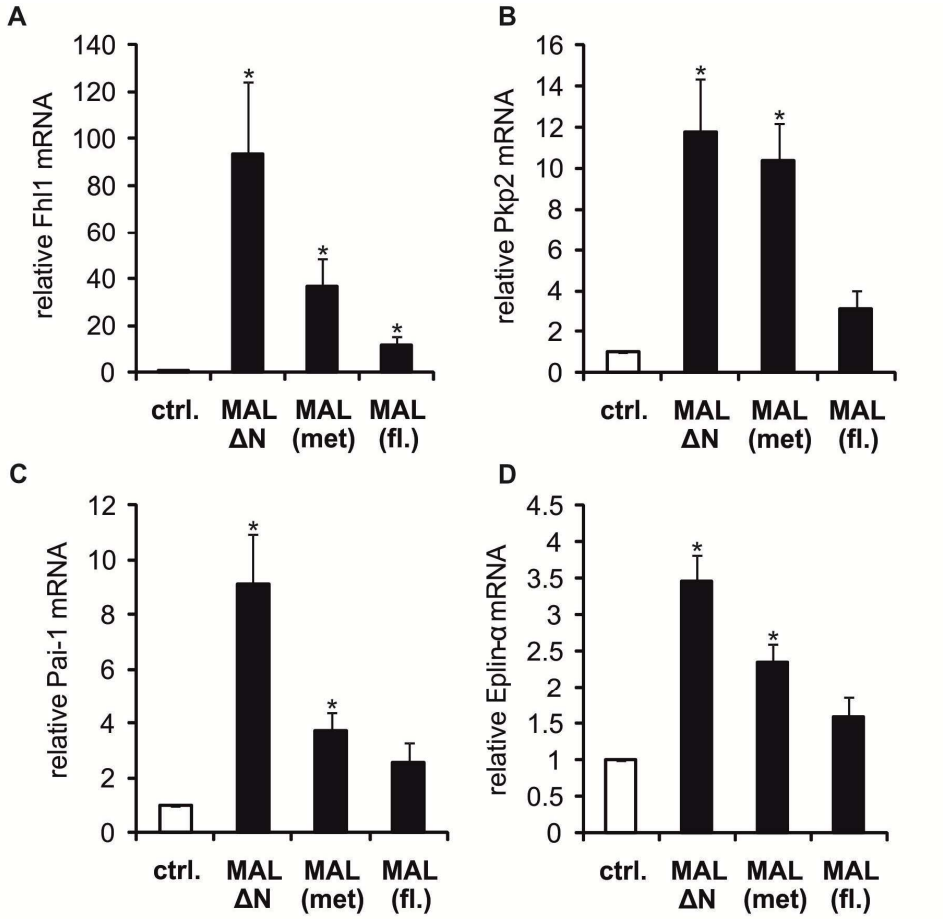

Figure VI-16: MAL/MRTF alone is sufficient to induce Fhl1, Pkp2, Pai-1, and Eplin-α. NIH 3T3 fibroblasts transiently infected with the indicated constructs were analyzed for mRNA expression of Fhl1 (A), Pkp2 (B), Pai-1 (C), and Eplin-α (D) by quantitative RT-PCR. Vector control used was pLPCX (ctrl.). Shown is the average induction of mRNA after normalization to Hprt. Error bars, SEM (n=3). Asterisk, significant change compared to the untreated control ($p<0.01$, unpaired student's t-test).

Immunoblotting was performed with antibodies against FHL1, PKP2 and PAI-1 and confirmed the MAL mediated upregulation of these targets on protein level (Figure VI-17).

Itga5 regulation by actin-MAL signaling has previously been examined by our group. Itga5 mRNA was induced upon transient overexpression of activated forms of MAL, SRF and RhoA (Descot et al., 2009). Moreover, a CArG-Box within the Itga5 promoter, which was shown to bind SRF in EMSA, had already been described (Sun et al., 2006a). It was shown to be upregulated by activated forms of MAL and SRF.

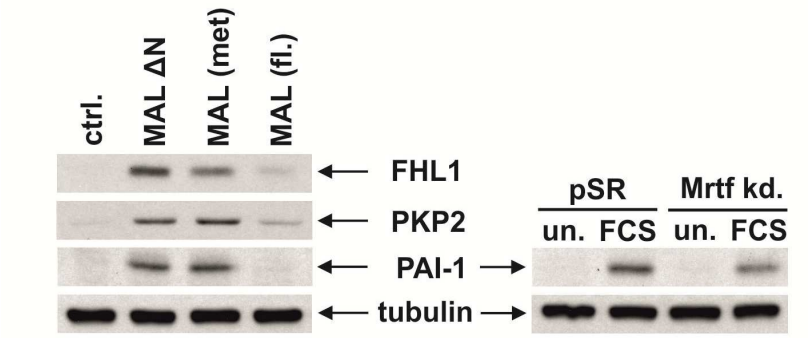

Figure VI-17: MAL/MRTF alone is sufficient to induce FHL1, PKP2, PAI-1, and Eplin-α on protein level. Target protein induction by MAL, and repression upon knockdown. Total lysates of transiently infected cells were analysed by immunoblotting with antibodies against PKP2, FHL1, PAI-1 and tubulin as a control

The results show that MAL alone is sufficient to induce expression of Fhl1, Pkp2, Pai-1 and Eplin-α. These genes are thus direct MAL targets. Conversely I tested whether MRTFs are required for serum induction of these genes. shRNA mediated knockdown of MRTFs resulted in considerably decreased inducibility of Fhl1, Pkp2 and Pai-1 by serum (Figure VI-18).

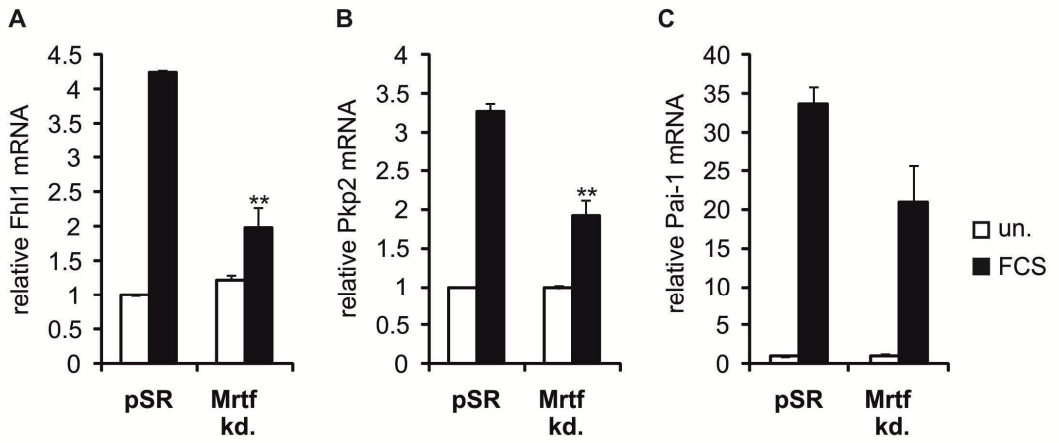

Figure VI-18: MAL/MRTF is necessary for FCS mediated induction of Fhl1, Pkp2, and Pai-1. NIH 3T3 fibroblasts transiently infected with the Mrtf knockdown construct or the vector control pSUPER-retro (pSR) were analyzed for mRNA expression of Fhl1 (A), Pkp2 (B), and Pai-1 (C) by quantitative RT-PCR. Cells were serum-starved (0.5%) prior to stimulation with fetal calf serum (15%, 90 min). Shown are the mean relative mRNA levels after normalization to Hprt. Error bars, SEM (n=3). double asterisk, significant repression ($p<0.05$, unpaired student's t-test).

The repression of serum mediated PAI-1 induction by MRTF knockdown was also observable on protein level as shown by immunoblotting (Figure VI-17). In contrast MRTF knockdown had little effect on the serum mediated upregulation of Eplin-α (Figure VI-19). I therefore tested the effect of ectopic expression of dominant negative MAL ΔNΔB and MAL ΔNΔC. Interestingly, only MAL ΔNΔC significantly inhibited serum induction of Eplin-α, whereas MAL ΔNΔB had like the partial Mrtf knockdown little effect (Figure VI-19).

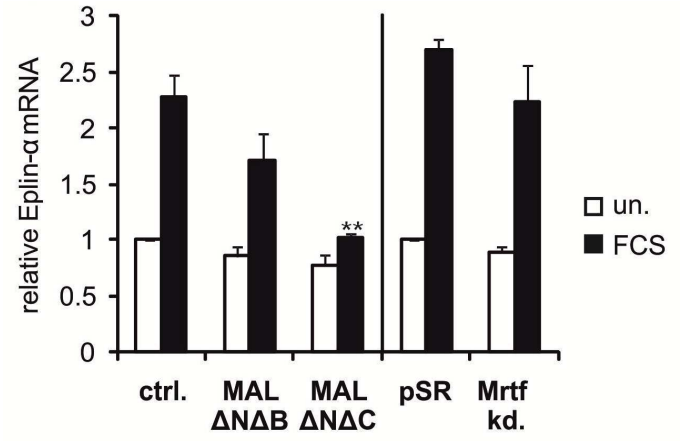

Figure VI-19: Effect of dominant negative MAL or Mrtf depletion on serum-stimulated Eplin-α expression. NIH 3T3 fibroblasts transiently infected with the indicated constructs were analyzed for mRNA expression of Eplin-α by quantitative RT-PCR. Cells were serum-starved (0.5%) prior to stimulation with fetal calf serum (15%, 90 min) Shown are the mean relative Eplin-α mRNA levels after normalization to Hprt. Error bars, SEM (n = 3). Asterisk, significant activation; double asterisk, significant repression ($p < 0.01$, unpaired student's t-test).

This result could be explained by a putative involvement MAPK signaling in Eplin-α regulation. MAL ΔNΔC is thought to block MAL/SRF function by forming a transcriptionally inactive SRF complex on target promoters. Binding of MAL ΔNΔC to SRF via its basic region does not allow association of SRF with the MAPK-regulated cofactors of the TCF-family (Wang et al., 2004; Zaromytidou et al., 2006). In contrast, MAL ΔNΔB retains MAL via its leucine zipper in an inactive, cytoplasmic state as mentioned above but does not compete with TCF binding to the common SRF surface (Knoll et al., 2006; Zaromytidou et al., 2006).

In order to determine the regulation of these target genes by MAL in epithelial cells, stably infected mouse mammary epithelial EpRas cells with active, dominant negative and knockdown constructs of MAL/Mrtf-B were analyzed. Upon whole RNA preparation I determined the relative mRNA levels of Eplin-α, Pkp2, Fhl1 and Pai-1 by quantitative RT-PCR (Figure VI-20). Eplin-α, Pkp2 and Fhl1 were elevated in EpRas cells stably expressing MAL ΔN and MAL (met), whereas Pai-1 was upregulated only by MAL (met). Conversely, Fhl1 was considerably decreased by the dominant negative MAL constructs, whereas Pai-1 and Pkp2 were little affected. Further analysis of the EpRas cells harboring a stable Mrtf knockdown revealed a significant reduction of all four target genes, with the strongest effect on Fhl1 (Figure VI-20). These results demonstrate that MRTFs are sufficient and required for the expression of the selected targets in epithelial cells.

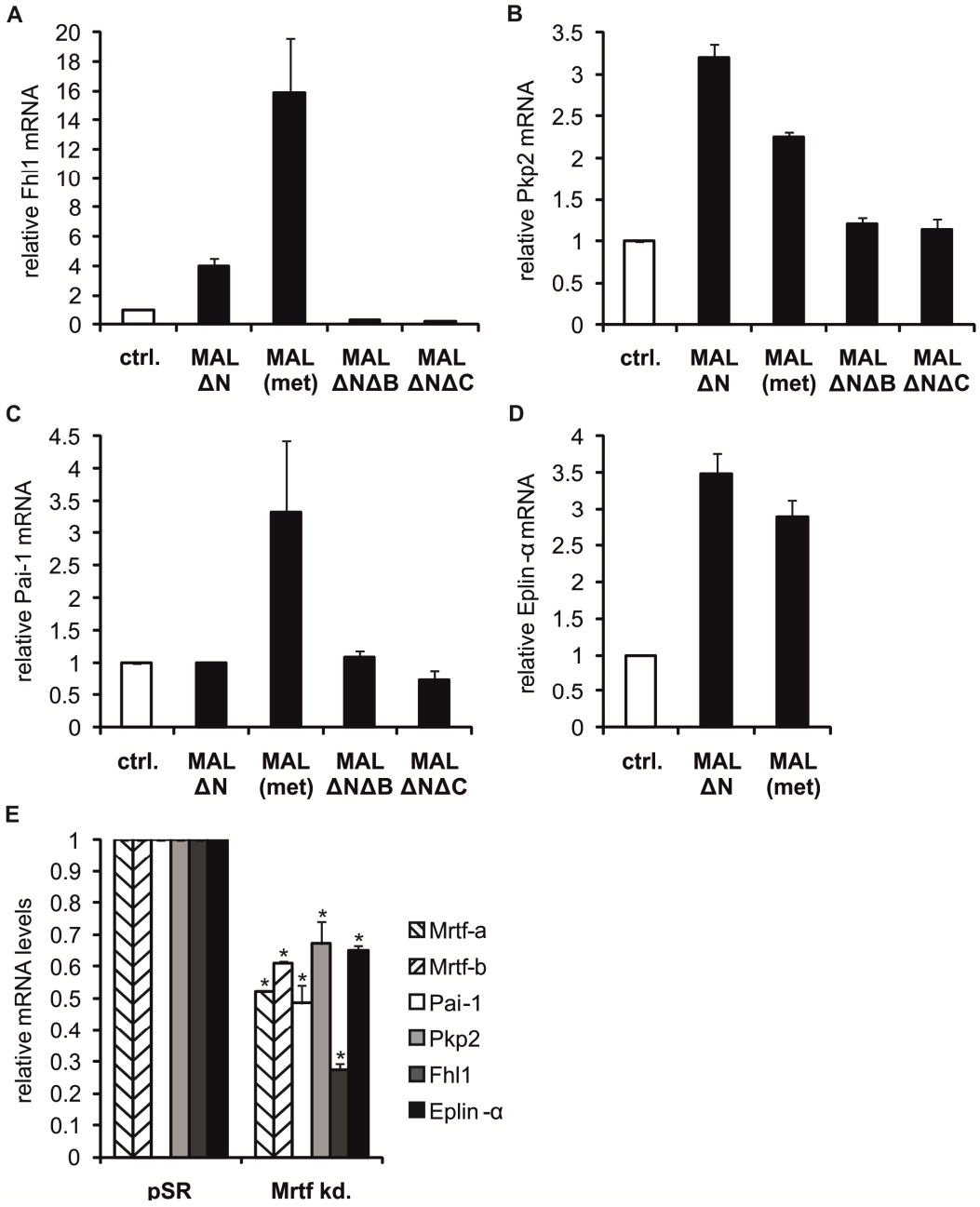

Figure VI-20: Effect of MAL on target expression in epithelial EpRas cells. Relative mRNA levels of Fhl1 (A), Pkp2 (B), Pai-1 (C), and Eplin-α (D) in EpRas epithelial cells stably infected with the indicated MAL constructs. Shown is the average mRNA amount, compared to the mock-infected control cells, of two independent experiments after normalisation to Hprt (Error bars indicate half range). (E) Relative mRNA levels of MAL, Mrtf-b, Fhl1, Pkp2, Pai-1, and Eplin-α in EpRas cells stably expressing MRTF shRNA in comparison to the pSR control. Quantitation of relative mRNA levels after normalization to Hprt is depicted. Asterisk, significant repression compared to the mock-infected control cells ($p<0.05$, unpaired student's t-test).

2.4 Recruitment of MAL and SRF to target promoters

To directly demonstrate the involvement of MAL in transcriptional regulation, I performed chromatin immunoprecipitations using MAL/MRTF-B and SRF specific antibodies. The chromatin was precipitated from NIH 3T3 cells treated with and without cytochalasin D. The known MAL target gene Srf and the “housekeeping” gene Gapdh were used as controls. In order to determine whether MAL and SRF are recruited to the Eplin-α promoter, I performed quantitative PCR following ChIP with primers flanking the proximal CArG-Box at -124 that was shown to mediate Eplin-α

responsiveness to MAL-SRF signaling in the luciferase assays. The Pkp2 gene contains a CArG-like element in the first intron at nucleotide 2894 after the transcription start site, which is conserved in human, rat and mouse. This region was analyzed for MRTF and SRF binding by ChIP. Upon treatment with cytochalasin D MAL was inducibly recruited to the analyzed Eplin-α and Pkp2 promoter regions, similarly to the known MAL target gene Srf (Figure VI-21). Quantitative PCR revealed that MAL recruitment to the Eplin-α and the Srf promoter was increased more than 10-fold. MAL-binding to the Pkp2 intronic region was significantly induced 5fold (Figure VI-22). SRF on the other hand proved to be constitutively present at the Eplin-α and the Srf promoter, and its binding was only slightly enhanced upon cytochalasin D treatment. This constitutive binding of SRF to promoter regions has been previously shown for other known target genes such as Vinc and Cyr61 (Descot et al., 2009; Miralles et al., 2003). Surprisingly the SRF recruitment to the Pkp2 intronic region is strongly increased upon induction of MAL-SRF signaling.

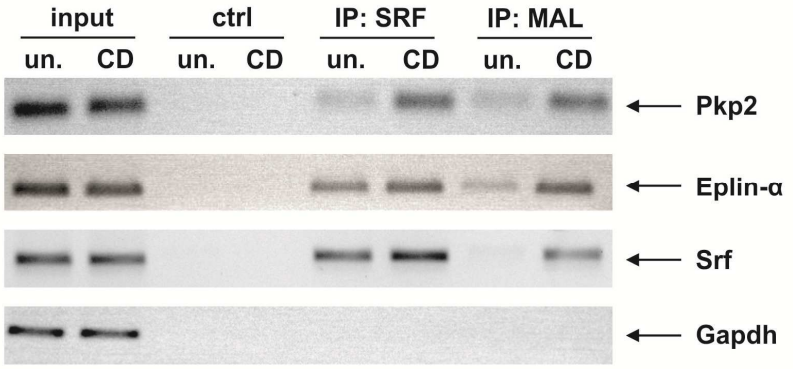

Figure VI-21: MAL and SRF are recruited to the Eplin-α and the Pkp2 promoter. Following chromatin preparation from starved (un.) and stimulated NIH 3T3 cells (CD, 2 µM; 30 min), antibodies specific for SRF and MAL, or a negative control antibody (ctrl), were used for Chromatin-IP. Immunoprecipitated and input Pkp2, Srf and Gapdh promoter fragments were amplified by conventional PCR and visualized by agarose gel electrophoresis.

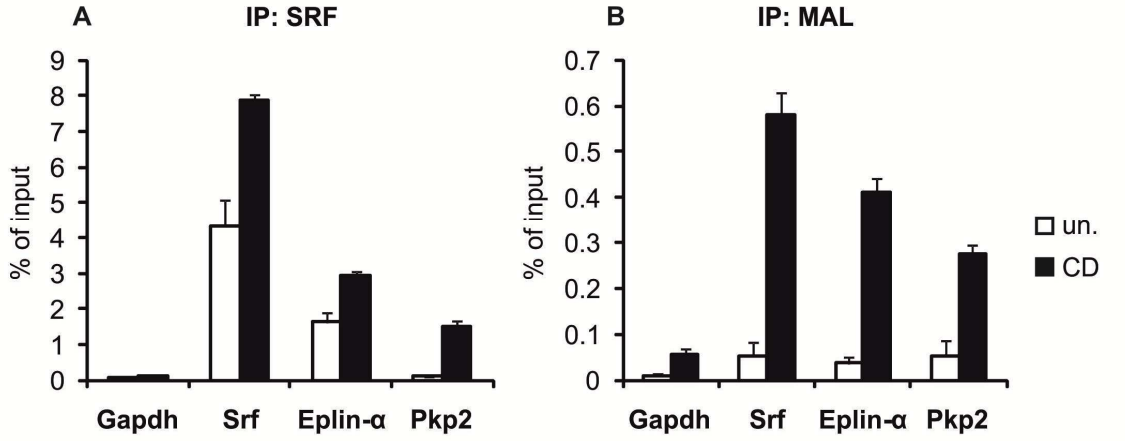

Figure VI-22: MAL and SRF are recruited to the Eplin-α and the Pkp2 promoter. Upon chromatin preparation form starved (un.) and stimulated NIH 3T3 cells (CD, 2 µM; 30 min) and chromatin-IP using SRF and MAL specific antibodies the relative amounts of precipitated promoter fragments were measured by real-time PCR. Shown is the relative quantitation of Gapdh, Srf, Eplin-α, and Pkp2 promoter fragments from three independent chromatin preparations and IPs, expressed in % of the input chromatin. Error bars, SEM (n=3). Asterisk, significant change compared to the untreated control ($p<0.01$, unpaired student's t-test).

SRF recruitment and inducible MAL recruitment to the Srf and the Eplin-α promoter was also detected after serum stimulation (Figure VI-23). The control antibody did not immunoprecipitate any of the analyzed promoter fragments, and neither MAL nor SRF were recruited to the Gapdh promoter.

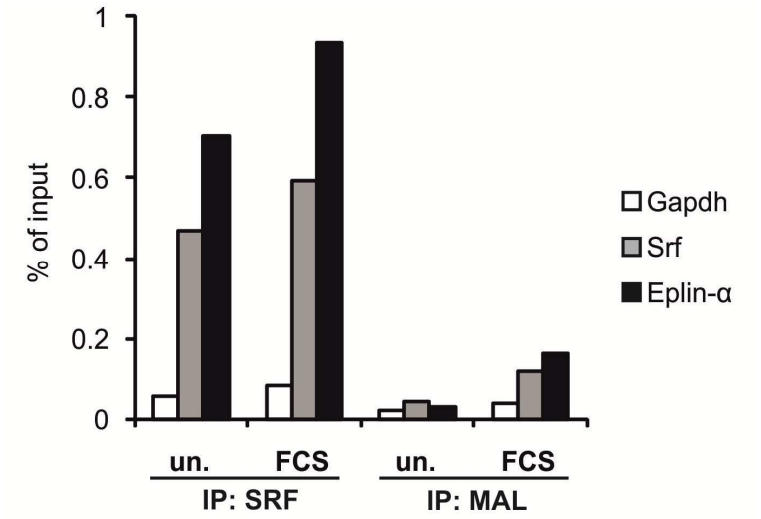

Figure VI-23: MAL is inducibly recruited to the Eplin-α promoter upon serum stimulation. Upon chromatin preparation form starved (un.) and stimulated NIH 3T3 cells (FCS, 15%; 30 min) and chromatin-IP using SRF and MAL specific antibodies the relative amounts of precipitated promoter fragments were measured by real-time PCR. Shown is the relative quantitation of Gapdh, Srf, and Eplin-α promoter fragments expressed in % of the input chromatin. Bound Eplin-α promoter fragment in MAL immunoprecipitates was increased 5.8 fold by FCS.

The ChIP results suggest that both the Eplin-α and the Pkp2 promoter are inducibly bound and regulated by MAL through its interaction with SRF.

2.5 Target regulation in other cellular systems

Furthermore I analyzed the responsiveness of Pkp2 and Fhl1 to MAL-SRF signaling in other cellular settings. In epithelial MDCK cells MAL dependent transcription is induced upon disruption of E-cadherins and Adherens Junctions, e.g. by reduction of extracellular calcium (Busche et al., 2008; Busche et al., 2010). Indeed PKP2 is upregulated upon dissociation of MDCK cell-cell contacts by calcium withdrawal as shown by immunoblotting (Figure VI-24). Similarly, FHL1 was induced in mouse embryo fibroblasts treated with cytochalasin D (Figure VI-24). This suggests that the regulation of the Pkp2 and Fhl1 genes through the actin-MAL pathway is a widespread mechanism and applies to various cell types and upstream stimuli.

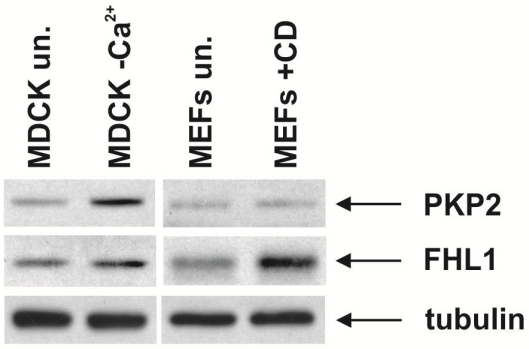

Figure VI-24: PKP2 and FHL1 are upregulated by various upstream stimuli inducing MAL-SRF signaling. Protein expression of PKP2 and FHL1 upon MAL/SRF induction by either calcium withdrawal in epithelial MDCK cells or cytochalasin D treatment (5 µM, 7 h) in mouse embryo fibroblasts as assessed by immunoblotting of 20 µg of total lysate .

Immunoblotting for PKP2, FHL1, and PAI-1 in total lysates of various cell lines revealed a rather heterogeneous expression pattern of those targets (Figure VI-25). As expected, PKP2 is most strongly expressed in non-invasive epithelial cell lines such as EpH4, EpRas, and MDCK cells. However, it is also detectable on protein level in the epithelial breast cancer cell lines MDA-MB-468 and MDA-MB -231 and in the NIH 3T3 fibroblasts. Endogenous basal FHL1 levels were low in most cell lines analyzed, although Fhl1 is detectable on mRNA level in EpRas cells, for instance. FHL1 protein was only visible in MDCK and NIH 3T3 cells. PAI-1 protein levels were detectable in all cell lines tested. Interestingly it was similarly to PKP2 very weakly expressed in the breast cancer cell lines MDA-MB-468 and MDA-MB-231 whereas the non-invasive epithelial mouse mammary cell lines EpH4 and EpRas contained high amounts of endogenous PAI-1 protein.

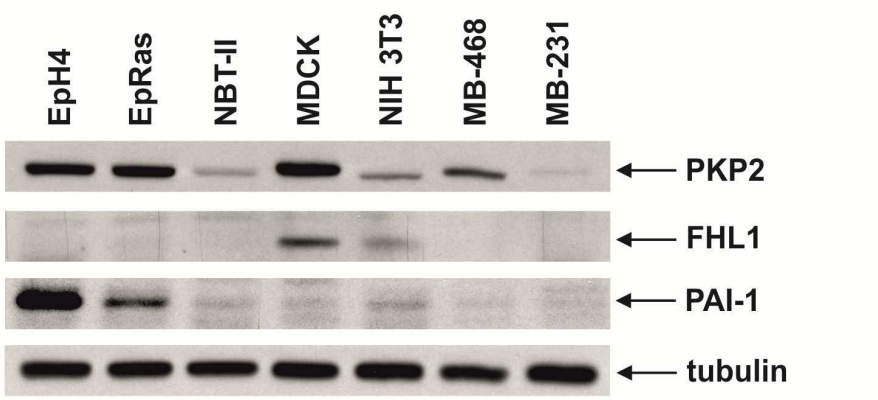

Figure VI-25: Protein expression of novel MAL-SRF targets in various cell lines. Protein expression of the G-actin regulated genes Pkp2, Fhl1 and Pai-1 was determined by immunoblotting of 20 µg of total lysate from the indicated cell lines.

3 MAL impairs cell motility of non-invasive fibroblasts

MAL-SRF signaling plays a pivotal role in cytoskeletal organization and actin homeostasis as demonstrated by the numerous target genes encoding structural and regulatory effectors of actin dynamics and components of focal adhesions. In order to test whether MAL/MRTFs affect cell

motility through such target genes, including the ones characterized above, I ectopically expressed various MAL constructs in non-invasive cell lines and examined the effect on the migratory behavior. As a non-invasive mesenchymal system I chose the NIH 3T3 cell line, in which actin MAL signaling was previously characterized and the regulation of the selected novel MAL targets was examined.

Upon transient retroviral infection of NIH 3T3 cells with the MAL constructs described above the effect on migration through uncoated transwell membranes was measured. The directed motility of NIH 3T3 cells towards growth medium containing 1% FCS as a chemoattractant was significantly impaired by ectopic expression of constitutive active MAL ΔN and MAL (met). Conversely dominant negative MAL ΔNΔB and MAL ΔNΔC as well as partial MAL/Mrtf-B knockdown enhanced directed migration through transwells (Figure VI-26, Figure VI-27A).

Constitutive active MAL ΔN and MAL (met) as well as wild type MAL also significantly decreased undirected transwell migration of fibroblasts in serum-containing medium (Figure VI-27B); ectopic expression of dominant negative MAL and MAL depletion had little effect under those conditions (data not shown).

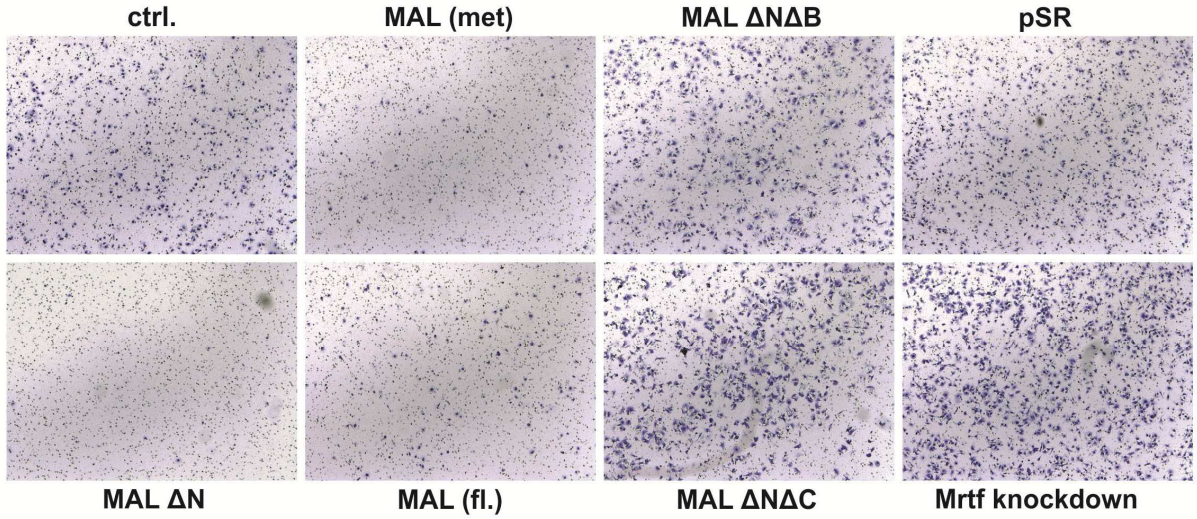

Figure VI-26: MAL/MRTF has an antimigratory effect in NIH 3T3 fibroblasts. Transient overexpression of constitutive active and wild type MAL impairs migration through uncoated transwell membrane in Boyden chamber assay whereas dominant negative MAL and MAL knockdown enhance cell motility. Directed cell migration was analyzed by letting cells migrate from FCS free medium towards 1% FCS containing medium for 2 hours. Representative micrographs of stained migrated cells on the lower side of the membrane are shown.

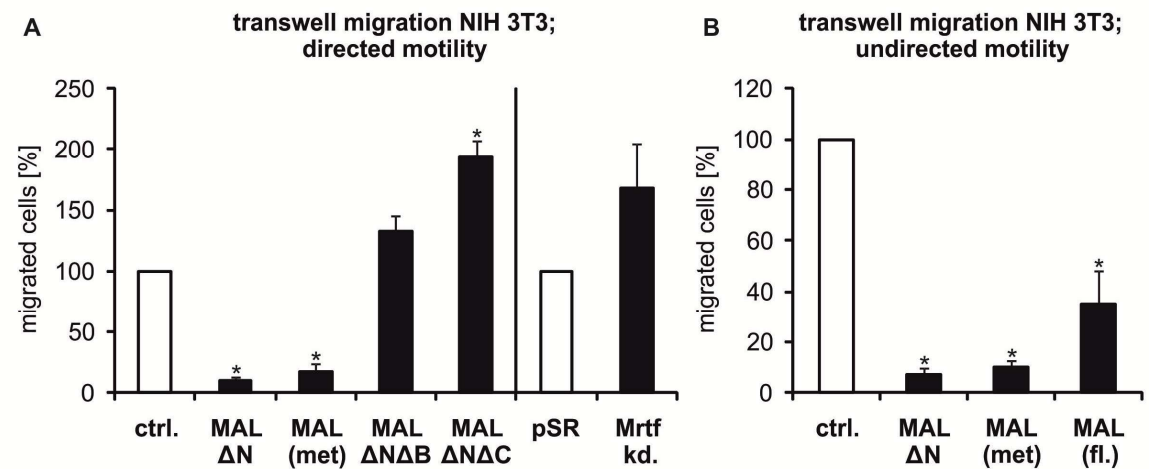

Figure VI-27: MAL/MRTF has an antimigratory effect in NIH 3T3 fibroblasts. Transient overexpression of constitutive active and wild type MAL impairs migration through uncoated transwell membrane in Boyden chamber assay whereas dominant negative MAL and MAL knockdown enhance cell motility. Directed cell migration was analyzed by letting cells migrate from FCS free medium towards 1% FCS containing medium for 2 hours (A). Undirected motility through transwell membranes was determined after 8 hours in growth medium containing 10% FCS (B). Expression of MAL constructs and shRNA was accomplished by transient retroviral infection. Quantitation of three independent infections is depicted with error bars indicating SEM. Asterisks: significant changes ($p<0.05$, unpaired student's t-test).

MAL ΔN showed the strongest negative effect on fibroblast migration consistent with the lack of negative regulation by G-actin binding.

Together these results suggest an antimigratory function of MAL activity in fibroblasts. Transwell migration is a rather artificial process in which cells have to squeeze through narrow pores of 8 μm in diameter. To examine whether the negative effect of MAL on fibroblast migration was a general feature that could be reproduced under different conditions I performed in vitro wound closure assays. To exclude an influence of altered proliferation I added mitomycin C, which blocks cell cycle progression. The NIH 3T3 cells' ability to migrate into a preformed wound in the cell layer was significantly impaired by ectopic expression of MAL ΔN, MAL (met) also slightly decreased wound closure (Figure VI-28, Figure VI-29A).

Conversely dominant negative MAL ΔNΔB and MAL ΔNΔC as well as partial MAL/Mrtf-B knockdown enhanced fibroblast migration into the cell free space (Figure VI-29B). The observed promigratory effect of MAL ΔNΔB was significant.

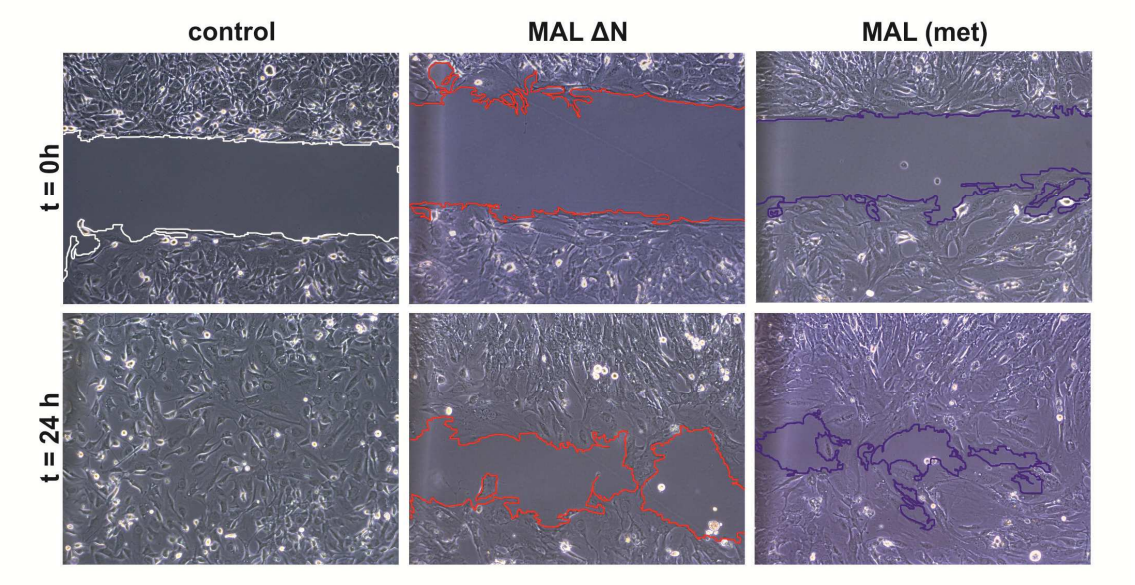

Figure VI-28: MAL/MRTF impairs 2-D migration in wound closure assays. Two days after infection cells were seeded into migration inserts at a density of 20.000 cells in 70 µl growth medium per reservoir. After attachment overnight the inserts were removed, and cells were allowed to migrate into the wound for 24 h in the presence of mitomycin C (10 µg/ml) to block proliferation. Micrographs of the wound closure with lines indicating the migration front are depicted.

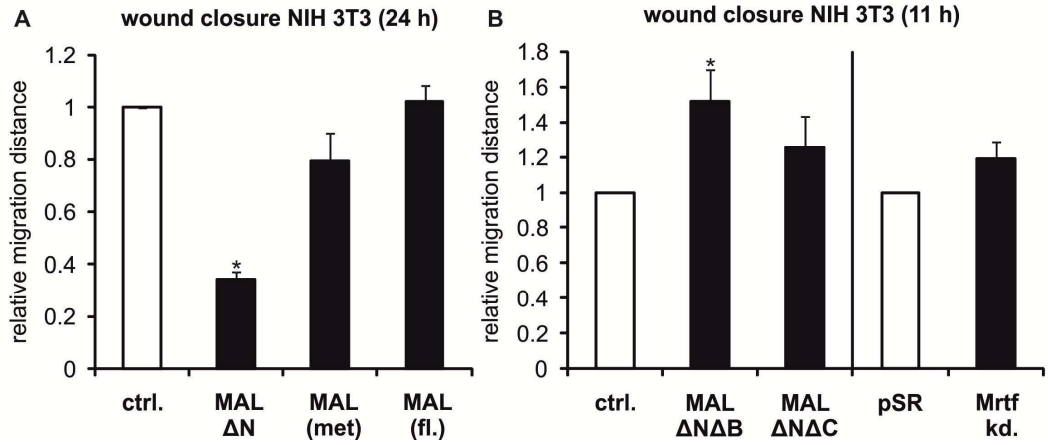

Figure VI-29: MAL/MRTF impairs 2-D migration in wound healing assays. Wound closure assays were conducted as described above (Figure VI-28). Wound closure was measured after 24 h to determine the effect of active MAL (A), and after 11 h to analyze the effect of dominant negative constructs and MAL knockdown (B), respectively. Quantitation of the relative migration distance is shown. Expression of MAL constructs and shRNA was accomplished by transient retroviral infection. Error bars indicate SEM of three independent experiments. Asterisks indicate significant changes ($p<0.05$, unpaired student's t-test).

MAL activity was therefore shown to negatively correlate with migration of non-invasive, mesenchymal cells under various conditions; directed and undirected migration through transwell membranes as well as two-dimensional wound closure was significantly impaired by active MAL. As observed before in the activation of target expression the ability of G-actin to negatively regulate the various active MAL constructs is reflected in the transactivation potential of the constructs; expression of wild type MAL has the weakest effects on target induction and migration of fibroblasts, consistent

with its tightest regulation through actin. As MAL ΔN lacks all RPEL-motifs, inhibition by G-actin is completely abolished and this construct therefore exhibits the strongest transactivation activity.

4 MAL exhibits similar antimigratory functions in non-invasive epithelial cells as in fibroblasts

To test whether MAL has different effects on migration of epithelial non-invasive cells, EpRas lines were selected which stably express wild type MAL, active MAL ΔN and MAL (met), dominant negative MAL ΔNΔB and MAL ΔNΔC and the MAL/Mrtf-B shRNA construct. The mouse mammary epithelial EpRas cell line was used as a model, since it exhibits many features characteristic of untransformed epithelial cells, including formation of proper junctions and expression of cytokeratin (Huber et al., 2004; Oft et al., 1996).

Retroviral infection of EpRas cells is considerably less efficient than NIH 3T3 infection. Therefore selection of stable lines was necessary. Ectopic expression of the activated MAL constructs was very weak and did not exceed endogenous MAL levels as judged by immunoblot analyses with antibodies against MAL/MRTF-B and the HA expressed by the constructs (Figure VI-30).

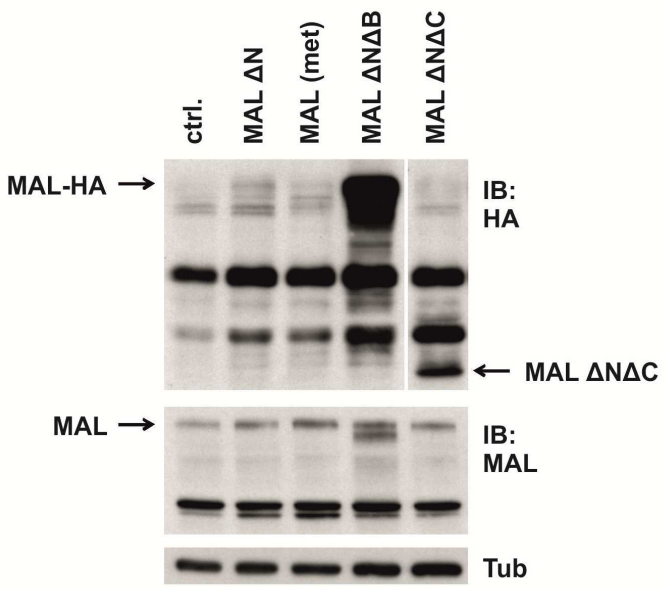

Figure VI-30: Expression analysis of MAL constructs in stably infected EpRas cells. MAL protein levels were determined by immunoblotting using anti-HA antibodies (top), anti-MAL antibodies (middle), and anti-tubulin as a control (bottom).

The weak expression of especially active MAL in stably selected cells is likely explained by impaired growth of high-expressing cells, due to recently reported antiproliferative MAL effects (Descot et al., 2009). To assess whether the obtained expression was sufficient for detectable activity of the various constructs, the stable EpRas cell lines were transfected with a MAL responsive luciferase reporter constructs and reporter activity was measured in untreated cells and upon cytochalasin D induction (Figure VI-31).

Active MAL ΔN and MAL (met) significantly enhanced basal reporter activity, but did not further enhance cytochalasin D mediated reporter activation. The dominant negative MAL constructs MAL ΔNΔB and MAL ΔNΔC both significantly decreased basal reporter activity and impaired the cytochalasin D mediated inducibility.

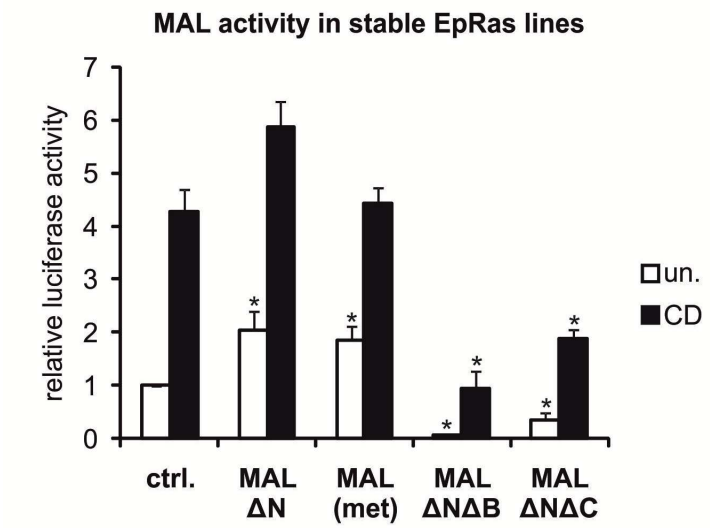

Figure VI-31: Stable expression of MAL constructs in EpRas cells effects MAL-SRF signaling. Analysis of SRF activity by transient luciferase assays in stably transfected EpRas cells. Shown is the mean relative luciferase activity, normalized to Renilla luciferase. Error bars, SEM (n=3). Asterisk, significant change compared to control ($p<0.05$, unpaired student's t-test).

The results of the luciferase assays suggested, that the ectopic expression of the MAL constructs was sufficient to considerably affect actin-MAL signaling activity in the stable EpRas cell lines. Thus, the migratory behavior of these cells was analyzed.

The effect of the different MAL constructs on cell motility of these non-invasive epithelial cells was strikingly similar to those observed in NIH 3T3 fibroblasts. Ectopic expression of both active MAL ΔN and MAL (met) significantly impaired undirected migration of EpRas cells through uncoated transwell membranes (Figure VI-32, Figure VI-33A). Conversely dominant negative MAL ΔNΔB and MAL ΔNΔC slightly enhanced undirected as well as directed transwell migration (Figure VI-32, Figure VI-33). Active MAL showed no effect on directed migration of EpRas cells through transwell membranes (Figure VI-33B).

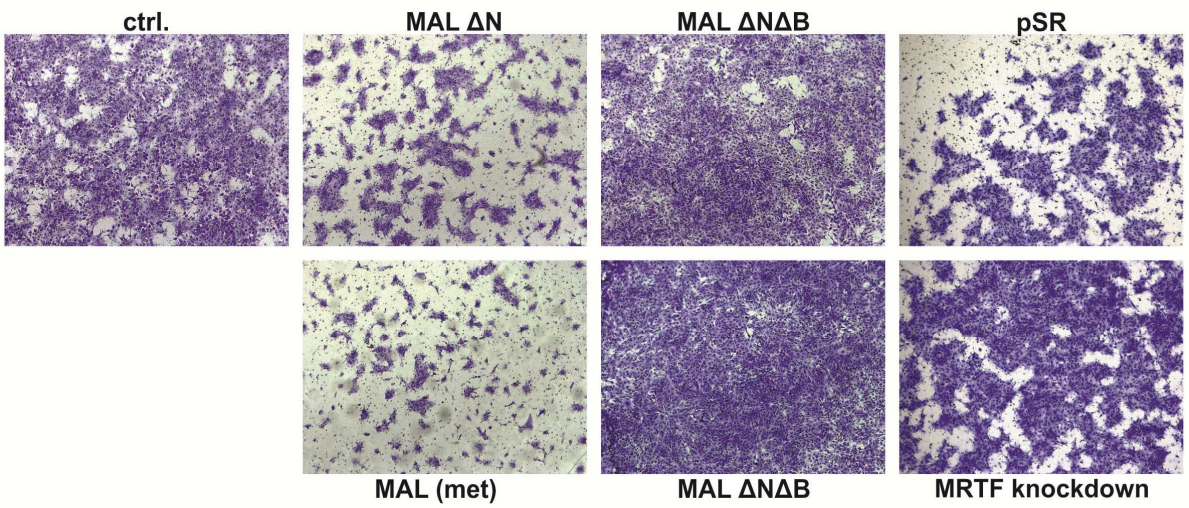

Figure VI-32: MAL/MRTF has an antimigratory effect in epithelial EpRas cells. EpRas cells stably expressing constitutive active MAL show impaired migration through uncoated transwell membrane in Boyden chamber assay, whereas cells stably expressing dominant negative MAL constructs or Mrtf shRNA exhibit increased cell motility. Undirected movement was assayed in serum-free growth medium for 23 h. Representative micrographs of stained migrated cells on the lower side of the membrane are shown.

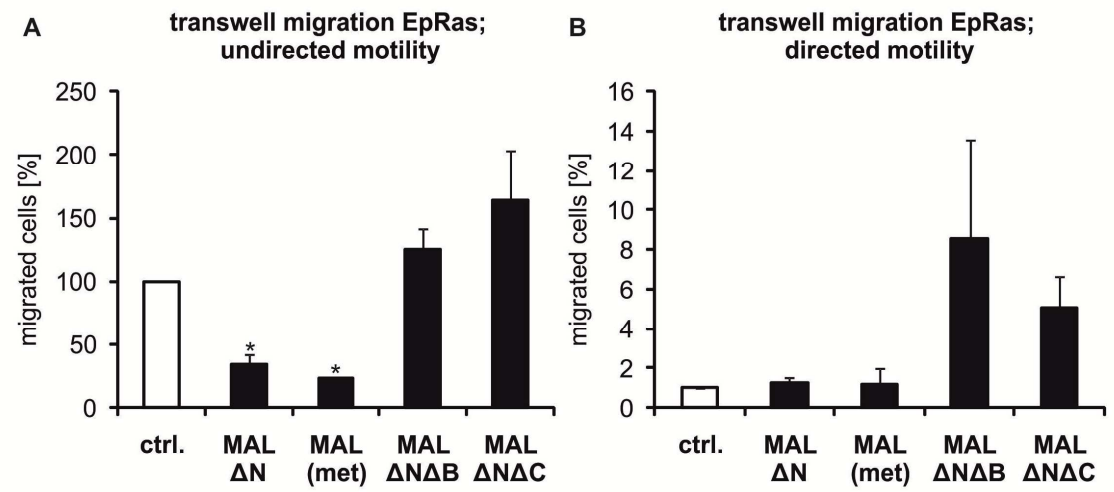

Figure VI-33: MAL/MRTF has an antimigratory effect in epithelial EpRas cells. EpRas cells stably expressing constitutive active MAL show impaired migration through uncoated transwell membrane in Boyden chamber assay, whereas cells stably expressing dominant negative MAL constructs exhibit increased cell motility. Undirected movement was assayed in serum-free growth medium for 23 h (A), directed movement occurred from serum-free medium towards 10% FCS containing medium for 14 h (B). Quantitation of three independent experiments is depicted with error bars indicating SEM. Asterisks: significant changes ($p<0.05$, unpaired student's t-test).

Partial MAL/Mrtf-B knockdown significantly enhanced both directed and undirected transwell migration of these non-invasive epithelial cells (Figure VI-34) although the knockdown efficiencies for MAL and Mrtf-B were only 50% and 40%, respectively, as shown above (Figure VI-20).

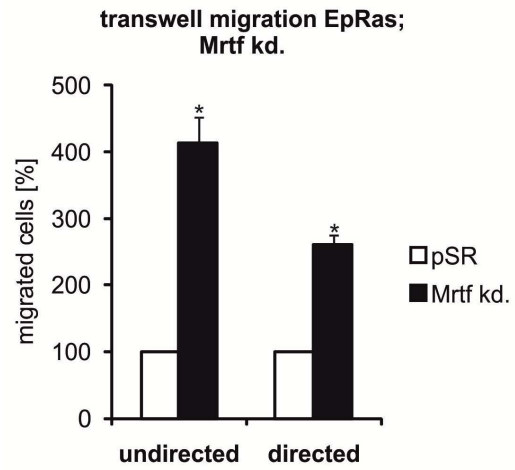

Figure VI-34: MAL/MRTF has an antimigratory effect in epithelial EpRas cells. Cells stably expressing Mrtf shRNA exhibit increased transwell migration. Undirected movement was assayed in serum-free growth medium for 23 h, directed movement occurred from serum-free medium towards 10% FCS containing medium for 14 h. Quantitation of three independent experiments is depicted with error bars indicating SEM. Asterisks: significant changes ($p<0.05$, unpaired student's t-test).

Our group previously described negative regulation of the EGFR-MAPK signaling axis by MAL dependent MIG6 induction (Descot et al., 2009). Inhibition of MAPK signaling could potentially impair cell motility, but since the effects of MAL on migration were also observed in serum free conditions, it is unlikely that they are solely mediated by MAL dependent MIG6 expression. The results of the transwell migration assays suggest that low levels of MAL are sufficient to exhibit both transcriptional and migratory responses and that MAL has similar antimigratory functions in non-invasive epithelial and mesenchymal cells.

5 MAL is required for cell motility of invasive tumorigenic cells

Interestingly MAL and MRTF-B have recently been implicated in tumor cell invasion and metastasis. Knockdown of both MAL and MRTF-B strongly reduced adhesion, spreading, invasion and motility of highly invasive breast cancer and melanoma cells (Medjkane et al., 2009). To address this apparent discrepancy between MAL/MRTF-B requirement for invasive cell motility and its antimigratory function in non-invasive epithelial and mesenchymal cells, I analyzed transwell migration and wound closure upon partial MAL depletion in the invasive breast cancer cell line MDA-MB-231, which was used in the study by Medjkane et al.

In spite of low transfection efficiencies, both migration through transwell membranes and wound closure were impaired by a partial MAL/Mrtf-B knockdown, essentially reproducing the antimigratory effect of Mrtf depletion (Figure VI-35).

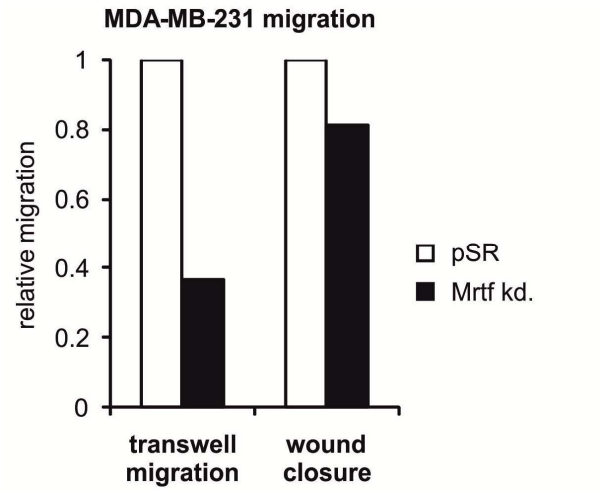

Figure VI-35: MAL is required for cell motility of invasive MDA-MB-231 cells. Depletion of MAL impairs migration of MDA-MB-231 through uncoated transwell membrane in Boyden chamber assay or in wound closure assay. MAL/Mrtf-B was depleted from MDA-MB-231 cells by transient transfection with Mrtf shRNA. To analyze transwell migration cells were allowed to migrate from FCS free medium in the upper compartment towards 10% FCS containing medium in the lower chamber for 15 h. Depicted is the quantitation of the relative transwell migration and the relative migrations distance, respectively.

Thus, differences in experimental procedures could be excluded as cause for the seemingly contradictory results. We therefore hypothesized that MAL could have opposite effects on migration in the different cells studied. To test whether MAL is required for cell motility of other invasive cells, I treated the stable MAL expressing EpRas lines with TGF-β for 6 days, which induces an epithelial-to-mesenchymal transition (EMT). The morphologically altered mesenchymal cells obtained are now termed EpRasXT and are able to develop invasive tumors in mice (Oft et al., 1996), similar to the highly invasive human breast cancer cell line MDA-MB-231. After the transition to the mesenchymal phenotype was completed, transwell migration assays with the EpRasXT lines stably expressing the various active and dominant negative MAL constructs were performed. Strikingly, the MAL constructs exhibited opposite effects on transwell migration of these invasive EpRasXT cells compared to the epithelial EpRas cells: active MAL strongly enhanced migration in transwell chambers, whereas dominant negative MAL had no effect or caused a slight reduction in motility (Figure VI-36, Figure VI-37). These findings suggest a fundamentally different migratory function of MRTFs in invasive and non-invasive cells.

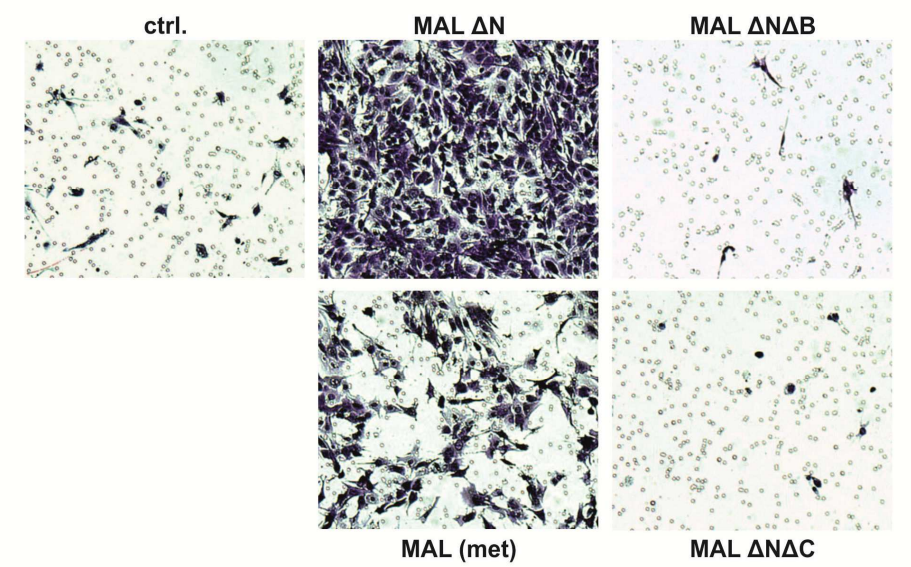

Figure VI-36: MAL enhances transwell migration of invasive EpRasXT cells. Stable mutant MAL expressing EpRas cells which had undergone epithelial-mesenchymal transition by TGF-β treatment for 7 days were assayed for directed transwell migration towards 10% FCS for 24 h. Representative micrographs of stained migrated cells on the lower side of the membrane are shown.

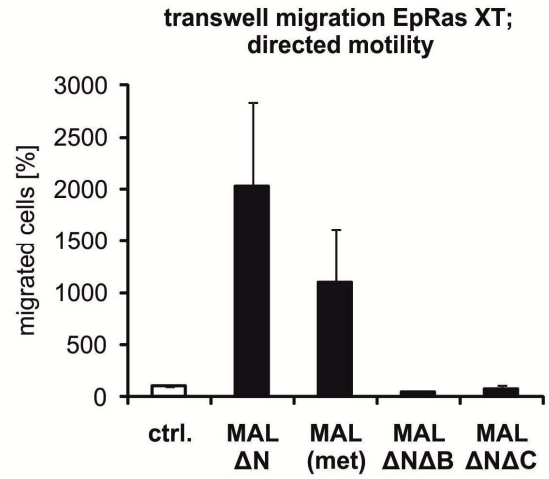

Figure VI-37: MAL enhances transwell migration of invasive EpRasXT cells. Stable mutant MAL expressing EpRas cells which had undergone epithelial-mesenchymal transition by TGF-β treatment for 7 days were assayed for directed transwell migration towards 10% FCS for 24 h. Quantitation of the relative transwell migration with error bars indicating half range (n=2) is depicted.

6 Identification of MAL targets mediating the antimigratory function of MAL in non-invasive cells

To identify MAL/MRTF targets that mediate the antimigratory effect of MAL in non-invasive epithelial and mesenchymal cells I depleted the selected newly identified G-actin regulated genes with potential roles in cell motility in our cellular model systems. Upon transient transfection of NIH 3T3 cells with siRNAs against Itga5, Pkp2, and Fhl1 I performed wound closure and transwell migration assays. Partial depletion of Itga5 and Pkp2 significantly enhanced NIH 3T3 wound closure whereas

Fhl1 knockdown had no effect (Figure VI-38A). Wound closure assays performed on dishes coated with the ITGA5 ligand fibronectin showed strikingly similar effects of Itga5 depletion (Figure VI-38B).

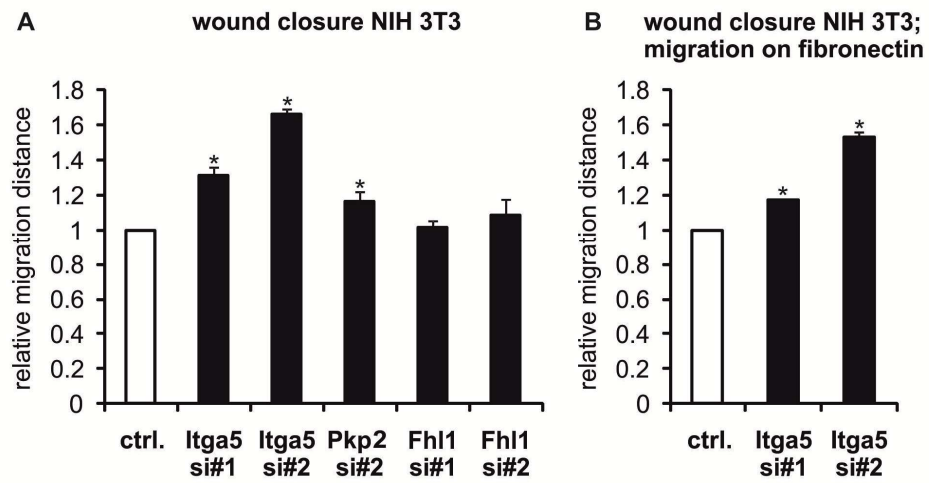

Figure VI-38: Knockdown of integrin α5 and plakophilin 2 enhances fibroblast wound closure. Cells were transiently transfected by RNAiMAX with the indicated siRNA and plated in wound closure chambers on non-coated cell culture dishes (A) or fibronectin coated dishes (10 µg/cm^2) (B) at a density of 20.000 cells in 70 µl growth medium per reservoir. After attachment overnight the inserts were removed, and cells were allowed to migrate into the wound for 12 h in the presence of mitomycin C (10 µg/ml) to block proliferation. A non-targeting siRNA was used as a control. Quantitation of the mean relative migration distance with error bars indicating SEM (n=3) is depicted. Asterisk, significant induction ($p<0.05$, unpaired student's t-test).

Similarly, Itga5 and Pkp2 knockdown enhanced undirected migration of NIH 3T3 cells through uncoated transwell membranes; the observed promigratory effect of Itga5 siRNA #2 was significant (Figure VI-39A). Again Fhl1 depletion had no effect on NIH 3T3 migration.

The knockdown efficiencies are shown in Figure VI-39B.

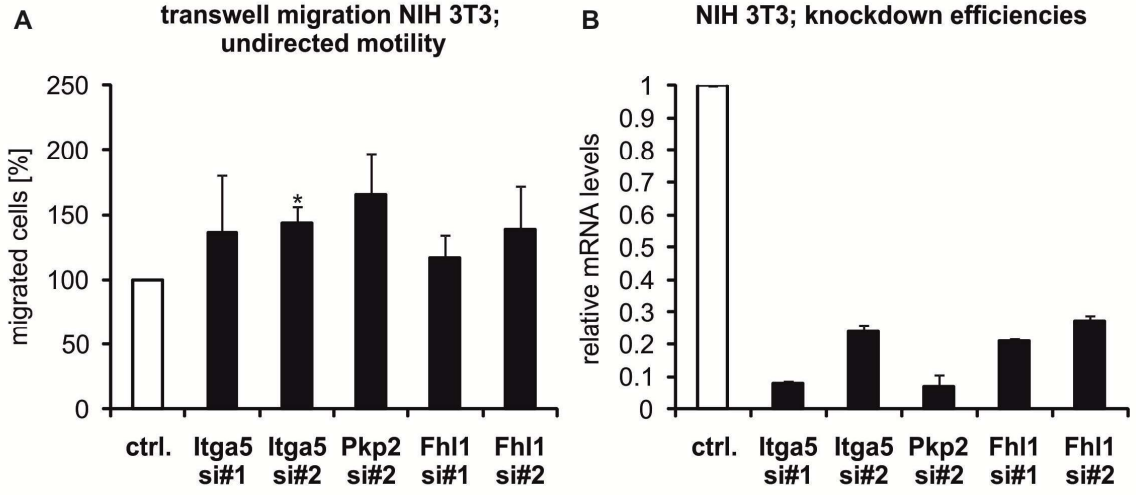

Figure VI-39: Knockdown of integrin α5 and plakophilin 2 enhances fibroblast transwell migration. Cells were transiently transfected by with the indicated siRNA and plated in uncoated as before. A non-targeting siRNA was used as a control. Quantitation of the mean relative transwell migration with error bars indicating SEM (n=3) is depicted (A). Asterisk, significant induction ($p<0.05$, unpaired student's t-test). The knockdown efficiencies of the indicated target genes in NIH 3T3 cells were measured by quantitative RT-PCR. Shown are the mean relative mRNA levels after normalization to Hprt. Error bars indicate SEM of three independent experiments.

Interestingly, the Itga5 siRNA#2 that yielded in lower knockdown efficiencies than the siRNA #1 showed in both migration assays stronger effects. This could be explained by a biphasic dependence of migration speed on integrin expression, which has been previously described (Palecek et al., 1997). The extremely low Itga5 levels attained with Itga5 siRNA #1 might be suboptimal for NIH 3T3 motility.
A second and even more efficient siRNA for Pkp2 was also tested, but its migratory effects were not interpretable due to cytotoxicity in NIH 3T3 cells (not shown).

Epithelial EpRas cells were transiently electroporated to achieve target depletion. The migratory effect was analysed in directed transwell migration assays. Pkp2 and Fhl1 knockdown strongly and significantly enhanced cell motility, as assessed with two different siRNAs each (Figure VI-40). The considerably smaller effect of Fhl1 siRNA #2 on EpRas cell motility was reflected by the lower knockdown efficiency obtained by this siRNA.

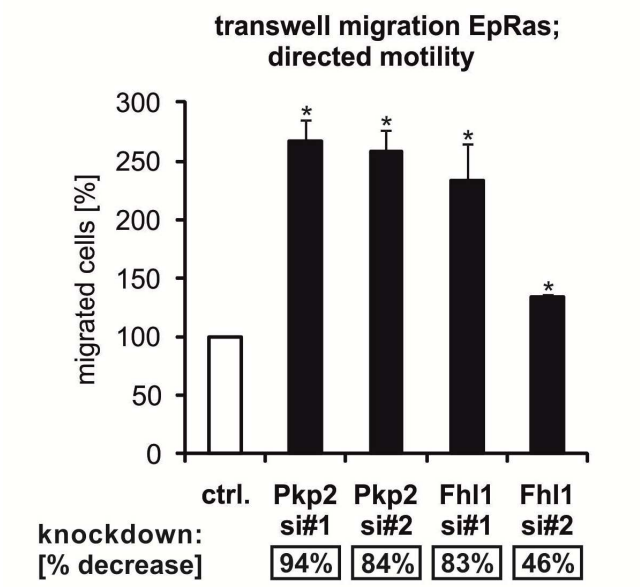

Figure VI-40: Pkp2 and Fhl1 knockdown affects migration of epithelial EpRas cells. Cells were transiently electroporated with the indicated siRNA and plated in uncoated as before. Directed transwell migration was analyzed by letting the cell migrate from serum-free medium towards 10% FCS containing medium for 16 h. A non-targeting siRNA was used as a control. Knockdown efficiencies as assessed by qRT-PCR are given below as percent decrease, compared to the control. Quantitation of the mean relative transwell migration with error bars indicating SEM (n=3) is depicted. Asterisk, significant induction ($p<0.05$, unpaired student's t-test).

These results indicate that both PKP2 and FHL1 are critically limiting the migratory potential of these non-invasive epithelial cells. I also tested the effect of Pai-1 depletion on motility of non-invasive epithelial and mesenchymal cells but due to very low knockdown efficiencies and apparent off-target effects, I was not able to determine its role in cell migration. Eplin-α knockdown had no effect on cell migration under the tested conditions (data not shown).

The strong and significant effects of Pkp2 and Fhl1 knockdown on EpRas migration suggested that these targets could contribute to the antimigratory function of MAL in these cells. Fhl1 was an especially promising target, as its expression in the EpRas lines stably expressing various MAL constructs strongly correlated with the observed migration rates through uncoated transwell membranes.

6.1 Knockdown of Pkp2 and Fhl1 partially rescues the antimigratory MAL effect in epithelial cells

To establish a contribution of these novel targets to the MAL mediated migration effect, I tested, whether a knockdown of Pkp2 and Fhl1 could restore normal transwell migration rates in the EpRas line stably expressing MAL (met). Depletion of either Pkp2 or Fhl1 by transient electroporation with two different siRNAs each resulted in a more than twofold increase in migrated cells compared to MAL (met) expressing cells transfected with a control siRNA (Figure VI-41A). The effects of both Pkp2 siRNAs were significant. Double knockdown of Fhl1 and Pkp2 also resulted in a significant and even slightly stronger enhancement of transmigration. However, comparison to EpRas cells stably infected with the vector control revealed, that migration was only partially restored (Figure VI-41A). Target mRNA levels in the different samples were analysed by quantitative RT-PCR (Figure VI-41B).

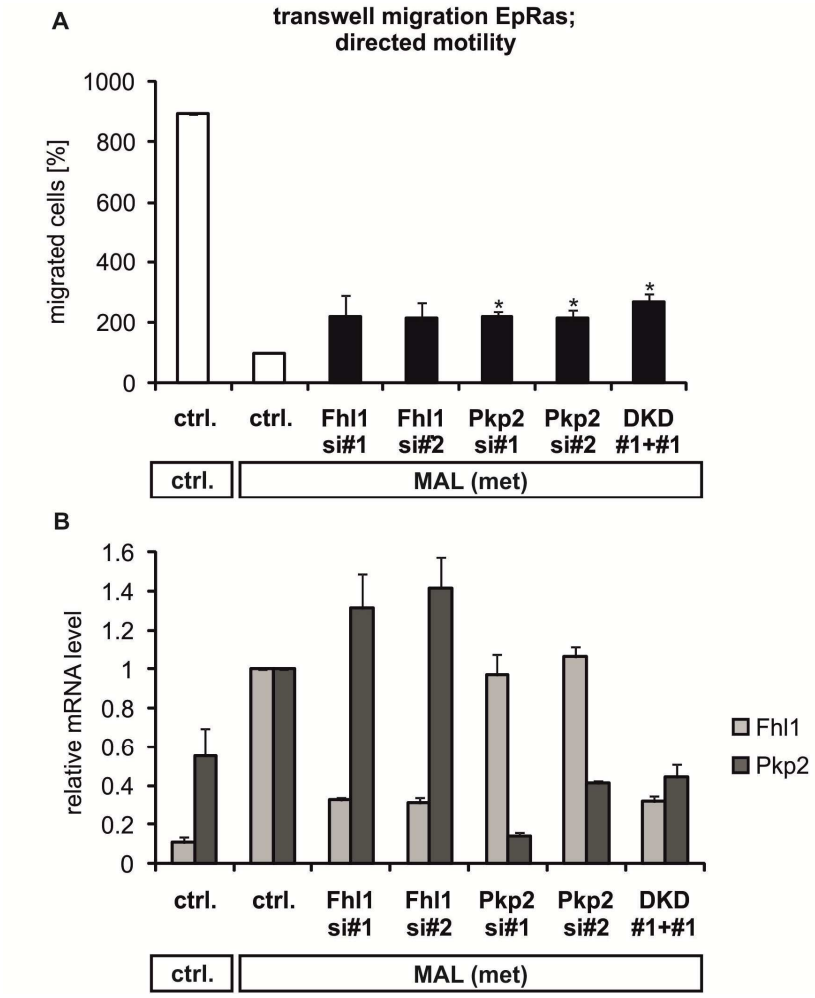

Figure VI-41: The antimigratory effect of MAL is partially rescued by knockdown of Fhl1 or Pkp2. EpRas cells stably infected with MAL (met) or vector control were transiently electroporated with the indicated siRNA (ctrl., non-targeting siRNA; DKD, double knockdown of Fhl1 and Pkp2). Directed cell migration was analyzed by letting cells migrate from FCS free medium in the upper transwell compartment towards 10% FCS containing medium in the lower chamber for 16 h. Shown is the mean relative transwell migration with error bars indicating SEM (n=3). Asterisk, significant induction compared to MAL expressing cells electroporated with control siRNA ($p<0.05$, unpaired student's t-test) (A). Relative Fhl1 and Pkp2 mRNA levels upon knockdown were measured by quantitative RT-PCR. Shown are the mean relative mRNA levels compared to MAL expressing cells electroporated with control siRNA after normalization to Hprt. Error bars, SEM (n=3).

The residual Pkp2 mRNA levels upon transfection with Pkp2 siRNA #1 and siRNA #2 as well as in the double knockdown fell below the endogenous Pkp2 mRNA levels in the vector control cells not stably overexpressing MAL (met) (Figure VI-41B). Insufficient Pkp2 knockdown efficiencies could therefore not explain the partial rescue of migration. In contrast, the remaining Fhl1 mRNA amount upon transient Fhl1 depletion in the MAL (met) expressing cells was still three times higher than in the control infected cells (Figure VI-41B). This demonstrates that insufficient Fhl1 knockdown efficiency could have prevented a complete rescue. Furthermore, Pkp2 and Fhl1 are most likely not the only targets contributing to the antimigratory function of MAL in non-invasive epithelial cells. Nevertheless, these results show that depletion of Fhl1 and Pkp2 partially restores the antimigratory effect of MAL and strongly suggest that their upregulation is involved in MAL regulation of cell motility.

7 Regulation of MAL during epithelial-mesenchymal transition

Carcinoma progression was shown often to involve a so called epithelial-mesenchymal transition (EMT); cell-cell contacts dissociate and epithelial cells transform into unpolarized motile cells as an early step of tumor progression (Perl et al., 1998).

Two recent reports have proposed that the transcriptional coactivators of the MAL/MRTF family are required for both EMT induction (Morita et al., 2007) and invasive cell motility (Medjkane et al., 2009).

In turn, we have recently demonstrated that MAL is activated during EMT and calcium-dependent disassembly of E-cadherin-mediated epithelial junctions through activation of Rac and dissociation of MAL from G-actin (Busche et al., 2008; Busche et al., 2010).

In order to investigate the involvement of MAL expression and activity in EMT I induced EMT with EGF or TGF-β in several model cell lines, including NBT-II (rat bladder carcinoma), PANC-1 (human pancreatic carcinoma), HaCaT (human keratinocytes) and EpRas. Phase contrast imaging confirmed the typical early morphological changes such as scattering and flattening (Figure VI-42).

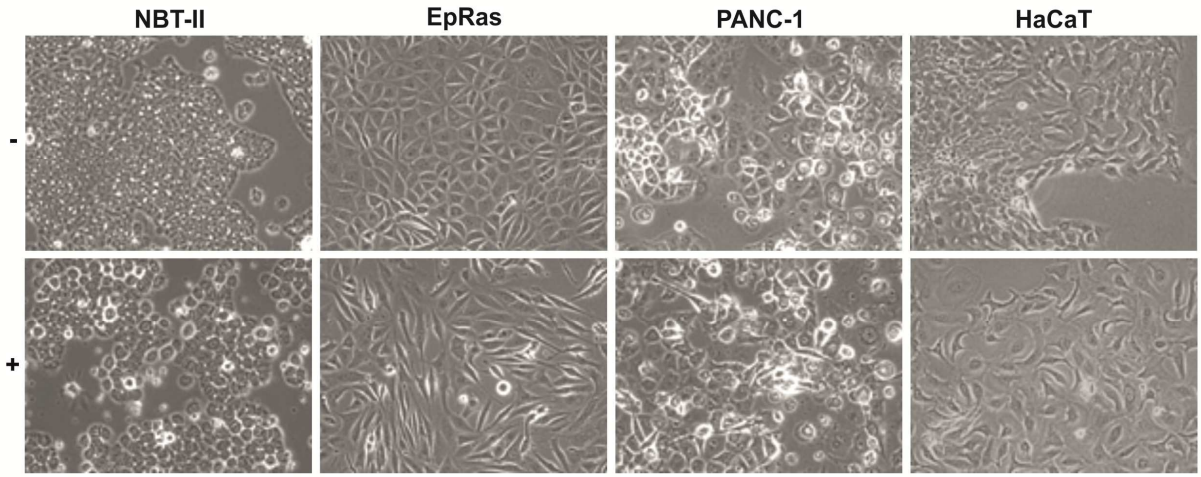

Figure VI-42: Induction of epithelial-mesenchymal transition in four model cell lines. To induce EMT, EpRas, PANC-1, and HaCaT cells were treated with recombinant human TGF-β1 (5 ng/ml, 10 ng/ml, and 2.5 ng/ml, respectively). NBT-II cells were treated with recombinant human EGF (10 ng/ml). The medium was changed every second day. Representative phase contrast micrographs were taken after three days.

As observed before in EpRas cells (Busche et al., 2008), EMT induction resulted in induced MAL dependent SRF activity in all four model cell-lines, as assessed by luciferase assays (Figure VI-43). I could therefore confirm that dissociation of epithelial junctions and epithelial-mesenchymal transition stimulates MAL transcriptional activity through signaling.

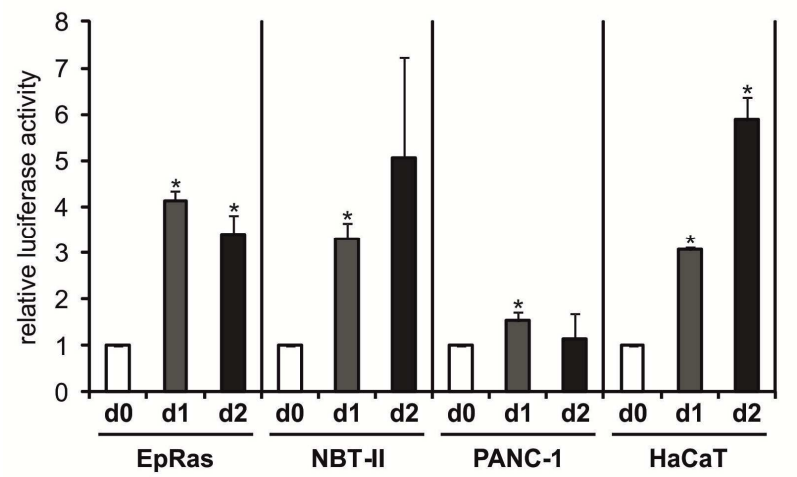

Figure VI-43: Induction of MAL dependent SRF activity during EMT. Relative SRF luciferase reporter activity in EMT model cell lines. Cells were transfected with a MAL responsive luciferase reporter. 24 hours later EMT was induced as described above (see Figure VI-42). Shown is the mean relative luciferase activity after normalization against renilla luciferase activity in comparison to untreated control cells. Error bars indicate SEM (n=3). Asterisk, significant induction ($p<0.05$, unpaired student's t-test).

Furthermore I analyzed the regulation of MAL expression upon EMT induction by immunoblotting. In all four model cell-lines MAL protein levels were quickly elevated at the onset of EMT, regardless of the used EMT inducing ligand (Figure VI-44). It is important to note, that the antibody used for immunoblotting recognizes both MAL and MRTF-B.

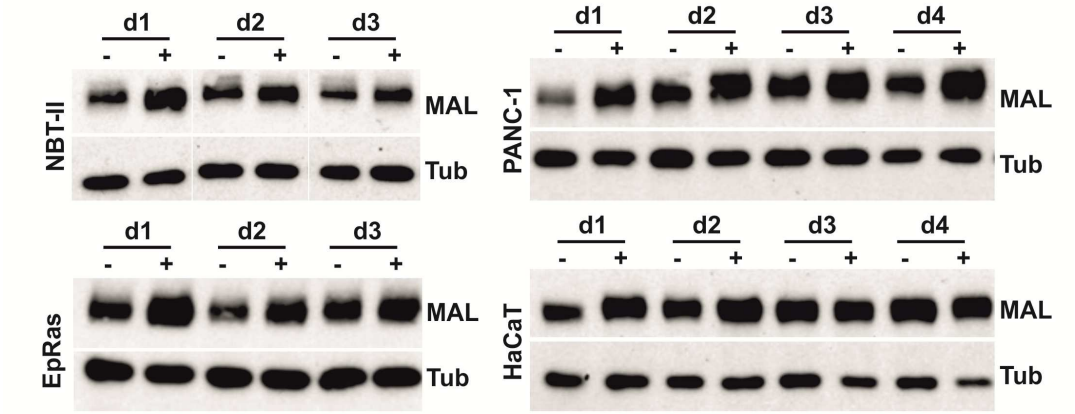

Figure VI-44: MAL protein is upregulated upon EMT induction. MAL Protein was determined by immunoblotting of 20 µg of total lysate from the indicated cell lines. EMT was induced as described above. Tubulin served as loading control.

Next I analyzed the effect of EMT induction in these model cell lines on MAL and Mrtf-B mRNA levels by quantitative RT-PCR. Endogenous MAL mRNA was quickly upregulated upon EMT induction (Figure VI-45). Thus, epithelial-mesenchymal transition not only stimulates MAL transcriptional activity through signaling but additionally induces MAL expression as observed on mRNA and protein level. Strikingly, Mrtf-B mRNA levels remained essentially unaffected (Figure VI-45).

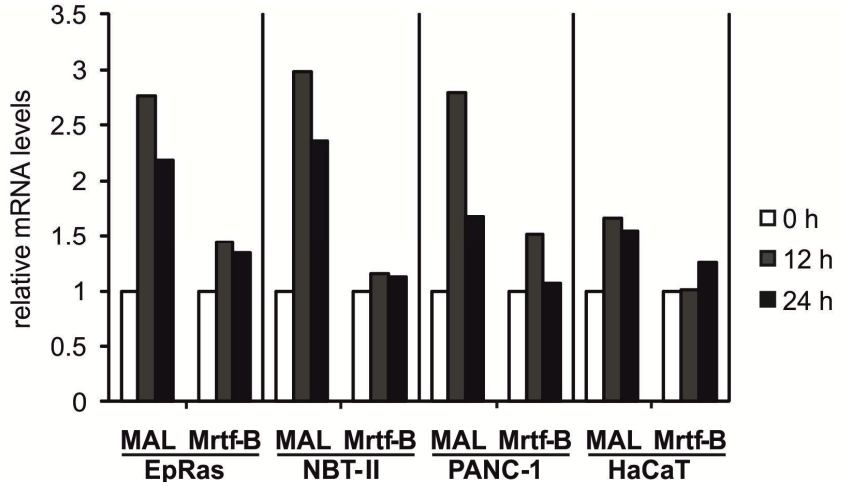

Figure VI-45: MAL mRNA is upregulated upon EMT induction. MAL and Mrtf-B mRNA regulation during EMT was analyzed by quantitative RT-PCR. EMT was induced as described above. Shown are the relative mRNA levels after normalization to Hprt (EpRas and NBT-II cells) or Alas1 (PANC-1 and HaCaT cells) in comparison to untreated cells. Error bars indicate SEM (n=3). Asterisk, significant induction ($p<0.05$, unpaired student's t-test).

Together, these results suggest a role of MAL during early steps of EMT. Whether the enhanced MAL expression at the onset of EMT represents a feed-forward regulation or rather a negative feedback mechanism has yet to be determined.

7.1 Contribution of miRNAs to the differential regulation of MAL

I thus asked which mechanisms might affect MAL expression during epithelial-mesenchymal transition. One possibility could be modulation by microRNAs, which fine-tune mRNA expression and stability (reviewed in (Bartel, 2004)). It has been estimated that 30% of all genes are subject to regulation by microRNAs. Cancer-associated EMT and metastasis are among the numerous processes regulated by miRNAs (reviewed by (Gregory et al., 2008; Ma and Weinberg, 2008).

Therefore I used the miRNA databases PICTAR and TargetScan to screen for miRNA binding sites in the 3'UTR of the MAL mRNA. Indeed, we found three miRNAs potentially targeting MAL. They are good candidate miRNAs because i) they are phylogenetically highly conserved (human, mouse, rat, dog, chicken); ii) they have highly-conserved binding sites in the MAL 3'UTR; iii) the free energy ($-\Delta G$) of the binding is high; and iv) they form excellent seeds comprising the nucleotides 2-8 of the miRNA (Fig. 4).

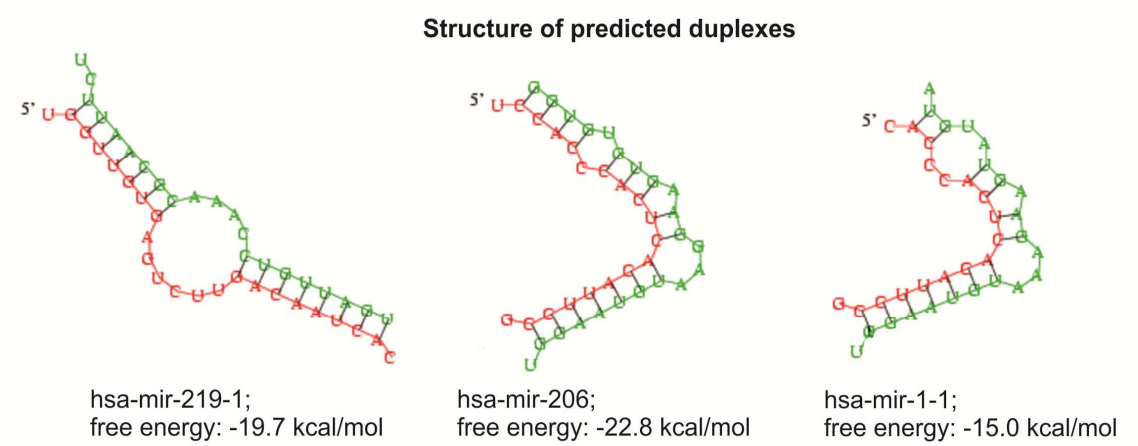

Figure VI-46: Schematic diagram of the predicted duplexes between MAL mRNA and the potential MAL targeting miRNAs. miRNAs (green), corresponding binding sites in the MAL 3'UTR (red), and the free energies of the binding are depicted. The predicted duplexes between the MAL 3'UTR and the potential targeting miRNAs show perfect-match base pairing comprising nucleotides 2-8 of the miRNA.

Of note, we did not find any miRNA potentially targeting Mrtf-B, which failed to show differential expression during EMT. The miRNA miR-1-1 is transcriptionally regulated by the MAL homolog myocardin and SRF itself and is prominently expressed in muscle cells (Chen et al., 2006; Zhao et al., 2005). However, it is repressed in metastasizing hepatocellular carcinoma, whereas miR-219 was found to be induced in the same study (Budhu et al., 2008). The miR-206 is also predominantly expressed in muscle (Sweetman et al., 2008), but suppresses breast cancer metastasis *in vivo* and reduces migration *in vitro* through as yet unknown mechanisms (Tavazoie et al., 2008).

I used synthetic 2'-O-methyl antisense-RNAs to target these endogenous miRNAs. The neuron-specific miR-124, which has no homology to MAL, was used as a negative control (Visvanathan et al., 2007). To monitor the effect on MAL expression, I cloned the 3'UTR of human, rat and mouse MAL behind a luciferase reporter gene under the control of a constitutive TK promoter. Assuming that the endogenous miRNAs under investigation are indeed targeting the putative binding sites in the MAL 3'UTR, inhibition of these miRNAs should lead to an increased reporter activity.

The EMT model cell lines were transiently transfected with the luciferase reporter plasmid containing the corresponding MAL 3'UTR (human, rat, and mouse, respectively) and the synthetic 2'-O-methyl antisense-RNAs. Two days after transfection with the antisense-RNA targeting miR-1-1 a significant induction of reporter activity as assessed by luciferase assays could be observed in murine EpRas and human PANC-1 cells. However, the effect was only transient, on day three reporter activity reached basal levels again. The antisense-RNAs targeting miR-206 and miR-219 had no significant effect on luciferase reporter activity (data not shown).

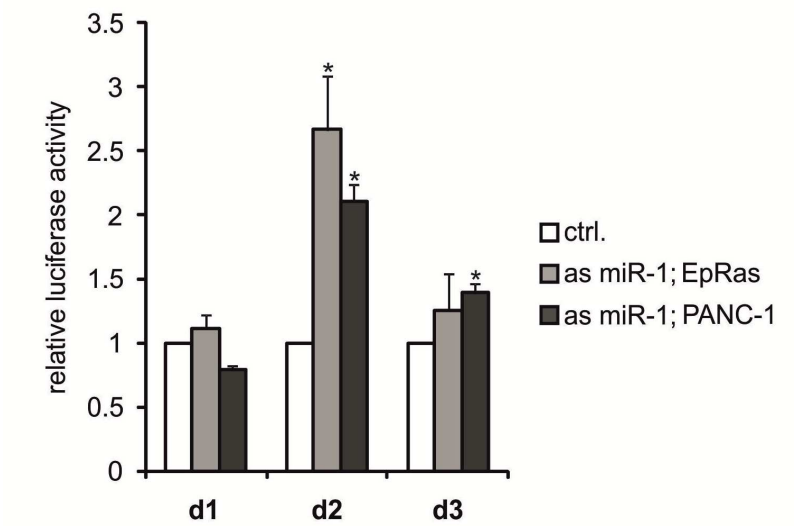

Figure VI-47: Inhibition of miR-1 induces MAL 3'UTR driven reporter activity. Cells were simultaneously transfected with a MAL 3'UTR containing luciferase reporter and a synthetic 2'-O-methyl anti-miR-1 antisense-RNA. Shown is the mean relative luciferase activity after normalization against renilla luciferase activity in comparison cells transfected with a control antisense RNA (2'-O-methyl anti-miR-124 antisense RNA). Error bars indicate SEM (n=3). Asterisk, significant induction ($p<0.05$, unpaired student's t-test).

These preliminary results suggest that miR-1-1 might be able to target the 3'UTR of MAL and thereby inhibit MAL expression.

I also analyzed the effect of miRNA inhibition by transient transfection with 2'-O-methyl antisense-RNAs on endogenous MAL protein levels but did not obtain reproducible results probably due to the rather weak regulation mediated by miRNAs that is considered to fine tune target expression.

Ectopic overexpression of miRNAs also yielded divergent results. I could not determine the underlying cause as I was unable to measure the obtained miRNA levels by Northernblotting. The establishment of a sensitive method to quantify miRNA levels will be critical not only as a quality control for experimental setups but also to measure the endogenous levels of miR-1, miR-206, and miR-219 in my cellular systems and analyze the regulation of these miRNAs during EMT.

Therefore, further analyses to establish the regulation of MAL expression by miRNAs and to relate the corresponding miRNAs to EMT induction will have to be carried out.

VII. Discussion

1 MAL/MRTF impairs migration on non-invasive cells

Cell migration is a highly regulated process that is fundamental for tissue formation, maintenance and regeneration. Efficient cell migration requires spatial and temporal coordination and a tightly regulated interplay between cell-cell adhesion, cell-matrix adhesion and localized cytoskeletal reorganization. Changes in the concentration of adhesion receptors, cytoskeleton-linking proteins and extracellular matrix ligands can affect cell motility (Huttenlocher et al., 1995).

The transcription factor SRF plays important roles in cytoskeletal organization and actin homeostasis (reviewed in (Miano et al., 2007). Srf depletion in mice results in embryonic lethality at gastrulation. Srf (-/-) embryonic stem cells show impaired cell spreading, adhesion and migration due to defective formation of actins stress fibers and focal adhesion plaques (Schratt et al., 2002). Numerous MRTF dependent SRF target genes are involved in contractile functions, actin microfilament dynamics and cell motility (reviewed in (Olson and Nordheim, 2010)) pointing towards an important role for MAL-SRF signaling in cell migration.

In this study I show that MAL impairs cell motility of non-invasive fibroblasts and epithelial cells. Ectopic expression of active MAL negatively affects NIH 3T3 migration in wound closure and transwell assays. Conversely, dominant negative and MAL knockdown constructs enhance NIH 3T3 migration. In line with this active MAL impairs transwell migration of epithelial EpRas cells whereas dominant negative and knockdown constructs enhance EpRas cell motility. Although mesenchymal and epithelial migration modes differ considerably, MAL-SRF signaling seems to influence motility of both fibroblasts and epithelial cells equally, pointing to a common function of MAL in non-invasive cell migration.

As numerous targets of MAL-SRF signaling encode cytoskeletal proteins associated with cell junctions, active MAL supposedly strengthens both cell-cell and cell-matrix adhesions. Two key steps in migration are focal adhesion (FA) formation and disassembly (Webb et al., 2002) and fast FA turnover correlates with high migration velocity. Increasing cell-matrix adhesiveness by MAL-mediated upregulation of integrin α5 might inhibit FA disassembly at the rear and therefore impair cell migration. Also, it is conceivable that MAL-mediated strengthening of cell-cell adhesions via upregulation of cytoskeletal proteins associated with cell-cell junctions such as Plakophilin 2 could hinder mesenchymal single cell movement. It has to be noted though, that mesenchymal and epithelial cell migration differ considerably, especially regarding the preservation of cell-cell adhesion during motility. Whereas mesenchymal cells migrate as individual cells, epithelial cells usually move collectively as epithelial sheets (Friedl and Wolf, 2010). Nevertheless, migration of EpRas cells through transwell membranes most likely does not resemble the typical collective epithelial mode of motility but rather reflects amoeboid-like motility or multicellular streaming. Ectopic expression of active MAL could lead to an upregulation of cytoskeletal proteins associated with cell-cell adhesions

such as Plakophilin 2. The resulting strengthening of desmosomal cell-cell contacts could therefore impair epithelial transwell motility.

Another mechanism by which MAL-SRF signaling could impair cell motility might be the MIG6 mediated negative crosstalk towards the EGFR-MAPK signaling axis (Descot et al., 2009). Nevertheless, the inhibitory effect on MAPK signaling most likely does not account solely for the antimigratory MAL effect, as it was also observable in the absence of any inducers of the MAPK signaling nodule.

The fact that a complete Mrtf-B knockout in MAL depleted non-invasive mouse embryonic fibroblasts results in impaired migration in wound healing assays (Mokalled et al., 2010) points to a biphasic dependence of migration speed on MAL expression. This might be explained by the numerous MRTF target genes involved in adhesiveness. Theoretical analyses predict that the cell-substratum adhesion strength contributes to the rate of locomotion in a biphasic manner, with maximal migration speed at intermediate adhesiveness (DiMilla et al., 1991) as the speed generated by the migration cycle is limited by the turnover rates of adhesion and de-adhesion events. Indeed this biphasic dependence could be demonstrated for integrin α5 and its ligand fibronectin: migration speed is highest at intermediate receptor and ligand concentrations and both increasing and decreasing the cell-substratum adhesion strength by altering the receptor or ligand concentration impairs migration (Palecek et al., 1997). If MAL activity correlates through its cytoskeletal targets with adhesiveness, altering MAL expression could have different outcomes depending on the adhesive/cytoskeletal repertoire of the cell. Figure VII-1 depicts this hypothesis.

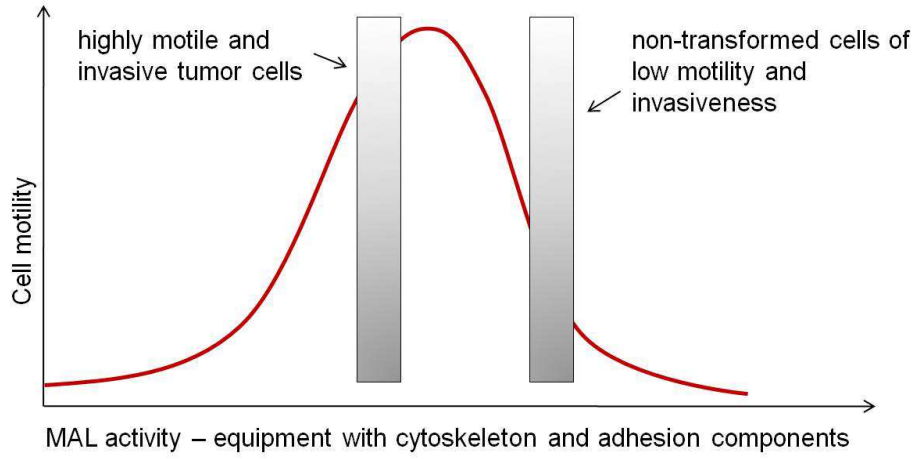

Figure VII-1 Migration speed might exhibit a biphasic dependence on MAL signaling activity due to numerous MRTF target genes involved in adhesiveness.

The highly-adherent cells investigated here may harbor a repertoire of adhesion receptors that is above the migratory optimum. Consistent with this hypothesis, MAL overexpression impairs migration, whereas a partial knockdown of MAL has a beneficial effect on cell motility. Unsurprisingly a further decrease in cytoskeletal target gene expression by a complete Mrtf knockout leads to drastic changes

in the cytoskeletal organization and impairs cell migration as reported for Mrtf double knockout MEFs (Mokalled et al., 2010).

MRTFs have recently been shown to be required for tumor cell invasion and metastasis (Medjkane et al., 2009). Knockdown of both MAL and Mrtf-B strongly reduced adhesion, spreading, invasion and motility of highly invasive breast cancer and melanoma cells (Medjkane et al., 2009).

These results seem to be contradictory to the antimigratory function of MAL I observed in non-invasive cells. I addressed this apparent discrepancy by Mrtf depletion in the previously used MDA-MB-231 cell line. The antimigratory effect of Mrtf knockdown in these highly invasive breast cancer cells could be reproduced, excluding experimental differences as a primary reason for the inconsistent results. In addition ectopic expression of the MAL constructs in TGF-β treated invasive EpRasXT cells that had undergone an epithelial-mesenchymal transition showed opposite effects on migration compared to the epithelial EpRas cells: active MAL strongly enhanced migration in transwell chambers, whereas dominant negative MAL had no effect or caused a slight reduction in motility. These findings suggest a fundamentally different migratory function of MRTFs in invasive and non-invasive cells.

One explanation could be that activated oncogenes or various induced signaling pathways in transformed and invasive cells distinctly affect the migratory response to altered MAL target genes expression.

The biphasic model for the dependence of migration speed on MAL activity might provide another explanation: invasive cells such as the human breast cancer cells MDA-MB 231 are less adherent to the ECM substrate or to neighboring cells as they are equipped with levels of cytoskeletal components and adhesion receptors that are optimized for migration. Knockdown of MRTFs and reductions of its cytoskeleton-associated targets therefore reduces motility.

In line with this both non-invasive and invasive cells ectopically expressing activated MAL show a large numbers of focal adhesions and a strongly spread-out morphology, which may be indicative for increased adhesion and less motile properties (Descot et al., 2009; Medjkane et al., 2009). Vice versa, transformation of rat intestinal epithelial cells with RAS or SRC suppressed the nuclear translocation of MRTF-A/B and resulted in disorganization of the actin cytoskeleton and reduced expression of the SRF/MRTF-regulated cytoskeletal proteins caldesmon and tropomyosin. Expression of constitutively active MRTF-A/B in these transformed cells reversed these effects and impaired their invasiveness and anchorage-independent growth (Yoshio et al., 2010).

Based on my results I suggest that MAL influences cell adhesiveness through the regulation of cytoskeleton-associated target genes, thereby controlling motility. Migration speed shows a biphasic dependence on adhesive strength which is not only contingent on integrin expression but numerous other cytoskeletal MRTF target genes. Thus I propose a biphasic model for the dependence of migration speed on MAL activity. It is conceivable, that in highly adherent non-invasive cells, the transcriptional upregulation of the cellular adhesive machinery by MAL results in a net reduced

migration. Ectopic overexpression of MAL might also negatively affect cell migration in highly invasive cells, consistent with the results of Yoshio et al. (Yoshio et al., 2010), but this remains to be tested for the invasive MDA-MB-231 cells.

Endogenous MAL activity and target gene expression is in turn regulated by actin microfilament dynamics, establishing an actin-MRTF-SRF circuit controlling cell motility. Thus, MAL-mediated transcription appears to be at the center of a negative feedback loop which functions to counteract inappropriate migration of non-invasive cells.

2 Cytoskeleton-associated target genes mediate motile functions of MAL

I wanted to identify target genes that mediate the motile functions of MAL in non-invasive cells. I deliberately focused on recently identified novel G-actin regulated genes that were shown to be upregulated by cytochalasin D and downregulated by latrunculin B (Descot et al., 2009). Among these targets cytoskeleton-associated genes with putative roles in cell migration were investigated further in this study.

Integrin receptors mediate attachment of the cell to the ECM and have crucial functions in cell migration. Thus, the novel G-actin target integrin α5 was an obvious choice for further characterization. It contains a CArG-like element (ACTTATAAGG) at position -1691 in its promoter that was shown to be bound by SRF in EMSA (Sun et al., 2006a). Furthermore we have recently shown that Itga5 is transcriptionally induced by activated forms of MAL and SRF (Descot et al., 2009). Preliminary results show, that the Itga5 promoter mediates regulation of a luciferase reporter. The promoter constructs are responsive to active MAL, serum, cytochalasin D and latrunculin B. The regulation of the Itga5 promoter by actin-MAL signalling seems to be mediated by the CArG-like element at position -1691, presumably in conjunction with another more proximal CArG Box at position -530 (CCAAGAAAGG) or -153 (CCTCATTAGG) as demonstrated by luciferase assays and ChIP (Mengel et al., unpublished data).

As mentioned above, migration speed shows a biphasic dependence on the concentration of integrin α5 and its ligand fibronectin (Palecek et al., 1997). In line with this, the Itga5 siRNA yielding better knockdown efficiencies showed in both migration assays weaker effects probably as the extremely low Itga5 levels attained with this siRNA might be suboptimal for NIH 3T3 motility. Thus, a complete depletion would presumably impair motility. Itga5 regulation through actin MAL might have a significant impact on cellular behavior as the ratio of integrin α subunit expression determines the composition of surface integrin heterodimers, which affects cell fate (Sastry et al., 1996). Moreover the α5 integrin displays a dynamic pattern of expression, for instance during muscle differentiation (Blaschuk and Holland, 1994).

I show that knockdown of the armadillo family member Pkp2 enhances motility of EpRas epithelial cells and NIH 3T3 fibroblasts. In addition Pkp2 knockdown partially rescues the antimigratory effects of MAL. PKP2 is a major regulator of desmosome composition and positioning (Chen et al., 2002;

Goossens et al., 2007). It coordinates actin-dependent maturation of desomosome precursors by interacting with the intermediate filament-desmoplakin complex, PKCα, and possibly F-actin (Bass-Zubek et al., 2008; Godsel et al., 2005). Among the plakophilins, PKP2 shows the broadest tissue distribution (Bonne et al., 1999; Mertens et al., 1996; Schmidt et al., 1999) and is the only plakophilin expressed in the heart. It is also detectable in fibroblasts (Figure VI-24; Figure VI-25) and mesenchymal cells, where it colocalizes with classical cadherins at sites of cell-cell contacts (Rickelt et al., 2009). PKP2 is essential for desmosome integrity in epithelial cells and cardiomyocytes (Grossmann et al., 2004; Pieperhoff et al., 2008). Ablation of Pkp2 in mouse results in lethal heart defects due to destabilized junctions (Grossmann et al., 2004). It is therefore conceivable, that the promigratory effect of Pkp2 knockdown reported here is mediated by weakening of cell-cell contacts, both in fibroblasts and epithelial cells. Furthermore dissolution of desmosomes might trigger intermediate filament remodeling, which has been implicated in cell migration (Beil et al., 2003; Bruel et al., 2001). However it has to be noted that PKP2 might affect cell migration by other mechanisms such as regulation of PKC or β-catenin signaling (reviewed in (Bass-Zubek et al., 2009; Chen et al., 2002) and it cannot be excluded that it exerts additional functions at catenin-containing junctions or in the nucleus (Bass-Zubek et al., 2009).

I characterized Pkp2 as a novel actin-MAL-SRF target gene. An intronic conserved CArG-like element is inducibly bound by both MAL and SRF as shown by chromatin IP. The inducible recruitment of SRF is somewhat unusual as consensus CArG Boxes in their proximal promoters of other known SRF targets such as Vinc, Srf, Cyr61 and Eplin-α, were shown to be constitutively bound by SRF (Descot et al., 2009; Leitner et al., 2010; Miralles et al., 2003). The slightly different occupation of the Pkp2 CArG-Box by SRF suggests cooperative binding of MAL and SRF, which might be caused by the intronic nature of this responsive element or the variation from the consensus sequence at position 5 (CCTTGTAAGG).

Intriguingly, the recently described skin-specific Srf knockout in mice resulted in a hyperproliferative skin disease, associated with impaired desmosome formation (Koegel et al., 2009). Whether PKP2 expression in the affected skin layers is decreased by Srf depletion, or even causative for desmosome malformation, remains to be investigated.

Similar to Pkp2 depletion Fhl1 knockdown enhanced cell motility of epithelial EpRas cells and partially rescued the antimigratory MAL effect. Migration of fibroblasts was however barely affected. Of note, among the target genes under investigation Fhl1 expression was most strongly and consistently affected by all MAL constructs in epithelial EpRas cells as well as in NIH 3T3 fibroblast (Figure VI-16; Figure VI-20), strongly suggesting that Fhl1 is a direct MAL-SRF target gene. Moreover, EpRas transwell migration persistently correlated well with low Fhl1 expression.

Consistent with my finding that Fhl1 is regulated by MAL-SRF signaling, a conserved intronic consensus CArG Box has been identified (Sun et al., 2006a). Moreover, the closely related Fhl2 gene is a known MAL/SRF target, and expression of Fhl1 follows that of Fhl2 (Philippar et al., 2004).
Together, this strongly suggests that Fhl1 is a direct MAL-SRF target that plays important roles in mediating the antimigratory effect of MAL epithelial cells.

FHL family members exert important roles in focal adhesion. FHL1 localizes to the actin cytoskeleton, intercellular junctions, and focal adhesions (Brown et al., 1999), and interferes with integrin-mediated processes (Robinson et al., 2003). It was shown to affect adhesion, spreading and migration of myoblasts (Robinson et al., 2003). In SRC-transformed fibroblasts, FHL1 has been shown to inhibit non-anchored tumor cell growth and migration unless it is suppressed by CAS phosphorylation (Shen et al., 2006).
It is important to note, that FHL1 could affect cell migration by means other than its cytoskeletal function, as it is also involved in transcriptional regulation by binding and modulating the activity of multiple transcription factors. For instance, FHL1 was reported to interact with SMAD family members mediating a TGF-ß like response that results in activation of Pai-1 and the tumor suppressor gene p21, and repression of the oncogene c-myc (Ding et al., 2009b).
Interestingly FHL1 expression is down-regulated in various types of malignancies and negatively correlates with tumor progression (Ding et al., 2009b; Shen et al., 2006). It is thus another addition to the increasing number of MAL-SRF regulated putative tumor suppressor genes, such as Mig6, Eplin-α and Cyr61.
Similar to FHL1, Epithelial Protein Lost in Neoplasm α is a novel cytoskeleton-associated tumor suppressor responsive to MAL-SRF signaling as judged by its induction in the unbiased microarray screen, its MAL-controlled transcriptional regulation, the responsiveness of its proximal promoter to G-actin binding drugs and mutant actins, and its chromatin IP, which identified a proximal consensus CArG Box that constitutively binds SRF and inducibly recruits MAL. Eplin crosslinks, bundles and stabilizes F-actin filaments and stress fibers, which correlates with its ability to suppress anchorage-independent growth in transformed cells (Han et al., 2007; Maul et al., 2003; Song et al., 2002). Furthermore it was shown to negatively affect cell motility (Jiang et al., 2008). Unfortunately I was not able to confirm this antimigratory function of Eplin-α in my model systems, probably due to insufficient knockdown, principally different functions of Eplin-α in the used cell lines or unsuitable migration assays.
As yet, I neither could address the migratory role of Pai-1 due to off-target effects but it could be established as a direct target of actin-MAL signaling, based on differential regulation by actin binding drugs and the consistent response to MAL overexpression and knockdown in both cell lines. Intriguingly, PAI-1 expression is induced during fibroblast scratch wounding, but transcriptionally inhibited by the ternary complex factor Net/Sap-2 which is required for optimal cell migration

(Buchwalter et al., 2005). Ternary complex factors and MRTF family members can compete for SRF binding, whereby the weaker transactivating properties of the ternary complex factors essentially result in inhibited gene expression (Wang et al., 2004; Zaromytidou et al., 2006). Pai-1 is typically known as a TGF-β induced SMAD target, but recent reports also proposed physical and functional interactions between MAL and SMADs, or FHL1 and SMADs (Ding et al., 2009b; Masszi et al., 2010; Morita et al., 2007). Importantly, although the induction of Pai-1 upon MAL overexpression could theoretically be an indirect effect mediated FHL1, the transcriptional upregulation of Pai-1 by G-actin binding drugs in the presence of the translation inhibitor cycloheximide strongly suggests, that Pai-1 is a direct MAL-SRF target. Precise analysis of Pai-1 transcriptional regulation remains an interesting subject to investigate.

Taken together, Itga5, Pkp2, and Fhl1 were shown to contribute to the MAL-mediated restriction of cell motility, but neither Pkp2 nor Fhl1 depletion nor double knockdown could fully rescue the antimigratory effects of MAL. Given the number of MAL target genes encoding structural and regulatory cytoskeletal components it seems likely that ITGA5, PKP2 and FHL1 cooperate with other known targets to mediate the antimigratory effect of MAL.

3 Involvement of MAL in epithelial-mesenchymal transition

Finally, I analyzed the regulation of MAL during epithelial-mesenchymal transition, as MRTFs have recently been implicated EMT. Our lab has recently demonstrated that MAL transcriptional activity is induced during EMT and calcium-dependent disassembly of epithelial junctions, which could be verified for all four EMT model systems I tested. Furthermore I demonstrated that MAL is upregulated on both mRNA and protein level upon EMT induction whereas MRTF-B expression is essentially unaffected.

Myocardin was shown to induce the expression of differentiation markers and block malignant growth in human sarcoma cells (Kimura et al., 2010; Milyavsky et al., 2007).

In contrast, MRTFs were reported to be critical mediators of EMT (Morita et al., 2007). In line with our own results TGF-β1 was shown to trigger the nuclear translocation of MRTFs. The authors further suggested the association of MRTFs with Smad3 and the subsequent binding and activation of the slug promoter by the MRTF-Smad3 complex. They propose that the transcriptional induction of slug mediated dissociation of cell-cell contacts.

It is however rather surprising that the levels of epithelial and mesenchymal marker proteins were already drastically changed after 24h of TGF-β1 treatment as they are normally assessed 5 to 7 days after EMT induction. Moreover the induction of EMT by MRTF signaling through Smads has been challenged by Medjkane et al. (Medjkane et al., 2009), as MRTF depletion did not affect expression of mesenchymal markers or regulators of EMT. The similarities between the cytoskeletal phenotypes of Mrtf and Srf-depleted cells suggested an SRF-mediated action of MRTFs.

Our own preliminary observations rather point to a long-term stabilization of the epithelial phenotype mediated by the induction of transcriptional MAL activity.

In line with this hypothesis, the group that initially suggested the requirement of MRTFs for EMT induction (Morita et al., 2007) recently reported that MRTFs suppress the oncogenic properties of v-ras- and v-src-mediated transformants, enhance the formation of stress fibers and focal adhesions and result in a flattened cell shape.

I therefore propose, that the fast upregulation of MRTF-A expression upon EMT induction might represent a negative feedback loop counteracting the loss of epithelial markers.

Luciferase reporter assays suggested that the MAL 3' UTR is targeted by endogenous miR-1. Interestingly the miR-1 gene is a direct transcriptional target of serum response factor (Zhao et al., 2005) and myocardin overexpression in human aortic smooth muscle cells was shown to induce miR-1 expression (Jiang et al., 2010).

Strikingly exogenous miR-1, which did not affect myocardin or SRF expression, suppressed the expression of contractile proteins, such as alpha-SMA and SM22, and impaired the actin cytoskeletal organization (Jiang et al., 2010). This reveals a negative feedback loop involving miR-1 in SMCs that regulates contractility induced by myocardin. I suggest that the myocardin-induced miR-1 upregulation might reduce MRTF-A expression, resulting in impaired actin cytoskeletal organization repression of alpha-SMA and SM22.

VIII. Abbreviations

Within this thesis the following abbreviations were used.

ADP	adenosine diphosphate
AJ	adherens junction
AMP	adenosine monophosphate
Amp	ampicilline
Ampr	ampicilline resistance
APS	ammonium peroxidsulfate
Arp2/3 complex	actin-related protein-2/3 complex
as	antisense strand
ATCC	American Type Culture Collection
ATP	adenosine triphosphate
B domain	basic domain
BCA	bicinchoninic acid
BSA	bovine serum albumin
CD	cytochalasin D
cDNA	complementary DNA
ChIP	chromatin immunoprecipitation
CMV	cytomegalovirus
CTGF	connective tissue growth factor
ctrl.	control
DAPI	4’,6-diamidino-2-phenylindole hydrochloride
DKD	double knock down
DMEM	Dulbecco’s Modified Eagle Medium
DMSO	dimethyl sulfoxide
DNA	deoxyribonucleic acid
DP	desmoplakin
DTT	dithiothreitol
E.coli	*Escherichia coli*
ECM	extracellular matrix
EDTA	ethylenediaminetetraacetic acid
EGF	epidermal-growth factor
EGFP	enhanced green fluorescent protein
EGFR	epidermal-growth factor-receptor
EMSA	electrophoretic mobility shift assay
EMT	epithelail-mesenchymal transition

EPLIN	epithelial protein lost in neoplasm
ES cells	embryonic stem cells
FA	focal adhesion
FAK	focal adhesion kinase
F-actin	filamentous actin
FCS	fetal calf serum
FHL	four-and-a-half LIM domains
fl	full length
FRAP	fluorescence recovery after photobleaching
G-actin	globular actin
GAP	GTPase-activating protein
GDI	GDP dissociation inhibitors
GDP	guanosine diphosphate
GEF	guanine nucleotide exchange factor
GTP	guanosine triphosphate
GTPase	small guanosine triphosphatase
HA	hemagglutinin
HEK	Human Embryonic Kidney
HEPES	4-(2-Hydroxyethyl)piperazine-1-ethanesulfonic acid
HPRT	hypoxanthine phosphoribosyltransferase
HPSF	high purity salt free
HRP	horseraddish peroxidase
IB	immunoblot
IF	intermediate filament
IgG	immunoglobulin G
IP	immunoprecipitation
IPTG	isopropyl thiogalactopyranoside
ITGA5	integrin α5
JAM	junctional adhesion molecules
Jas	jasplakinolide
Kan	kanamycine
kd.	knockdwon
LB	latrunculin B
LB broth	Luria-Bertani broth
LIM domain	Lin11, Isl-1 & Mec-3 domain
LIMK	LIM kinase
LPA	lysophosphatidic acid

LZ	leucine zipper
MADS	MCM1, Agamous, Deficiens, SRF
MAL	Megakaryoblastic leukemia protein
MAP	mitogen-activated protein
MAPK	mitogen-activated protein kinase
MAT	mesenchymal-to-amoeboid transition
MDCK	Madin-Darby Canine Kidney
mDia	murine diaphanous
MEK	MAPK/ERK kinase
MET	mesenchymal-epithelial transition
miRNA	microRNA
MLC	myosin light-chain
MLCK	myosin light-chain kinase
MPI	Max Planck Institute
mRNA	messenger RNA
MRTF	myocardin related transcription factor
MT	microtubule
MTOC	microtubule-organizing center
MW	molecular weight
PAGE	polyacrylamid gel electrophoresis
PAI-1	plasminogen activator inhibitor 1
PAK	p21-activated kinase
PBS	phosphate buffered saline
PCR	polymerase chain reaction
PDZ domain	post synaptic density protein, *Drosophila* disc large tumor suppressor, and zonula occludens-1 protein domain
Pg	plakoglobin
PI3K	phosphatidylinositol-3 kinase
PKC	protein kinase C
PKP	plakophilin
PLB	passive lysis buffer
PMSF	phenylmethylsulfonylfluoride
pSR	pSUPER.retro
Puror	puromycine resistance
PVDF	polyvinylidene fluoride
RNA	ribonucleic acid
RIPA	radioimmunoprecipitation assay

ROCK	RhoA activated coiled-coil kinase
RS	restriction site
RT	room temperature
RT-PCR	real time PCR
s.e.m.	standard error of the mean
SAP-1	sphingolipid activator protein-1
SDS	sodium dodecyl sulfate
shRNA	small hairpin RNA
siRNA	small interfering RNA
SOB	super optimal broth
SOC	super optimal broth with catabolite repression
SRF	serum response factor
ss	sense strand
TAT	trans-activator of transcription
TCF	ternary complex factor
TGF-β	transforming growth factor-β
+TIP	plus end interactin protein
TJ	Tight junction
TK	thymidine kinase
TR	transfection reagent
un.	untreated
UTR	untranslated region
VASP	vasodilator stimulated phosphoprotein
WASP	Wiskott-Aldrich syndrome protein
WAVE	WASP-family verprolin-homolougous protein
wt	wild type
ZO	zonula occludens protein

IX. References

Abe, K., and Takeichi, M. (2008). EPLIN mediates linkage of the cadherin catenin complex to F-actin and stabilizes the circumferential actin belt. Proc Natl Acad Sci U S A *105*, 13-19.

Adams, J.C. (2001). Cell-matrix contact structures. Cell Mol Life Sci *58*, 371-392.

Affolter, M., Montagne, J., Walldorf, U., Groppe, J., Kloter, U., LaRosa, M., and Gehring, W.J. (1994). The Drosophila SRF homolog is expressed in a subset of tracheal cells and maps within a genomic region required for tracheal development. Development *120*, 743-753.

Alberti, S., Krause, S.M., Kretz, O., Philippar, U., Lemberger, T., Casanova, E., Wiebel, F.F., Schwarz, H., Frotscher, M., Schutz, G., *et al.* (2005). Neuronal migration in the murine rostral migratory stream requires serum response factor. Proc Natl Acad Sci U S A *102*, 6148-6153.

Alexander, S., Koehl, G.E., Hirschberg, M., Geissler, E.K., and Friedl, P. (2008). Dynamic imaging of cancer growth and invasion: a modified skin-fold chamber model. Histochem Cell Biol *130*, 1147-1154.

Allen, W.E., Zicha, D., Ridley, A.J., and Jones, G.E. (1998). A role for Cdc42 in macrophage chemotaxis. J Cell Biol *141*, 1147-1157.

Arsenian, S., Weinhold, B., Oelgeschlager, M., Ruther, U., and Nordheim, A. (1998). Serum response factor is essential for mesoderm formation during mouse embryogenesis. EMBO J *17*, 6289-6299.

Bartel, D.P. (2004). MicroRNAs: genomics, biogenesis, mechanism, and function. Cell *116*, 281-297.

Bass-Zubek, A.E., Godsel, L.M., Delmar, M., and Green, K.J. (2009). Plakophilins: multifunctional scaffolds for adhesion and signaling. Curr Opin Cell Biol *21*, 708-716.

Bass-Zubek, A.E., Hobbs, R.P., Amargo, E.V., Garcia, N.J., Hsieh, S.N., Chen, X., Wahl, J.K., 3rd, Denning, M.F., and Green, K.J. (2008). Plakophilin 2: a critical scaffold for PKC alpha that regulates intercellular junction assembly. J Cell Biol *181*, 605-613.

Batlle E., S.E., Francí C., Domínguez D., Monfar M., Baulida J., García de Herreros A. (2000). The transcription factor Snail is a repressor of E-cadherin gene expression in epithelial tumour cells. Nat Cell Biol *2*, 84-89.

Bazzoni, G., Martinez-Estrada, O.M., Orsenigo, F., Cordenonsi, M., Citi, S., and Dejana, E. (2000). Interaction of junctional adhesion molecule with the tight junction components ZO-1, cingulin, and occludin. J Biol Chem *275*, 20520-20526.

Beil, M., Micoulet, A., von Wichert, G., Paschke, S., Walther, P., Omary, M.B., Van Veldhoven, P.P., Gern, U., Wolff-Hieber, E., Eggermann, J., *et al.* (2003). Sphingosylphosphorylcholine regulates keratin network architecture and visco-elastic properties of human cancer cells. Nat Cell Biol *5*, 803-811.

Blaschuk, K.L., and Holland, P.C. (1994). The regulation of alpha 5 beta 1 integrin expression in human muscle cells. Dev Biol *164*, 475-483.

Bonne, S., van Hengel, J., Nollet, F., Kools, P., and van Roy, F. (1999). Plakophilin-3, a novel armadillo-like protein present in nuclei and desmosomes of epithelial cells. J Cell Sci *112 (Pt 14)*, 2265-2276.

Brandt, D.T., Baarlink, C., Kitzing, T.M., Kremmer, E., Ivaska, J., Nollau, P., and Grosse, R. (2009). SCAI acts as a suppressor of cancer cell invasion through the transcriptional control of beta1-integrin. Nat Cell Biol *11*, 557-568.

Brennan, J.K., Mansky, J., Roberts, G., and Lichtman, M.A. (1975). Improved methods for reducing calcium and magnesium concentrations in tissue culture medium: application to studies of lymphoblast proliferation in vitro. In Vitro *11*, 354-360.

Brown, S., McGrath, M.J., Ooms, L.M., Gurung, R., Maimone, M.M., and Mitchell, C.A. (1999). Characterization of two isoforms of the skeletal muscle LIM protein 1, SLIM1. Localization of SLIM1 at focal adhesions and the isoform slimmer in the nucleus of myoblasts and cytoplasm of myotubes

suggests distinct roles in the cytoskeleton and in nuclear-cytoplasmic communication. J Biol Chem *274*, 27083-27091.

Bruel, A., Paschke, S., Jainta, S., Zhang, Y., Vassy, J., Rigaut, J.P., and Beil, M. (2001). Remodeling of vimentin cytoskeleton correlates with enhanced motility of promyelocytic leukemia cells during differentiation induced by retinoic acid. Anticancer Res *21*, 3973-3980.

Buchwalter, G., Gross, C., and Wasylyk, B. (2004). Ets ternary complex transcription factors. Gene *324*, 1-14.

Buchwalter, G., Gross, C., and Wasylyk, B. (2005). The ternary complex factor Net regulates cell migration through inhibition of PAI-1 expression. Mol Cell Biol *25*, 10853-10862.

Budhu, A., Jia, H.L., Forgues, M., Liu, C.G., Goldstein, D., Lam, A., Zanetti, K.A., Ye, Q.H., Qin, L.X., Croce, C.M., *et al.* (2008). Identification of metastasis-related microRNAs in hepatocellular carcinoma. Hepatology *47*, 897-907.

Busche, S., Descot, A., Julien, S., Genth, H., and Posern, G. (2008). Epithelial cell-cell contacts regulate SRF-mediated transcription via Rac-actin-MAL signalling. J Cell Sci *121*, 1025-1035.

Busche, S., Kremmer, E., and Posern, G. (2010). E-cadherin regulates MAL-SRF-mediated transcription in epithelial cells. J Cell Sci *123*, 2803-2809.

Calderwood, D.A. (2004). Integrin activation. J Cell Sci *117*, 657-666.

Calderwood, D.A., Yan, B., de Pereda, J.M., Alvarez, B.G., Fujioka, Y., Liddington, R.C., and Ginsberg, M.H. (2002). The phosphotyrosine binding-like domain of talin activates integrins. J Biol Chem *277*, 21749-21758.

Campbell, I.D., and Ginsberg, M.H. (2004). The talin-tail interaction places integrin activation on FERM ground. Trends Biochem Sci *29*, 429-435.

Cano, A., Perez-Moreno, M.A., Rodrigo, I., Locascio, A., Blanco, M.J., del Barrio, M.G., Portillo, F., and Nieto, M.A. (2000). The transcription factor snail controls epithelial-mesenchymal transitions by repressing E-cadherin expression. Nat Cell Biol *2*, 76-83.

Carlier, M.F. (1990). Actin polymerization and ATP hydrolysis. Adv Biophys *26*, 51-73.

Carlier, M.F., Pantaloni, D., and Korn, E.D. (1984). Evidence for an ATP cap at the ends of actin filaments and its regulation of the F-actin steady state. J Biol Chem *259*, 9983-9986.

Carter, W.G., Wayner, E.A., Bouchard, T.S., and Kaur, P. (1990). The role of integrins alpha 2 beta 1 and alpha 3 beta 1 in cell-cell and cell-substrate adhesion of human epidermal cells. J Cell Biol *110*, 1387-1404.

Cau, J., and Hall, A. (2005). Cdc42 controls the polarity of the actin and microtubule cytoskeletons through two distinct signal transduction pathways. J Cell Sci *118*, 2579-2587.

Charvet, C., Houbron, C., Parlakian, A., Giordani, J., Lahoute, C., Bertrand, A., Sotiropoulos, A., Renou, L., Schmitt, A., Melki, J., *et al.* (2006). New role for serum response factor in postnatal skeletal muscle growth and regeneration via the interleukin 4 and insulin-like growth factor 1 pathways. Mol Cell Biol *26*, 6664-6674.

Chen, J.F., Mandel, E.M., Thomson, J.M., Wu, Q., Callis, T.E., Hammond, S.M., Conlon, F.L., and Wang, D.Z. (2006). The role of microRNA-1 and microRNA-133 in skeletal muscle proliferation and differentiation. Nat Genet *38*, 228-233.

Chen, S., Maul, R.S., Kim, H.R., and Chang, D.D. (2000). Characterization of the human EPLIN (Epithelial Protein Lost in Neoplasm) gene reveals distinct promoters for the two EPLIN isoforms. Gene *248*, 69-76.

Chen, X., Bonne, S., Hatzfeld, M., van Roy, F., and Green, K.J. (2002). Protein binding and functional characterization of plakophilin 2. Evidence for its diverse roles in desmosomes and beta -catenin signaling. J Biol Chem *277*, 10512-10522.

Cheng, E.C., Luo, Q., Bruscia, E.M., Renda, M.J., Troy, J.A., Massaro, S.A., Tuck, D., Schulz, V., Mane, S.M., Berliner, N., *et al.* (2009). Role for MKL1 in megakaryocytic maturation. Blood *113*, 2826-2834.

Choi, C.K., Vicente-Manzanares, M., Zareno, J., Whitmore, L.A., Mogilner, A., and Horwitz, A.R. (2008). Actin and alpha-actinin orchestrate the assembly and maturation of nascent adhesions in a myosin II motor-independent manner. Nat Cell Biol *10*, 1039-1050.

Chu, P.H., Ruiz-Lozano, P., Zhou, Q., Cai, C., and Chen, J. (2000). Expression patterns of FHL/SLIM family members suggest important functional roles in skeletal muscle and cardiovascular system. Mech Dev *95*, 259-265.

Cooke, R. (1975). The role of the bound nucleotide in the polymerization of actin. Biochemistry *14*, 3250-3256.

Copeland, J.W., and Treisman, R. (2002). The diaphanous-related formin mDia1 controls serum response factor activity through its effects on actin polymerization. Mol Biol Cell *13*, 4088-4099.

Cory, G.O., and Ridley, A.J. (2002). Cell motility: braking WAVEs. Nature *418*, 732-733.

Coulombe, P.A., Bousquet, O., Ma, L., Yamada, S., and Wirtz, D. (2000). The 'ins' and 'outs' of intermediate filament organization. Trends Cell Biol *10*, 420-428.

Cox, E.A., and Huttenlocher, A. (1998). Regulation of integrin-mediated adhesion during cell migration. Microsc Res Tech *43*, 412-419.

Davis, E.M., and Trinkaus, J.P. (1981). Significance of cell-to cell contacts for the directional movement of neural crest cells within a hydrated collagen lattice. J Embryol Exp Morphol *63*, 29-51.

De La Cruz, E.M., Mandinova, A., Steinmetz, M.O., Stoffler, D., Aebi, U., and Pollard, T.D. (2000). Polymerization and structure of nucleotide-free actin filaments. J Mol Biol *295*, 517-526.

De La Cruz, E.M., and Pollard, T.D. (1995). Nucleotide-free actin: stabilization by sucrose and nucleotide binding kinetics. Biochemistry *34*, 5452-5461.

Demlehner, M.P., Schafer, S., Grund, C., and Franke, W.W. (1995). Continual assembly of half-desmosomal structures in the absence of cell contacts and their frustrated endocytosis: a coordinated Sisyphus cycle. J Cell Biol *131*, 745-760.

Desai, B.V., Harmon, R.M., and Green, K.J. (2009). Desmosomes at a glance. J Cell Sci *122*, 4401-4407.

Descot, A. (2010). Identification and Functional Characterisation of Genes regulated by Monomeric Actin. Doctoral dissertation.

Descot, A., Hoffmann, R., Shaposhnikov, D., Reschke, M., Ullrich, A., and Posern, G. (2009). Negative regulation of the EGFR-MAPK cascade by actin-MAL-mediated Mig6/Errfi-1 induction. Mol Cell *35*, 291-304.

DiMilla, P.A., Barbee, K., and Lauffenburger, D.A. (1991). Mathematical model for the effects of adhesion and mechanics on cell migration speed. Biophys J *60*, 15-37.

Ding, L., Niu, C., Zheng, Y., Xiong, Z., Liu, Y., Lin, J., Sun, H., Huang, K., Yang, W., Li, X., *et al.* (2009a). FHL1 interacts with estrogen receptors and regulates breast cancer cell growth. J Cell Mol Med.

Ding, L., Wang, Z., Yan, J., Yang, X., Liu, A., Qiu, W., Zhu, J., Han, J., Zhang, H., Lin, J., *et al.* (2009b). Human four-and-a-half LIM family members suppress tumor cell growth through a TGF-beta-like signaling pathway. J Clin Invest *119*, 349-361.

dos Remedios, C.G., Chhabra, D., Kekic, M., Dedova, I.V., Tsubakihara, M., Berry, D.A., and Nosworthy, N.J. (2003). Actin binding proteins: regulation of cytoskeletal microfilaments. Physiol Rev *83*, 433-473.

Du, K.L., Chen, M., Li, J., Lepore, J.J., Mericko, P., and Parmacek, M.S. (2004). Megakaryoblastic leukemia factor-1 transduces cytoskeletal signals and induces smooth muscle cell differentiation from undifferentiated embryonic stem cells. J Biol Chem *279*, 17578-17586.

Etkin, A., Alarcon, J.M., Weisberg, S.P., Touzani, K., Huang, Y.Y., Nordheim, A., and Kandel, E.R. (2006). A role in learning for SRF: deletion in the adult forebrain disrupts LTD and the formation of an immediate memory of a novel context. Neuron *50*, 127-143.

Ezratty, E.J., Partridge, M.A., and Gundersen, G.G. (2005). Microtubule-induced focal adhesion disassembly is mediated by dynamin and focal adhesion kinase. Nat Cell Biol *7*, 581-590.

Fanning, A. (2001). Organization and the regulation of the tight junction by the actin-myosin cytoskeleton. Tight Junctions (ed J M Anderson and M Cereijido), 265-284.

Farooqui, R., and Fenteany, G. (2005). Multiple rows of cells behind an epithelial wound edge extend cryptic lamellipodia to collectively drive cell-sheet movement. J Cell Sci *118*, 51-63.

Franco, S.J., Rodgers, M.A., Perrin, B.J., Han, J., Bennin, D.A., Critchley, D.R., and Huttenlocher, A. (2004). Calpain-mediated proteolysis of talin regulates adhesion dynamics. Nat Cell Biol *6*, 977-983.

Friedl, P., Borgmann, S., and Brocker, E.B. (2001). Amoeboid leukocyte crawling through extracellular matrix: lessons from the Dictyostelium paradigm of cell movement. J Leukoc Biol *70*, 491-509.

Friedl, P., Noble, P.B., Walton, P.A., Laird, D.W., Chauvin, P.J., Tabah, R.J., Black, M., and Zanker, K.S. (1995). Migration of coordinated cell clusters in mesenchymal and epithelial cancer explants in vitro. Cancer Res *55*, 4557-4560.

Friedl, P., and Wolf, K. (2010). Plasticity of cell migration: a multiscale tuning model. J Cell Biol *188*, 11-19.

Friedl, P., Zanker, K.S., and Brocker, E.B. (1998). Cell migration strategies in 3-D extracellular matrix: differences in morphology, cell matrix interactions, and integrin function. Microsc Res Tech *43*, 369-378.

Furuse, M., and Tsukita, S. (2006). Claudins in occluding junctions of humans and flies. Trends Cell Biol *16*, 181-188.

Gaietta, G., Deerinck, T.J., Adams, S.R., Bouwer, J., Tour, O., Laird, D.W., Sosinsky, G.E., Tsien, R.Y., and Ellisman, M.H. (2002). Multicolor and electron microscopic imaging of connexin trafficking. Science *296*, 503-507.

Garrod, D.R. (1993). Desmosomes and hemidesmosomes. Curr Opin Cell Biol *5*, 30-40.

Garrod, D.R., Merritt, A.J., and Nie, Z. (2002). Desmosomal cadherins. Curr Opin Cell Biol *14*, 537-545.

Geiger, B., Bershadsky, A., Pankov, R., and Yamada, K.M. (2001). Transmembrane crosstalk between the extracellular matrix--cytoskeleton crosstalk. Nat Rev Mol Cell Biol *2*, 793-805.

Geneste, O., Copeland, J.W., and Treisman, R. (2002). LIM kinase and Diaphanous cooperate to regulate serum response factor and actin dynamics. J Cell Biol *157*, 831-838.

Gerull, B., Heuser, A., Wichter, T., Paul, M., Basson, C.T., McDermott, D.A., Lerman, B.B., Markowitz, S.M., Ellinor, P.T., MacRae, C.A., *et al.* (2004). Mutations in the desmosomal protein plakophilin-2 are common in arrhythmogenic right ventricular cardiomyopathy. Nat Genet *36*, 1162-1164.

Gilles, L., Bluteau, D., Boukour, S., Chang, Y., Zhang, Y., Robert, T., Dessen, P., Debili, N., Bernard, O.A., Vainchenker, W., *et al.* (2009). MAL/SRF complex is involved in platelet formation and megakaryocyte migration by regulating MYL9 (MLC2) and MMP9. Blood *114*, 4221-4232.

Gineitis, D., and Treisman, R. (2001). Differential usage of signal transduction pathways defines two types of serum response factor target gene. J Biol Chem *276*, 24531-24539.

Godsel, L.M., Getsios, S., Huen, A.C., and Green, K.J. (2004). The molecular composition and function of desmosomes. Handb Exp Pharmacol, 137-193.

Godsel, L.M., Hsieh, S.N., Amargo, E.V., Bass, A.E., Pascoe-McGillicuddy, L.T., Huen, A.C., Thorne, M.E., Gaudry, C.A., Park, J.K., Myung, K., *et al.* (2005). Desmoplakin assembly dynamics in four dimensions: multiple phases differentially regulated by intermediate filaments and actin. J Cell Biol *171*, 1045-1059.

Goldberg, G.S., Lampe, P.D., and Nicholson, B.J. (1999). Selective transfer of endogenous metabolites through gap junctions composed of different connexins. Nat Cell Biol *1*, 457-459.

Goldman, R.D. (1971). The role of three cytoplasmic fibers in BHK-21 cell motility. I. Microtubules and the effects of colchicine. J Cell Biol *51*, 752-762.

Goossens, S., Janssens, B., Bonne, S., De Rycke, R., Braet, F., van Hengel, J., and van Roy, F. (2007). A unique and specific interaction between alphaT-catenin and plakophilin-2 in the area composita, the mixed-type junctional structure of cardiac intercalated discs. J Cell Sci *120*, 2126-2136.

Gotlieb, A.I., May, L.M., Subrahmanyan, L., and Kalnins, V.I. (1981). Distribution of microtubule organizing centers in migrating sheets of endothelial cells. J Cell Biol *91*, 589-594.

Green, K.J., and Jones, J.C. (1996). Desmosomes and hemidesmosomes: structure and function of molecular components. FASEB J *10*, 871-881.

Green, K.J., Kowalczyk, A.P., Bornslaeger, E.A., Palka, H.L., and Norvell, S.M. (1998). Desmosomes: integrators of mechanical integrity in tissues. Biol Bull *194*, 374-376; discussion 376-377.

Gregory, P.A., Bracken, C.P., Bert, A.G., and Goodall, G.J. (2008). MicroRNAs as regulators of epithelial-mesenchymal transition. Cell Cycle *7*, 3112-3118.

Gregory, S.L., and Brown, N.H. (1998). kakapo, a gene required for adhesion between and within cell layers in Drosophila, encodes a large cytoskeletal linker protein related to plectin and dystrophin. J Cell Biol *143*, 1271-1282.

Grossmann, K.S., Grund, C., Huelsken, J., Behrend, M., Erdmann, B., Franke, W.W., and Birchmeier, W. (2004). Requirement of plakophilin 2 for heart morphogenesis and cardiac junction formation. J Cell Biol *167*, 149-160.

Guillemin, K., Groppe, J., Ducker, K., Treisman, R., Hafen, E., Affolter, M., and Krasnow, M.A. (1996). The pruned gene encodes the Drosophila serum response factor and regulates cytoplasmic outgrowth during terminal branching of the tracheal system. Development *122*, 1353-1362.

Gumbiner, B.M. (1996). Cell adhesion: the molecular basis of tissue architecture and morphogenesis. Cell *84*, 345-357.

Gundersen, G.G., Gomes, E.R., and Wen, Y. (2004). Cortical control of microtubule stability and polarization. Curr Opin Cell Biol *16*, 106-112.

Han, M.Y., Kosako, H., Watanabe, T., and Hattori, S. (2007). Extracellular signal-regulated kinase/mitogen-activated protein kinase regulates actin organization and cell motility by phosphorylating the actin cross-linking protein EPLIN. Mol Cell Biol *27*, 8190-8204.

Hatzfeld, M., Kristjansson, G.I., Plessmann, U., and Weber, K. (1994). Band 6 protein, a major constituent of desmosomes from stratified epithelia, is a novel member of the armadillo multigene family. J Cell Sci *107 (Pt 8)*, 2259-2270.

Hegerfeldt, Y., Tusch, M., Brocker, E.B., and Friedl, P. (2002). Collective cell movement in primary melanoma explants: plasticity of cell-cell interaction, beta1-integrin function, and migration strategies. Cancer Res *62*, 2125-2130.

Herrmann, H., and Aebi, U. (2000). Intermediate filaments and their associates: multi-talented structural elements specifying cytoarchitecture and cytodynamics. Curr Opin Cell Biol *12*, 79-90.

Hesse, M., Magin, T.M., and Weber, K. (2001). Genes for intermediate filament proteins and the draft sequence of the human genome: novel keratin genes and a surprisingly high number of pseudogenes related to keratin genes 8 and 18. J Cell Sci *114*, 2569-2575.

Huber, M.A., Azoitei, N., Baumann, B., Grunert, S., Sommer, A., Pehamberger, H., Kraut, N., Beug, H., and Wirth, T. (2004). NF-kappaB is essential for epithelial-mesenchymal transition and metastasis in a model of breast cancer progression. J Clin Invest *114*, 569-581.

Humphries, J.D., Byron, A., and Humphries, M.J. (2006). Integrin ligands at a glance. J Cell Sci *119*, 3901-3903.

Huttenlocher, A., Sandborg, R.R., and Horwitz, A.F. (1995). Adhesion in cell migration. Curr Opin Cell Biol *7*, 697-706.

Hynes, R.O. (1992). Integrins: versatility, modulation, and signaling in cell adhesion. Cell *69*, 11-25.

Hynes, R.O. (2002). Integrins: bidirectional, allosteric signaling machines. Cell *110*, 673-687.

Ikenouchi, J., Furuse, M., Furuse, K., Sasaki, H., and Tsukita, S. (2005). Tricellulin constitutes a novel barrier at tricellular contacts of epithelial cells. J Cell Biol *171*, 939-945.

Ikenouchi, J., Matsuda, M., Furuse, M., and Tsukita, S. (2003). Regulation of tight junctions during the epithelium-mesenchyme transition: direct repression of the gene expression of claudins/occludin by Snail. J Cell Sci *116*, 1959-1967.

Ivaska, J., Vuoriluoto, K., Huovinen, T., Izawa, I., Inagaki, M., and Parker, P.J. (2005). PKCepsilon-mediated phosphorylation of vimentin controls integrin recycling and motility. EMBO J *24*, 3834-3845.

Jiang, W.G., Martin, T.A., Lewis-Russell, J.M., Douglas-Jones, A., Ye, L., and Mansel, R.E. (2008). Eplin-alpha expression in human breast cancer, the impact on cellular migration and clinical outcome. Mol Cancer *7*, 71.

Jiang, Y., Yin, H., and Zheng, X.L. (2010). MicroRNA-1 inhibits myocardin-induced contractility of human vascular smooth muscle cells. J Cell Physiol *225*, 506-511.

Johannessen, M., Moller, S., Hansen, T., Moens, U., and Van Ghelue, M. (2006). The multifunctional roles of the four-and-a-half-LIM only protein FHL2. Cell Mol Life Sci *63*, 268-284.

Jones, J.C., Asmuth, J., Baker, S.E., Langhofer, M., Roth, S.I., and Hopkinson, S.B. (1994). Hemidesmosomes: extracellular matrix/intermediate filament connectors. Exp Cell Res *213*, 1-11.

Kabsch, W., Mannherz, H.G., Suck, D., Pai, E.F., and Holmes, K.C. (1990). Atomic structure of the actin:DNase I complex. Nature *347*, 37-44.

Karakesisoglou, I., Yang, Y., and Fuchs, E. (2000). An epidermal plakin that integrates actin and microtubule networks at cellular junctions. J Cell Biol *149*, 195-208.

Kasai, M., Asakura, S., and Oosawa, F. (1962). The cooperative nature of G-F transformation of actin. Biochim Biophys Acta *57*, 22-31.

Kasai, M., Nakano, E., and Oosawa, F. (1965). Polymerization of Actin Free from Nucleotides and Divalent Cations. Biochim Biophys Acta *94*, 494-503.

Kaverina, I., Krylyshkina, O., and Small, J.V. (1999). Microtubule targeting of substrate contacts promotes their relaxation and dissociation. J Cell Biol *146*, 1033-1044.

Kaverina, I., Rottner, K., and Small, J.V. (1998). Targeting, capture, and stabilization of microtubules at early focal adhesions. J Cell Biol *142*, 181-190.

Kawakatsu, T., Shimizu, K., Honda, T., Fukuhara, T., Hoshino, T., and Takai, Y. (2002). Trans-interactions of nectins induce formation of filopodia and Lamellipodia through the respective activation of Cdc42 and Rac small G proteins. J Biol Chem *277*, 50749-50755.

Kaye, G.I., Siegel, L.F., and Pascal, R.R. (1971). Cell replication of mesenchymal elements in adult tissues. I. The replication and migration of mesenchymal cells in the adult rabbit dermis. Anat Rec *169*, 593-611.

Kim, Y.J., Sauer, C., Testa, K., Wahl, J.K., Svoboda, R.A., Johnson, K.R., Wheelock, M.J., and Knudsen, K.A. (2005). Modulating the strength of cadherin adhesion: evidence for a novel adhesion complex. J Cell Sci *118*, 3883-3894.

Kimura, Y., Morita, T., Hayashi, K., Miki, T., and Sobue, K. (2010). Myocardin functions as an effective inducer of growth arrest and differentiation in human uterine leiomyosarcoma cells. Cancer Res *70*, 501-511.

King, I.A., Sullivan, K.H., Bennett, R., Jr., and Buxton, R.S. (1995). The desmocollins of human foreskin epidermis: identification and chromosomal assignment of a third gene and expression patterns of the three isoforms. J Invest Dermatol *105*, 314-321.

Kinosian, H.J., Selden, L.A., Estes, J.E., and Gershman, L.C. (1993). Nucleotide binding to actin. Cation dependence of nucleotide dissociation and exchange rates. J Biol Chem *268*, 8683-8691.

Kirchhoff, S., Nelles, E., Hagendorff, A., Kruger, O., Traub, O., and Willecke, K. (1998). Reduced cardiac conduction velocity and predisposition to arrhythmias in connexin40-deficient mice. Curr Biol *8*, 299-302.

Kirschner, M., and Mitchison, T. (1986). Beyond self-assembly: from microtubules to morphogenesis. Cell *45*, 329-342.

Knoll, B., Kretz, O., Fiedler, C., Alberti, S., Schutz, G., Frotscher, M., and Nordheim, A. (2006). Serum response factor controls neuronal circuit assembly in the hippocampus. Nat Neurosci *9*, 195-204.

Koch, P.J., and Franke, W.W. (1994). Desmosomal cadherins: another growing multigene family of adhesion molecules. Curr Opin Cell Biol *6*, 682-687.

Koch, P.J., Goldschmidt, M.D., Zimbelmann, R., Troyanovsky, R., and Franke, W.W. (1992). Complexity and expression patterns of the desmosomal cadherins. Proc Natl Acad Sci U S A *89*, 353-357.

Kodama, A., Karakesisoglou, I., Wong, E., Vaezi, A., and Fuchs, E. (2003). ACF7: an essential integrator of microtubule dynamics. Cell *115*, 343-354.

Koegel, H., von Tobel, L., Schafer, M., Alberti, S., Kremmer, E., Mauch, C., Hohl, D., Wang, X.J., Beer, H.D., Bloch, W., *et al.* (2009). Loss of serum response factor in keratinocytes results in hyperproliferative skin disease in mice. J Clin Invest *119*, 899-910.

Komarova, Y.A., Akhmanova, A.S., Kojima, S., Galjart, N., and Borisy, G.G. (2002). Cytoplasmic linker proteins promote microtubule rescue in vivo. J Cell Biol *159*, 589-599.

Kottke, M.D., Delva, E., and Kowalczyk, A.P. (2006). The desmosome: cell science lessons from human diseases. J Cell Sci *119*, 797-806.

Kowalczyk, A.P., Navarro, P., Dejana, E., Bornslaeger, E.A., Green, K.J., Kopp, D.S., and Borgwardt, J.E. (1998). VE-cadherin and desmoplakin are assembled into dermal microvascular endothelial intercellular junctions: a pivotal role for plakoglobin in the recruitment of desmoplakin to intercellular junctions. J Cell Sci *111 (Pt 20)*, 3045-3057.

Kowalczyk, A.P., Palka, H.L., Luu, H.H., Nilles, L.A., Anderson, J.E., Wheelock, M.J., and Green, K.J. (1994). Posttranslational regulation of plakoglobin expression. Influence of the desmosomal cadherins on plakoglobin metabolic stability. J Biol Chem *269*, 31214-31223.

Kreis, S., Schonfeld, H.J., Melchior, C., Steiner, B., and Kieffer, N. (2005). The intermediate filament protein vimentin binds specifically to a recombinant integrin alpha2/beta1 cytoplasmic tail complex and co-localizes with native alpha2/beta1 in endothelial cell focal adhesions. Exp Cell Res *305*, 110-121.

Kundu, S.T., Gosavi, P., Khapare, N., Patel, R., Hosing, A.S., Maru, G.B., Ingle, A., Decaprio, J.A., and Dalal, S.N. (2008). Plakophilin3 downregulation leads to a decrease in cell adhesion and promotes metastasis. Int J Cancer *123*, 2303-2314.

Kuwahara, K., Barrientos, T., Pipes, G.C., Li, S., and Olson, E.N. (2005). Muscle-specific signaling mechanism that links actin dynamics to serum response factor. Mol Cell Biol *25*, 3173-3181.

Laemmli, U.K. (1970). Cleavage of structural proteins during the assembly of the head of bacteriophage T4. Nature *227*, 680-685.

Lammermann, T., and Sixt, M. (2009). Mechanical modes of 'amoeboid' cell migration. Curr Opin Cell Biol *21*, 636-644.

Langhofer, M., Hopkinson, S.B., and Jones, J.C. (1993). The matrix secreted by 804G cells contains laminin-related components that participate in hemidesmosome assembly in vitro. J Cell Sci *105 (Pt 3)*, 753-764.

Latasa, M.U., Couton, D., Charvet, C., Lafanechere, A., Guidotti, J.E., Li, Z., Tuil, D., Daegelen, D., Mitchell, C., and Gilgenkrantz, H. (2007). Delayed liver regeneration in mice lacking liver serum response factor. Am J Physiol Gastrointest Liver Physiol *292*, G996-G1001.

Lauf, U., Giepmans, B.N., Lopez, P., Braconnot, S., Chen, S.C., and Falk, M.M. (2002). Dynamic trafficking and delivery of connexons to the plasma membrane and accretion to gap junctions in living cells. Proc Natl Acad Sci U S A *99*, 10446-10451.

Lauffenburger, D.A., and Horwitz, A.F. (1996). Cell migration: a physically integrated molecular process. Cell *84*, 359-369.

Lee, S.M., Vasishtha, M., and Prywes, R. (2010). Activation and repression of cellular immediate early genes by serum response factor cofactors. J Biol Chem *285*, 22036-22049.

Legate, K.R., Wickstrom, S.A., and Fassler, R. (2009). Genetic and cell biological analysis of integrin outside-in signaling. Genes Dev *23*, 397-418.

Leitner, L., Shaposhnikov, D., Descot, A., Hoffmann, R., and Posern, G. (2010). Epithelial Protein Lost in Neoplasm alpha (Eplin-alpha) is transcriptionally regulated by G-actin and MAL/MRTF coactivators. Mol Cancer *9*, 60.

Leung, C.L., Sun, D., Zheng, M., Knowles, D.R., and Liem, R.K. (1999). Microtubule actin cross-linking factor (MACF): a hybrid of dystonin and dystrophin that can interact with the actin and microtubule cytoskeletons. J Cell Biol *147*, 1275-1286.

Li, J., Zhu, X., Chen, M., Cheng, L., Zhou, D., Lu, M.M., Du, K., Epstein, J.A., and Parmacek, M.S. (2005a). Myocardin-related transcription factor B is required in cardiac neural crest for smooth muscle differentiation and cardiovascular development. Proc Natl Acad Sci U S A *102*, 8916-8921.

Li, S., Chang, S., Qi, X., Richardson, J.A., and Olson, E.N. (2006). Requirement of a myocardin-related transcription factor for development of mammary myoepithelial cells. Mol Cell Biol *26*, 5797-5808.

Li, S., Czubryt, M.P., McAnally, J., Bassel-Duby, R., Richardson, J.A., Wiebel, F.F., Nordheim, A., and Olson, E.N. (2005b). Requirement for serum response factor for skeletal muscle growth and maturation revealed by tissue-specific gene deletion in mice. Proc Natl Acad Sci U S A *102*, 1082-1087.

Liao, G., Nagasaki, T., and Gundersen, G.G. (1995). Low concentrations of nocodazole interfere with fibroblast locomotion without significantly affecting microtubule level: implications for the role of dynamic microtubules in cell locomotion. J Cell Sci *108 (Pt 11)*, 3473-3483.

Litjens, S.H., de Pereda, J.M., and Sonnenberg, A. (2006). Current insights into the formation and breakdown of hemidesmosomes. Trends Cell Biol *16*, 376-383.

Lockman, K., Hinson, J.S., Medlin, M.D., Morris, D., Taylor, J.M., and Mack, C.P. (2004). Sphingosine 1-phosphate stimulates smooth muscle cell differentiation and proliferation by activating separate serum response factor co-factors. J Biol Chem *279*, 42422-42430.

Ma, L., and Weinberg, R.A. (2008). Micromanagers of malignancy: role of microRNAs in regulating metastasis. Trends Genet *24*, 448-456.

Malech, H.L., Root, R.K., and Gallin, J.I. (1977). Structural analysis of human neutrophil migration. Centriole, microtubule, and microfilament orientation and function during chemotaxis. J Cell Biol *75*, 666-693.

Masszi, A., Speight, P., Charbonney, E., Lodyga, M., Nakano, H., Szaszi, K., and Kapus, A. (2010). Fate-determining mechanisms in epithelial-myofibroblast transition: major inhibitory role for Smad3. J Cell Biol *188*, 383-399.

Mathur, M., Goodwin, L., and Cowin, P. (1994). Interactions of the cytoplasmic domain of the desmosomal cadherin Dsg1 with plakoglobin. J Biol Chem *269*, 14075-14080.

Matter, K., and Balda, M.S. (2007). Epithelial tight junctions, gene expression and nucleo-junctional interplay. J Cell Sci *120*, 1505-1511.

Maul, R.S., and Chang, D.D. (1999). EPLIN, epithelial protein lost in neoplasm. Oncogene *18*, 7838-7841.

Maul, R.S., Song, Y., Amann, K.J., Gerbin, S.C., Pollard, T.D., and Chang, D.D. (2003). EPLIN regulates actin dynamics by cross-linking and stabilizing filaments. J Cell Biol *160*, 399-407.

McGough, A., Pope, B., Chiu, W., and Weeds, A. (1997). Cofilin changes the twist of F-actin: implications for actin filament dynamics and cellular function. J Cell Biol *138*, 771-781.

McGrath, J.A., McMillan, J.R., Shemanko, C.S., Runswick, S.K., Leigh, I.M., Lane, E.B., Garrod, D.R., and Eady, R.A. (1997). Mutations in the plakophilin 1 gene result in ectodermal dysplasia/skin fragility syndrome. Nat Genet *17*, 240-244.

McGrath, M.J., Mitchell, C.A., Coghill, I.D., Robinson, P.A., and Brown, S. (2003). Skeletal muscle LIM protein 1 (SLIM1/FHL1) induces alpha 5 beta 1-integrin-dependent myocyte elongation. Am J Physiol Cell Physiol *285*, C1513-1526.

McKoy, G., Protonotarios, N., Crosby, A., Tsatsopoulou, A., Anastasakis, A., Coonar, A., Norman, M., Baboonian, C., Jeffery, S., and McKenna, W.J. (2000). Identification of a deletion in plakoglobin in arrhythmogenic right ventricular cardiomyopathy with palmoplantar keratoderma and woolly hair (Naxos disease). Lancet *355*, 2119-2124.

Medjkane, S., Perez-Sanchez, C., Gaggioli, C., Sahai, E., and Treisman, R. (2009). Myocardin-related transcription factors and SRF are required for cytoskeletal dynamics and experimental metastasis. Nat Cell Biol *11*, 257-268.

Mertens, C., Kuhn, C., and Franke, W.W. (1996). Plakophilins 2a and 2b: constitutive proteins of dual location in the karyoplasm and the desmosomal plaque. J Cell Biol *135*, 1009-1025.

Miano, J.M. (2003). Serum response factor: toggling between disparate programs of gene expression. J Mol Cell Cardiol *35*, 577-593.

Miano, J.M., Long, X., and Fujiwara, K. (2007). Serum response factor: master regulator of the actin cytoskeleton and contractile apparatus. Am J Physiol Cell Physiol *292*, C70-81.

Miano, J.M., Ramanan, N., Georger, M.A., de Mesy Bentley, K.L., Emerson, R.L., Balza, R.O., Jr., Xiao, Q., Weiler, H., Ginty, D.D., and Misra, R.P. (2004). Restricted inactivation of serum response factor to the cardiovascular system. Proc Natl Acad Sci U S A *101*, 17132-17137.

Mikhailov, A., and Gundersen, G.G. (1998). Relationship between microtubule dynamics and lamellipodium formation revealed by direct imaging of microtubules in cells treated with nocodazole or taxol. Cell Motil Cytoskeleton *41*, 325-340.

Milyavsky, M., Shats, I., Cholostoy, A., Brosh, R., Buganim, Y., Weisz, L., Kogan, I., Cohen, M., Shatz, M., Madar, S., *et al.* (2007). Inactivation of myocardin and p16 during malignant transformation contributes to a differentiation defect. Cancer Cell *11*, 133-146.

Miralles, F., Posern, G., Zaromytidou, A.I., and Treisman, R. (2003). Actin dynamics control SRF activity by regulation of its coactivator MAL. Cell *113*, 329-342.

Mokalled, M.H., Johnson, A., Kim, Y., Oh, J., and Olson, E.N. (2010). Myocardin-related transcription factors regulate the Cdk5/Pctaire1 kinase cascade to control neurite outgrowth, neuronal migration and brain development. Development *137*, 2365-2374.

Morita, T., Mayanagi, T., and Sobue, K. (2007). Dual roles of myocardin-related transcription factors in epithelial mesenchymal transition via slug induction and actin remodeling. J Cell Biol *179*, 1027-1042.

Mouilleron, S., Guettler, S., Langer, C.A., Treisman, R., and McDonald, N.Q. (2008). Molecular basis for G-actin binding to RPEL motifs from the serum response factor coactivator MAL. EMBO J *27*, 3198-3208.

Mullis, K.B., and Faloona, F.A. (1987). Specific synthesis of DNA in vitro via a polymerase-catalyzed chain reaction. Methods Enzymol *155*, 335-350.

Murai, K., and Treisman, R. (2002). Interaction of serum response factor (SRF) with the Elk-1 B box inhibits RhoA-actin signaling to SRF and potentiates transcriptional activation by Elk-1. Mol Cell Biol *22*, 7083-7092.

Nabi, I.R. (1999). The polarization of the motile cell. J Cell Sci *112 (Pt 12)*, 1803-1811.

Neidl, C., and Engel, J. (1979). Exchange of ADP, ATP and 1: N6-ethenoadenosine 5'-triphosphate at G-actin. Equilibrium and kinetics. Eur J Biochem *101*, 163-169.

Niu, Z., Yu, W., Zhang, S.X., Barron, M., Belaguli, N.S., Schneider, M.D., Parmacek, M., Nordheim, A., and Schwartz, R.J. (2005). Conditional mutagenesis of the murine serum response factor gene blocks cardiogenesis and the transcription of downstream gene targets. J Biol Chem *280*, 32531-32538.

Norgett, E.E., Hatsell, S.J., Carvajal-Huerta, L., Cabezas, J.C., Common, J., Purkis, P.E., Whittock, N., Leigh, I.M., Stevens, H.P., and Kelsell, D.P. (2000). Recessive mutation in desmoplakin disrupts desmoplakin-intermediate filament interactions and causes dilated cardiomyopathy, woolly hair and keratoderma. Hum Mol Genet *9*, 2761-2766.

Oft, M., Peli, J., Rudaz, C., Schwarz, H., Beug, H., and Reichmann, E. (1996). TGF-beta1 and Ha-Ras collaborate in modulating the phenotypic plasticity and invasiveness of epithelial tumor cells. Genes Dev *10*, 2462-2477.

Oh, J., Richardson, J.A., and Olson, E.N. (2005). Requirement of myocardin-related transcription factor-B for remodeling of branchial arch arteries and smooth muscle differentiation. Proc Natl Acad Sci U S A *102*, 15122-15127.

Olson, E.N., and Nordheim, A. (2010). Linking actin dynamics and gene transcription to drive cellular motile functions. Nat Rev Mol Cell Biol *11*, 353-365.

Omary, M.B., Ku, N.O., Liao, J., and Price, D. (1998). Keratin modifications and solubility properties in epithelial cells and in vitro. Subcell Biochem *31*, 105-140.

Oosawa, F., Asakura, S., Hotta, K., and T., O. (1959). G-F transformation of actin as a fibrous condensation. J Polymer Sci, 323-326.

Orlova, A., Chen, X., Rubenstein, P.A., and Egelman, E.H. (1997). Modulation of yeast F-actin structure by a mutation in the nucleotide-binding cleft. J Mol Biol *271*, 235-243.

Orlova, A., and Egelman, E.H. (1995). Structural dynamics of F-actin: I. Changes in the C terminus. J Mol Biol *245*, 582-597.

Owen, C., and DeRosier, D. (1993). A 13-A map of the actin-scruin filament from the limulus acrosomal process. J Cell Biol *123*, 337-344.

Palecek, S.P., Loftus, J.C., Ginsberg, M.H., Lauffenburger, D.A., and Horwitz, A.F. (1997). Integrin-ligand binding properties govern cell migration speed through cell-substratum adhesiveness. Nature *385*, 537-540.

Pardee, J.D., Simpson, P.A., Stryer, L., and Spudich, J.A. (1982). Actin filaments undergo limited subunit exchange in physiological salt conditions. J Cell Biol *94*, 316-324.

Parlakian, A., Charvet, C., Escoubet, B., Mericskay, M., Molkentin, J.D., Gary-Bobo, G., De Windt, L.J., Ludosky, M.A., Paulin, D., Daegelen, D., *et al.* (2005). Temporally controlled onset of dilated cardiomyopathy through disruption of the SRF gene in adult heart. Circulation *112*, 2930-2939.

Peifer, M., McCrea, P.D., Green, K.J., Wieschaus, E., and Gumbiner, B.M. (1992). The vertebrate adhesive junction proteins beta-catenin and plakoglobin and the Drosophila segment polarity gene armadillo form a multigene family with similar properties. J Cell Biol *118*, 681-691.

Perl, A.K., Wilgenbus, P., Dahl, U., Semb, H., and Christofori, G. (1998). A causal role for E-cadherin in the transition from adenoma to carcinoma. Nature *392*, 190-193.

Philippar, U., Schratt, G., Dieterich, C., Muller, J.M., Galgoczy, P., Engel, F.B., Keating, M.T., Gertler, F., Schule, R., Vingron, M., *et al.* (2004). The SRF target gene Fhl2 antagonizes RhoA/MAL-dependent activation of SRF. Mol Cell *16*, 867-880.

Pieperhoff, S., Schumacher, H., and Franke, W.W. (2008). The area composita of adhering junctions connecting heart muscle cells of vertebrates. V. The importance of plakophilin-2 demonstrated by small interference RNA-mediated knockdown in cultured rat cardiomyocytes. Eur J Cell Biol *87*, 399-411.

Pipes, G.C., Creemers, E.E., and Olson, E.N. (2006). The myocardin family of transcriptional coactivators: versatile regulators of cell growth, migration, and myogenesis. Genes Dev *20*, 1545-1556.

Pollard, T.D. (1984). Polymerization of ADP-actin. J Cell Biol *99*, 769-777.

Posern, G., Miralles, F., Guettler, S., and Treisman, R. (2004). Mutant actins that stabilise F-actin use distinct mechanisms to activate the SRF coactivator MAL. EMBO J *23*, 3973-3983.

Posern, G., Sotiropoulos, A., and Treisman, R. (2002). Mutant actins demonstrate a role for unpolymerized actin in control of transcription by serum response factor. Mol Biol Cell *13*, 4167-4178.

Posern, G., and Treisman, R. (2006). Actin' together: serum response factor, its cofactors and the link to signal transduction. Trends Cell Biol *16*, 588-596.

Ragu, C., Elain, G., Mylonas, E., Ottolenghi, C., Cagnard, N., Daegelen, D., Passegue, E., Vainchenker, W., Bernard, O.A., and Penard-Lacronique, V. (2010). The transcription factor SRF regulates hematopoietic stem cells adhesion. Blood.

Ramanan, N., Shen, Y., Sarsfield, S., Lemberger, T., Schutz, G., Linden, D.J., and Ginty, D.D. (2005). SRF mediates activity-induced gene expression and synaptic plasticity but not neuronal viability. Nat Neurosci *8*, 759-767.

Regen, C.M., and Horwitz, A.F. (1992). Dynamics of beta 1 integrin-mediated adhesive contacts in motile fibroblasts. J Cell Biol *119*, 1347-1359.

Rickelt, S., Winter-Simanowski, S., Noffz, E., Kuhn, C., and Franke, W.W. (2009). Upregulation of plakophilin-2 and its acquisition to adherens junctions identifies a novel molecular ensemble of cell-cell-attachment characteristic for transformed mesenchymal cells. Int J Cancer *125*, 2036-2048.

Robinson, P.A., Brown, S., McGrath, M.J., Coghill, I.D., Gurung, R., and Mitchell, C.A. (2003). Skeletal muscle LIM protein 1 regulates integrin-mediated myoblast adhesion, spreading, and migration. Am J Physiol Cell Physiol *284*, C681-695.

Roh, J.Y., and Stanley, J.R. (1995). Plakoglobin binding by human Dsg3 (pemphigus vulgaris antigen) in keratinocytes requires the cadherin-like intracytoplasmic segment. J Invest Dermatol *104*, 720-724.

Roper, K., and Brown, N.H. (2003). Maintaining epithelial integrity: a function for gigantic spectraplakin isoforms in adherens junctions. J Cell Biol *162*, 1305-1315.

Rousselle, P., and Aumailley, M. (1994). Kalinin is more efficient than laminin in promoting adhesion of primary keratinocytes and some other epithelial cells and has a different requirement for integrin receptors. J Cell Biol *125*, 205-214.

Saez, J.C., Connor, J.A., Spray, D.C., and Bennett, M.V. (1989). Hepatocyte gap junctions are permeable to the second messenger, inositol 1,4,5-trisphosphate, and to calcium ions. Proc Natl Acad Sci U S A *86*, 2708-2712.

Sahai, E., and Marshall, C.J. (2003). Differing modes of tumour cell invasion have distinct requirements for Rho/ROCK signalling and extracellular proteolysis. Nat Cell Biol *5*, 711-719.

Sambrook, J., Fritsch, E. F., and Maniatis, M. (1989). Molecular Cloning: A laboratory manual. Cold

Spring Habor Laboratory Press: Cold Spring Habor.

Sambrook, J., Russel, DW. (2001). Molecular Cloning: A laboratory manual. Third Edition. Cold

Spring Habor Laboratory Press: Cold Spring Habor.

Sampath, P., and Pollard, T.D. (1991). Effects of cytochalasin, phalloidin, and pH on the elongation of actin filaments. Biochemistry *30*, 1973-1980.

Sanz-Moreno, V., Gadea, G., Ahn, J., Paterson, H., Marra, P., Pinner, S., Sahai, E., and Marshall, C.J. (2008). Rac activation and inactivation control plasticity of tumor cell movement. Cell *135*, 510-523.

Sastry, S.K., Lakonishok, M., Thomas, D.A., Muschler, J., and Horwitz, A.F. (1996). Integrin alpha subunit ratios, cytoplasmic domains, and growth factor synergy regulate muscle proliferation and differentiation. J Cell Biol *133*, 169-184.

Schmidt, A., Heid, H.W., Schafer, S., Nuber, U.A., Zimbelmann, R., and Franke, W.W. (1994). Desmosomes and cytoskeletal architecture in epithelial differentiation: cell type-specific plaque components and intermediate filament anchorage. Eur J Cell Biol *65*, 229-245.

Schmidt, A., and Jager, S. (2005). Plakophilins--hard work in the desmosome, recreation in the nucleus? Eur J Cell Biol *84*, 189-204.

Schmidt, A., Langbein, L., Pratzel, S., Rode, M., Rackwitz, H.R., and Franke, W.W. (1999). Plakophilin 3--a novel cell-type-specific desmosomal plaque protein. Differentiation *64*, 291-306.

Schmidt, A., Langbein, L., Rode, M., Pratzel, S., Zimbelmann, R., and Franke, W.W. (1997). Plakophilins 1a and 1b: widespread nuclear proteins recruited in specific epithelial cells as desmosomal plaque components. Cell Tissue Res *290*, 481-499.

Schratt, G., Philippar, U., Berger, J., Schwarz, H., Heidenreich, O., and Nordheim, A. (2002). Serum response factor is crucial for actin cytoskeletal organization and focal adhesion assembly in embryonic stem cells. J Cell Biol *156*, 737-750.

Schuyler, S.C., and Pellman, D. (2001). Microtubule "plus-end-tracking proteins": The end is just the beginning. Cell *105*, 421-424.

Selvaraj, A., and Prywes, R. (2004). Expression profiling of serum inducible genes identifies a subset of SRF target genes that are MKL dependent. BMC Mol Biol *5*, 13.

Shen, Y., Jia, Z., Nagele, R.G., Ichikawa, H., and Goldberg, G.S. (2006). SRC uses Cas to suppress Fhl1 in order to promote nonanchored growth and migration of tumor cells. Cancer Res *66*, 1543-1552.

Shore, P., and Sharrocks, A.D. (1995). The MADS-box family of transcription factors. Eur J Biochem *229*, 1-13.

Simon, A.M., Goodenough, D.A., and Paul, D.L. (1998). Mice lacking connexin40 have cardiac conduction abnormalities characteristic of atrioventricular block and bundle branch block. Curr Biol *8*, 295-298.

Smilenov, L.B., Mikhailov, A., Pelham, R.J., Marcantonio, E.E., and Gundersen, G.G. (1999). Focal adhesion motility revealed in stationary fibroblasts. Science *286*, 1172-1174.

Smith-Hicks, C., Xiao, B., Deng, R., Ji, Y., Zhao, X., Shepherd, J.D., Posern, G., Kuhl, D., Huganir, R.L., Ginty, D.D., *et al.* (2010). SRF binding to SRE 6.9 in the Arc promoter is essential for LTD in cultured Purkinje cells. Nat Neurosci *13*, 1082-1089.

Song, Y., Maul, R.S., Gerbin, C.S., and Chang, D.D. (2002). Inhibition of anchorage-independent growth of transformed NIH3T3 cells by epithelial protein lost in neoplasm (EPLIN) requires localization of EPLIN to actin cytoskeleton. Mol Biol Cell *13*, 1408-1416.

Sotiropoulos, A., Gineitis, D., Copeland, J., and Treisman, R. (1999). Signal-regulated activation of serum response factor is mediated by changes in actin dynamics. Cell *98*, 159-169.

South, A.P., Wan, H., Stone, M.G., Dopping-Hepenstal, P.J., Purkis, P.E., Marshall, J.F., Leigh, I.M., Eady, R.A., Hart, I.R., and McGrath, J.A. (2003). Lack of plakophilin 1 increases keratinocyte migration and reduces desmosome stability. J Cell Sci *116*, 3303-3314.

Stritt, C., Stern, S., Harting, K., Manke, T., Sinske, D., Schwarz, H., Vingron, M., Nordheim, A., and Knoll, B. (2009). Paracrine control of oligodendrocyte differentiation by SRF-directed neuronal gene expression. Nat Neurosci *12*, 418-427.

Strzelecka-Golaszewska, H. (2001). Divalent cations, nucleotides, and actin structure. Results Probl Cell Differ *32*, 23-41.

Subramanian, A., Prokop, A., Yamamoto, M., Sugimura, K., Uemura, T., Betschinger, J., Knoblich, J.A., and Volk, T. (2003). Shortstop recruits EB1/APC1 and promotes microtubule assembly at the muscle-tendon junction. Curr Biol *13*, 1086-1095.

Sun, Q., Chen, G., Streb, J.W., Long, X., Yang, Y., Stoeckert, C.J., Jr., and Miano, J.M. (2006a). Defining the mammalian CArGome. Genome Res *16*, 197-207.

Sun, Y., Boyd, K., Xu, W., Ma, J., Jackson, C.W., Fu, A., Shillingford, J.M., Robinson, G.W., Hennighausen, L., Hitzler, J.K., *et al.* (2006b). Acute myeloid leukemia-associated Mkl1 (Mrtf-a) is a key regulator of mammary gland function. Mol Cell Biol *26*, 5809-5826.

Sweetman, D., Goljanek, K., Rathjen, T., Oustanina, S., Braun, T., Dalmay, T., and Munsterberg, A. (2008). Specific requirements of MRFs for the expression of muscle specific microRNAs, miR-1, miR-206 and miR-133. Dev Biol *321*, 491-499.

Takai, Y., and Nakanishi, H. (2003). Nectin and afadin: novel organizers of intercellular junctions. J Cell Sci *116*, 17-27.

Takai, Y., Sasaki, T., and Matozaki, T. (2001). Small GTP-binding proteins. Physiol Rev *81*, 153-208.

Taniguchi, Y., Furukawa, T., Tun, T., Han, H., and Honjo, T. (1998). LIM protein KyoT2 negatively regulates transcription by association with the RBP-J DNA-binding protein. Mol Cell Biol *18*, 644-654.

Tavazoie, S.F., Alarcon, C., Oskarsson, T., Padua, D., Wang, Q., Bos, P.D., Gerald, W.L., and Massague, J. (2008). Endogenous human microRNAs that suppress breast cancer metastasis. Nature *451*, 147-152.

Thiery, J.P. (2002). Epithelial-mesenchymal transitions in tumour progression. Nat Rev Cancer *2*, 442-454.

Tirnauer, J.S., Grego, S., Salmon, E.D., and Mitchison, T.J. (2002). EB1-microtubule interactions in Xenopus egg extracts: role of EB1 in microtubule stabilization and mechanisms of targeting to microtubules. Mol Biol Cell *13*, 3614-3626.

Treisman, R. (1994). Ternary complex factors: growth factor regulated transcriptional activators. Curr Opin Genet Dev *4*, 96-101.

Troyanovsky, S.M., Troyanovsky, R.B., Eshkind, L.G., Leube, R.E., and Franke, W.W. (1994). Identification of amino acid sequence motifs in desmocollin, a desmosomal glycoprotein, that are required for plakoglobin binding and plaque formation. Proc Natl Acad Sci U S A *91*, 10790-10794.

Tsuruta, D., and Jones, J.C. (2003). The vimentin cytoskeleton regulates focal contact size and adhesion of endothelial cells subjected to shear stress. J Cell Sci *116*, 4977-4984.

Tullai, J.W., Schaffer, M.E., Mullenbrock, S., Kasif, S., and Cooper, G.M. (2004). Identification of transcription factor binding sites upstream of human genes regulated by the phosphatidylinositol 3-kinase and MEK/ERK signaling pathways. J Biol Chem *279*, 20167-20177.

Vandekerckhove, J., and Weber, K. (1978). At least six different actins are expressed in a higher mammal: an analysis based on the amino acid sequence of the amino-terminal tryptic peptide. J Mol Biol *126*, 783-802.

Vartiainen, M.K., Guettler, S., Larijani, B., and Treisman, R. (2007). Nuclear actin regulates dynamic subcellular localization and activity of the SRF cofactor MAL. Science *316*, 1749-1752.

Vasiliev, J.M., Gelfand, I.M., Domnina, L.V., Ivanova, O.Y., Komm, S.G., and Olshevskaja, L.V. (1970). Effect of colcemid on the locomotory behaviour of fibroblasts. J Embryol Exp Morphol *24*, 625-640.

Visvanathan, J., Lee, S., Lee, B., Lee, J.W., and Lee, S.K. (2007). The microRNA miR-124 antagonizes the anti-neural REST/SCP1 pathway during embryonic CNS development. Genes Dev *21*, 744-749.

Wang, D., Chang, P.S., Wang, Z., Sutherland, L., Richardson, J.A., Small, E., Krieg, P.A., and Olson, E.N. (2001). Activation of cardiac gene expression by myocardin, a transcriptional cofactor for serum response factor. Cell *105*, 851-862.

Wang, Z., Wang, D.Z., Hockemeyer, D., McAnally, J., Nordheim, A., and Olson, E.N. (2004). Myocardin and ternary complex factors compete for SRF to control smooth muscle gene expression. Nature *428*, 185-189.

Wear, M.A., Schafer, D.A., and Cooper, J.A. (2000). Actin dynamics: assembly and disassembly of actin networks. Curr Biol *10*, R891-895.

Webb, D.J., Parsons, J.T., and Horwitz, A.F. (2002). Adhesion assembly, disassembly and turnover in migrating cells -- over and over and over again. Nat Cell Biol *4*, E97-100.

Weinhold, B., Schratt, G., Arsenian, S., Berger, J., Kamino, K., Schwarz, H., Ruther, U., and Nordheim, A. (2000). Srf(-/-) ES cells display non-cell-autonomous impairment in mesodermal differentiation. EMBO J *19*, 5835-5844.

Welch, M.D., and Mullins, R.D. (2002). Cellular control of actin nucleation. Annu Rev Cell Dev Biol *18*, 247-288.

Winer, J., Jung, C.K., Shackel, I., and Williams, P.M. (1999). Development and validation of real-time quantitative reverse transcriptase-polymerase chain reaction for monitoring gene expression in cardiac myocytes in vitro. Anal Biochem *270*, 41-49.

Wixler, V., Hirner, S., Muller, J.M., Gullotti, L., Will, C., Kirfel, J., Gunther, T., Schneider, H., Bosserhoff, A., Schorle, H., *et al.* (2007). Deficiency in the LIM-only protein Fhl2 impairs skin wound healing. J Cell Biol *177*, 163-172.

Yang, Y., Bauer, C., Strasser, G., Wollman, R., Julien, J.P., and Fuchs, E. (1999). Integrators of the cytoskeleton that stabilize microtubules. Cell *98*, 229-238.

Yoshio, T., Morita, T., Tsujii, M., Hayashi, N., and Sobue, K. (2010). MRTF-A/B suppress the oncogenic properties of v-ras- and v-src-mediated transformants. Carcinogenesis *31*, 1185-1193.

Yue, K.K., Holton, J.L., Clarke, J.P., Hyam, J.L., Hashimoto, T., Chidgey, M.A., and Garrod, D.R. (1995). Characterisation of a desmocollin isoform (bovine DSC3) exclusively expressed in lower layers of stratified epithelia. J Cell Sci *108 (Pt 6)*, 2163-2173.

Zaromytidou, A.I., Miralles, F., and Treisman, R. (2006). MAL and ternary complex factor use different mechanisms to contact a common surface on the serum response factor DNA-binding domain. Mol Cell Biol *26*, 4134-4148.

Zhang, S.X., Garcia-Gras, E., Wycuff, D.R., Marriot, S.J., Kadeer, N., Yu, W., Olson, E.N., Garry, D.J., Parmacek, M.S., and Schwartz, R.J. (2005). Identification of direct serum-response factor gene targets during Me2SO-induced P19 cardiac cell differentiation. J Biol Chem *280*, 19115-19126.

Zhao, Y., Samal, E., and Srivastava, D. (2005). Serum response factor regulates a muscle-specific microRNA that targets Hand2 during cardiogenesis. Nature *436*, 214-220.

X. Acknowledgements

I want to thank all those who have contributed to this scientific project and who have accompanied and supported me during my thesis.

In particular, I am very grateful to Prof. Dr. Kay Schneitz for supervising and promoting my thesis at the Technical University of Munich.

My special thanks go to Dr. Guido Posern for giving me the chance to work on this exciting project, for supporting my ideas and for the many valuable discussions, suggestions and all advice.

Many thanks also go to Prof. Dr. Axel Ullrich for giving me with the opportunity to work in this great scientific environment at the Department of Molecular Biology at the Max Planck Institute of Biochemistry and for all support.

Many thanks to my PhD advisory committee members Dr. Markus Moser and Dr. Gunter Meister and especially to Dr.Michael Sixt for productive discussions, guidance and advice.

My current and former lab members, particularly Stephan Busche, Carolin Schächterle, Arnaud Descot, Dmitry Shaposhnikov and Angela Kurz for all their help, discussions, the relaxed lab atmosphere and the great time I had, working with you.

My student Alexander Mengel for his great contribution to this project, his constant motivation and thorough work.

I want to thank all members of the Department of Molecular Biology for their help and friendship, especially Simone Gusenbauer, Philipp Mertins, Wolfgang Reindl, Robert Torka, Pavlos Stampolidis, Martin Gräber and Bianca Sperl.

Abschließend möchte ich ganz besonders meiner Familie für die andauernde Unterstützung und die erholsamen Aufenthalte zu Hause während der Zeit dieser Doktorarbeit danken.